ISSN 2434-1088
KURNS-EKR- 1

京都大学臨界集合体実験装置での加速器駆動システムにおけるウラン-鉛領域炉心の中性子特性に関する実験ベンチマーク

Experimental Benchmarks of Neutron Characteristics on Uranium-Lead Zoned Core in Accelerator-Driven System at Kyoto University Critical Assembly

編集： 卞　哲浩、山中正朗
Edited by : Cheol Ho Pyeon and Masao Yamanaka

京 都 大 学 複 合 原 子 力 科 学 研 究 所
Institute for Integrated Radiation and Nuclear Science, Kyoto University

Preface

These experimental benchmarks were contributed to the Coordinated Research Project (CRP) T33002 in the International Atomic Energy Agency (IAEA), as entitled "**Accelerator Driven Systems (ADS) and Use of Low-Enriched Uranium in ADS**," from 2016 to 2019.

The main objective of these benchmarks is to contribute to research and development of neutronics on Uranium-Lead (U-Pb) cores in ADS through the experimental data with the use of differing external neutron (14 MeV neutrons generated by D-T reactions; spallation neutrons generated by 100 MeV protons and Pb-Bi target), carried out at the Kyoto University Critical Assembly (KUCA) A-core.

Special thanks are due the KUCA and the fixed-filed alternative gradient (FFAG) accelerator staff for support and patience throughout a series of ADS experiments carried out at KUCA.

Cheol Ho Pyeon and Masao Yamanaka

June 2018

Keywords:
ADS, KUCA, FFAG accelerator, 14 MeV neutrons, Spallation neutrons, U-Pb zoned core

要　旨

この実験ベンチマーク問題は、国際原子力機関（IAEA）において 2016 年から 2019 年にかけて行われた国際共同研究プロジェクト T33002「加速器駆動システム（ADS）と ADS における低濃縮ウラニウムの利用」の一部として採択された「京都大学臨界集合体実験装置での加速器駆動システムにおけるウラン-鉛領域炉心の中性子特性に関する実験ベンチマーク」である。

この実験ベンチマーク問題は、KUCA の A 架台において行われた 2 種類の異なる外部中性子源（コッククロフト・ウォルトン加速器の DT 反応から 14 MeV 中性子、または FFAG 加速器と Pb-Bi ターゲットを組み合わせて得られる核破砕中性子）を用いた実験を通して、ADS におけるウラン-鉛領域炉心の中性子特性に関する基礎研究の発展に貢献することを目的としている。

最後に、KUCA において ADS 実験を準備および運転にご協力をいただいた KUCA および FFAG 加速器のスタッフに心から感謝の意を表します。

卞　哲浩、山中正朗

2018 年 6 月

Contents

Experimental Benchmarks of Neutron Characteristics on Uranium-Lead Zoned Core in Accelerator-Driven System at Kyoto University Critical Assembly

目　次

京都大学臨界集合体実験装置での加速器駆動システムにおけるウラン-鉛領域炉心の中性子特性に関する実験ベンチマーク

Experimental Benchmarks of Neutron Characteristics on Uranium-Lead Zoned Core in Accelerator-Driven System at Kyoto University Critical Assembly

Institute for Integrated for Radiation and Nuclear Science

(former Research Reactor Institute), Kyoto University, Japan

Cheol Ho Pyeon and Masao Yamanaka

Phase I

Study on Kinetics Parameters

11th June, 2018

1. Collaborative Work Specifications

1-1. Introduction

The accelerator-driven system (ADS) was developed for producing energy and for transmuting minor actinides and long-lived fission products. ADS has attracted worldwide attention in recent years because of its superior safety characteristics and potential for burning plutonium and nuclear waste. An outstanding advantage of its use is the anticipated absence of reactivity accidents, provided sufficient subcriticality is ensured. At the Institute for Integrated Radiation and Nuclear Science (KURNS), Kyoto University (former the Research Reactor Institute, Kyoto University: KURRI), a series of experiments on ADS was launched in fiscal year 2003 at the Kyoto University Critical Assembly (KUCA) [1]-[36]. A new accelerator was attached to the KUCA facility in March 2008, and the high-energy neutrons generated by the interaction of 100 MeV protons with tungsten target was injected into KUCA on March 2009. The new accelerator is called the fixed-field alternating gradient (FFAG) [37]-[38] accelerator of the synchrotron type developed by the High Energy Accelerator Research Organization (KEK) in Japan.

The experimental studies on ADS are being conducted for nuclear transmutation analyses with the combined use of KUCA and the FFAG accelerator. The ADS experiments [18]-[36] with 100 MeV protons obtained from the FFAG accelerator had been carried out to investigate the neutron characteristics of ADS, and the static and kinetic parameters were accurately analyzed through both the measurements and the Monte Carlo simulations of reactor physics parameters, including the reaction rates, the neutron spectrum, the neutron multiplication, the neutron decay constants and the subcriticality.

In this study, special attention was given to neutron characteristics of the ^{235}U-lead (U-Pb) zoned core in ADS with differing external neutron source: 14 MeV neutrons; 100 MeV protons with lead-bismuth (Pb-Bi) target. In a series of ADS experiments at KUCA, kinetic parameters, including the prompt neutron decay constant (α) and the subcriticality (ρ) in dollar units, were mainly obtained by the pulsed neutron source (PNS) method, the Feynman-α (Noise) method and the α-fitting method with the use of BF_3 neutron detector, optical fiber detectors [39]-[40] and LiCaF detector [41]-[43]. Among two external neutron sources, the Pb-Bi target was notably consisted of a mixture ratio of 44.5% (Pb) and 55.5% (Bi). Then, the high-energy neutrons were generated by the injection of 100 MeV protons onto the Pb-Bi target. In addition to the kinetic parameters, reaction rate distributions were experimentally measured by the foil activation method for analyzing the k-source value in a subcritical state.

The objective of this study was to investigate experimentally the neutron characteristics of U-Pb zoned core in ADS with differing external neutron source, and to evaluate the accuracy of stochastic and deterministic approaches with standard nuclear data libraries.

1-2. Experimental Settings

1-2-1. Description of KUCA core

KUCA comprises solid-moderated and -reflected type-A and -B cores, and a water-moderated and -reflected type-C core. In the present series of experiments, the solid-moderated and -reflected type-A core was combined with a Cockcroft-Walton type pulsed neutron generator and the FFAG accelerator at KUCA.

The A-core (A(1/8”p60EUEU(3)+1/8”Pb40p20EUEU)) configuration used for measuring the kinetic parameters and reaction rates is shown in Fig. 1-1. The core were composed of a combination of normal fuel “F” (1/8”p60EUEU) and special fuel “f” (1/8”p10EUEU<1/8”Pb40EUEU>1/8”p10EUEU) assemblies that were loaded on the grid plate. The materials used in the critical assemblies were always in the form of rectangular parallelepipe, 2” sq. with thickness ranging between 1/16” and 2”. The upper and lower parts of the fuel region were polyethylene reflector layers of more than 500 mm long, as shown in Fig. 1-2. The fuel rod, a highly-enriched uranium-aluminum (U-Al) alloy, consisted of 60 cells of polyethylene plate 1/8” thick, and a U-Al plate 1/16” thick and 2” sq. The functional height of the core was approximately 400 mm.

1-2-2. Description of FFAG accelerator

100 MeV protons generated from the FFAG accelerator were injected onto the Pb-Bi target. The main characteristics are under the following parameters: 100 MeV energy, 0.05 nA intensity, 20 Hz pulsed frequency, 100 ns pulsed width and 25 mm diameter spot size at the target. The thickness of target was determined on the basis of previous analyses [19] in the reaction rates for the high-energy protons. A level of the neutron yield generated at the target was around 1.0×10^{7} 1/*s* by the injection of 100 MeV protons onto the Pb-Bi target.

1-3. Experimental Results

1-3-1. Critical position and Excess reactivity

The critical state was adjusted by maintaining the control rods in certain positions, and the excess reactivity was attained on the basis of its integral calibration curve obtained by the positive period method.

1-3-2. Time evolution data of PNS and Noise methods

For 14 MeV neutrons and 100 MeV protons, to monitor carefully the prompt and delayed neutron behaviors, each core was set with four (or five) BF_3 detectors (1/2" and 1" diameters; 300 mm long) at the axial central position, three optical fibers and LiCaF detector, as shown in Fig. 1-1. Through the time evolution data of prompt and delayed neutrons, the prompt neutron decay constant was deduced by the Feynman-α method and the α-fitting method: the least-square fitting of the time evolution of the neutrons to an exponential function over the time optimal duration. Subcriticality was deduced by the extrapolated area ratio method on the basis of the prompt and delayed neutron behaviors.

1-3-3. Indium (In) reaction rate distribution

Indium (In) wire 1.0 mm diameter and 800 mm long was set in the axial center position along (13-14, A-P) the vertical direction shown in Fig. 2-3 for measuring the reaction rate distribution. The experimental results of the In wire were obtained by measuring total counts of the peak energy of γ-ray emittance and normalized by the counts of irradiated In foil (10*10*1 mm) emitted from ^{115}In(n, n')^{115m}In (threshold energy 0.3 MeV) reactions set at the location of the Pb-Bi target.

1-4. References

ADS with 14 MeV Neutrons

[1] C. H. Pyeon, Y. Hirano, T. Misawa, *et al.*, "Preliminary Experiments on Accelerator Driven Subcritical Reactor with Pulsed Neutron Generator in Kyoto University Critical Assembly," *J. Nucl. Sci. Technol.,* **44**, 1368 (2007).

[2] C. H. Pyeon, M. Hervault, T. Misawa, *et al.*, "Static and Kinetic Experiments on Accelerator Driven Subcritical Reactor with 14 MeV Neutrons in Kyoto University Critical Assembly," *J. Nucl. Sci. Technol.,* **45**, 1171 (2008).

[3] C. H. Pyeon, H. Shiga, T. Misawa, *et al.*, "Reaction Rate Analyses for an Accelerator-Driven System with 14 MeV Neutrons in Kyoto University Critical Assembly," *J. Nucl. Sci. Technol.*, **46**, 965 (2009).

[4] H. Shahbunder, C. H. Pyeon, T. Misawa and S. Shiroya, "Experimental Analysis for Neutron Multiplication by using Reaction Rate Distribution in Accelerator-Driven System," *Ann. Nucl. Energy*, **37**, 592 (2010).

[5] H. Taninaka, K. Hashimoto, C. H. Pyeon, *et al.,* "Determination of Lambda-Mode Eigenvalue Separation of a Thermal Accelerator-Driven System from Pulsed Neutron Experiment," *J. Nucl. Sci. Technol.*, **47**, 376 (2010).

[6] H. Shahbunder, C. H. Pyeon, T. Misawa, *et al.*, "Subcritical Multiplication Factor and Source Efficiency in Accelerator-Driven System," *Ann. Nucl. Energy*, **37**, 1214 (2010).

[7] H. Shahbunder, C. H. Pyeon, T. Misawa, *et al.*, "Effects of Neutron Spectrum and External Neutron Source on Neutron Multiplication Parameters in Accelerator-Driven System," *Ann. Nucl. Energy*, **37**, 1785 (2010).

[8] H. Taninaka, K. Hashimoto, C. H. Pyeon, *et al.,* "Determination of Subcritical Reactivity of a Thermal Accelerator-Driven System from Beam Trip and Restart Experiment," *J. Nucl. Sci. Technol.*, **48**, 873 (2011).

[9] H. Taninaka, A. Miyoshi, K. Hashimoto, *et al.,* "Feynman-α Analysis for a Thermal Subcritical Reactor System Driven by an Unstable 14MeV-Neutron Source," *J. Nucl. Sci. Technol.*, **48**, 1272 (2011).

[10] C. H. Pyeon, Y. Takemoto, T. Yagi, *et al.*, "Accuracy of Reaction Rates in the Accelerator-Driven System with 14 MeV Neutrons at the Kyoto University Critical Assembly," *Ann. Nucl. Energy*, **40**, 229 (2012).

[11] A. Sakon, K. Hashimoto, W. Sugiyama, *et al.*, "Power Spectral Analysis for a Thermal Subcritical Reactor System Driven by a Pulsed 14 MeV Neutron Source," *J. Nucl. Sci. Technol.*, **50**, 481 (2013).

[12] A. Sakon, K. Hashimoto, M. A. Maarof, *et al.*, "Measurement of Large Negative Reactivity of an Accelerator-Driven System in the Kyoto University Critical Assembly," *J. Nucl. Sci. Technol.,* **51**, 116 (2014).

[13] A. Sakon, K. Hashimoto, W. Sugiyama, *et al.*, "Determination of Prompt-Neutron Decay Constant from Phase Shift between Beam Current and Neutron Detection Signals for an

Accelerator-Driven System in the Kyoto University Critical Assembly," *J. Nucl. Sci. Technol.*, **52**, 204-213 (2015).

[14] W. K. Kim, H. C. Lee, C. H. Pyeon, *et al.*, "Monte Carlo Analysis of the Accelerator-Driven System at Kyoto University Research Reactor Institute," *Nucl. Eng. Technol.*, **48**, 304 (2016).

[15] T. Endo, A. Yamamoto, T. Yagi and C. H. Pyeon, "Statistical Error Estimation of the Feynman-α Method using the Bootstrap Method," *J. Nucl. Sci. Technol.*, **53**, 1447 (2016).

[16] W. F. G. Rooijen, T. Endo, G. Chiba and C. H. Pyeon, "Analysis of the KUCA ADS Benchmarks with Diffusion Theory," *Prog. Nucl. Energy*, **101**, 243 (2017).

[17] C. D. Kong, J. W. Choe, S. P. Yum, *et al.*, "Application of Advanced Rossi-alpha Technique to Reactivity Measurements at Kyoto University Critical Assembly," *Ann. Nucl. Energy*, **118**, 92 (2018).

ADS with 100 MeV Protons

[18] C. H. Pyeon, T. Misawa, J. Y. Lim *et al.*, "First Injection of Spallation Neutrons Generated by High-Energy Protons into the Kyoto University Critical Assembly," *J. Nucl. Sci. Technol.*, **46**, 1091 (2009).

[19] C. H. Pyeon, H. Shiga, K. Abe, *et al.*, "Reaction Rate Analysis of Nuclear Spallation Reactions Generated by 150, 190 and 235 MeV Protons," *J. Nucl. Sci. Technol.*, **47**, 1090 (2010).

[20] C. H. Pyeon, J. Y. Lim, Y. Takemoto, *et al.*, "Preliminary Study on the Thorium-Loaded Accelerator-Driven System with 100 MeV Protons at the Kyoto University Critical Assembly," *Ann. Nucl. Energy*, **38**, 2298 (2011).

[21] J. Y. Lim, C. H. Pyeon, T. Yagi and T. Misawa, "Subcritical Multiplication Parameters of the Accelerator-Driven System with 100 MeV Protons at the Kyoto University Critical Assembly," *Sci. Technol. Nucl. Install.*, **2012**, ID: 395878, 9 pages, (2012).

[22] Y. Takahashi, T. Azuma, T. Nishio, *et al.*, "Conceptual Design of Multi-Targets for Accelerator-Driven System Experiments with 100 MeV Protons," *Ann. Nucl. Energy*, **54**, 162 (2013).

[23] C. H. Pyeon, T. Azuma, Y. Takemoto, *et al.*, "Experimental Analyses of External Neutron Source Generated by 100 MeV Protons at the Kyoto University Critical Assembly," *Nucl. Eng. Technol.*, **45**, 81 (2013).

[24] C. H. Pyeon, T. Yagi, K. Sukawa, *et al.*, "Mockup Experiments on the Thorium-Loaded Accelerator-Driven System in the Kyoto University Critical Assembly," *Nucl. Sci. Eng.*, **177**, 156 (2014).

[25] C. H. Pyeon, H. Nakano, M. Yamanaka, *et al.*, "Neutron Characteristics of Solid Targets in Accelerator-Driven System with 100 MeV Protons at Kyoto University Critical Assembly," *Nucl. Technol.*, **192**, 181 (2015).

[26] M. Yamanaka, C. H. Pyeon, T. Yagi and T. Misawa, "Accuracy of Reactor Physics Parameters in Thorium-Loaded Accelerator-Driven System Experiments at Kyoto University Critical Assembly," *Nucl. Sci. Eng.*, **183**, 96 (2016).

[27] T. Endo, A. Yamamoto, T. Yagi and C. H. Pyeon, "Statistical Error Estimation of the Feynman-α

Method using the Bootstrap Method," *J. Nucl. Sci. Technol.*, **53**, 1447 (2016).

[28] M. Yamanaka, C. H. Pyeon and T. Misawa, "Monte Carlo Approach of Effective Delayed Neutron Fraction by k-ratio Method with External Neutron Source," *Nucl. Sci. Eng.*, **184**, 551 (2016).

[29] S. Dulla, S. S. Hoh, G. Marana, *et al.*, "Analysis of KUCA Measurements by the Reactivity Monitoring MAρTA Method," *Ann. Nucl. Energy*, **101**, 397 (2017).

[30] M. Yamanaka, C. H. Pyeon, S. H. Kim, *et al.*, "Effective Delayed Neutron Fraction in Accelerator-Driven System Experiments with 100 MeV Protons at Kyoto University Critical Assembly," *J. Nucl. Sci. Technol.*, **54**, 293 (2017).

[31] H. Iwamoto, K. Nishihara, T. Yagi and C. H. Pyeon, "On-line Subcriticality Measurement using A Pulsed Spallation Neutron Source," *J. Nucl. Sci. Technol.*, **54**, 432 (2017).

[32] C. H. Pyeon, M. Yamanaka, T. Endo, *et al.*, "Experimental Benchmarks on Kinetic Parameters in Accelerator-Driven System with 100 MeV Protons at Kyoto University Critical Assembly," *Ann. Nucl. Energy*, **105**, 346 (2017).

[33] C. H. Pyeon, M. Yamanaka, S. H. Kim, *et al.*, "Benchmarks of Subcriticality in Accelerator-Driven System Experiments at Kyoto University Critical Assembly," *Nucl. Eng. Technol.*, **49**, 1234 (2017).

[34] A. Talamo, Y. Gohar, F. Gabrielli, *et al.*, "Coupling Sjostrand and Feynman Methods in Prompt Neutron Decay Constant Analyses," *Prog. Nucl. Energy*, **101**, 299 (2017).

[35] C. H. Pyeon, T. M. Vu, M. Yamanaka, *et al.*, "Reaction Rate Analyses of Accelerator-Driven System Experiments with 100 MeV Protons at Kyoto University Critical Assembly," *J. Nucl. Sci. Technol.*, **55**, 190 (2018).

[36] T. Endo, G. Chiba, W. F. G. van Rooijen, *et al.*, "Experimental Analysis and Uncertainty Quantification using Random Sampling Technique for ADS Experiments at KUCA," *J. Nucl. Sci. Technol.*, **55**, 450 (2018).

FFAG Accelerator (100 MeV Protons)

[37] J. B. Lagrange, T. Planche, E. Yamakawa *et al.*, "Straight Scaling FFAG Beam Line," *Nucl. Instrum. Methods A*, **691**, 55 (2013).

[38] E. Yamakawa, T. Uesugi, J. B. Lagrange *et al.*, "Serpentine Acceleration in Zero-Chromatic FFAG Accelerators," *Nucl. Instrum. Methods A*, **716**, 46 (2013).

Optical Fiber and LiCaF Fiber Detectors

[39] T. Yagi, T. Misawa, C. H. Pyeon *et al.*, "A Small High Sensitivity Neutron Detector using a Wavelength Shifting Fiber," *Appl. Radiat. Isot.*, **69**, 176 (2011).

[40] T. Yagi, C. H. Pyeon and T. Misawa, "Application of Wavelength Shifting Fiber to Subcriticality Measurements," *Appl. Radiat. Isot.*, **72**, 11 (2013).

[41] K. Watanabe, Y. Kondo, A. Yamazaki *et al.*, "Study on Fast Luminescence Component Induced by Gamma-rays in Ce Doped $LiCaAlF_6$ Scintillators," *Radiation Measurement*, **71**, 158 (2014).

[42] K. Watanabe, Y. Kawabata, A. Yamazaki *et al.*, "Development of an Optical Fiber Type Detector

using a Eu:LiCaAlF6 Scintillator for Neutron Monitoring in Boron Neutron Capture Therapy," *Nucl. Instrum. Methods A*, **802**, 1 (2015).

[43] K. Watanabe, T. Yamazaki, D. Sugimoto *et al.*, "Wavelength-Shifting Fiber Signal Readout from Transparent RUbber SheeT (TRUST) Type $LiCaAlF_6$ Neutron Scintillator," *Nucl. Instrum. Methods A*, **784**, 260 (2015).

Appendix-I

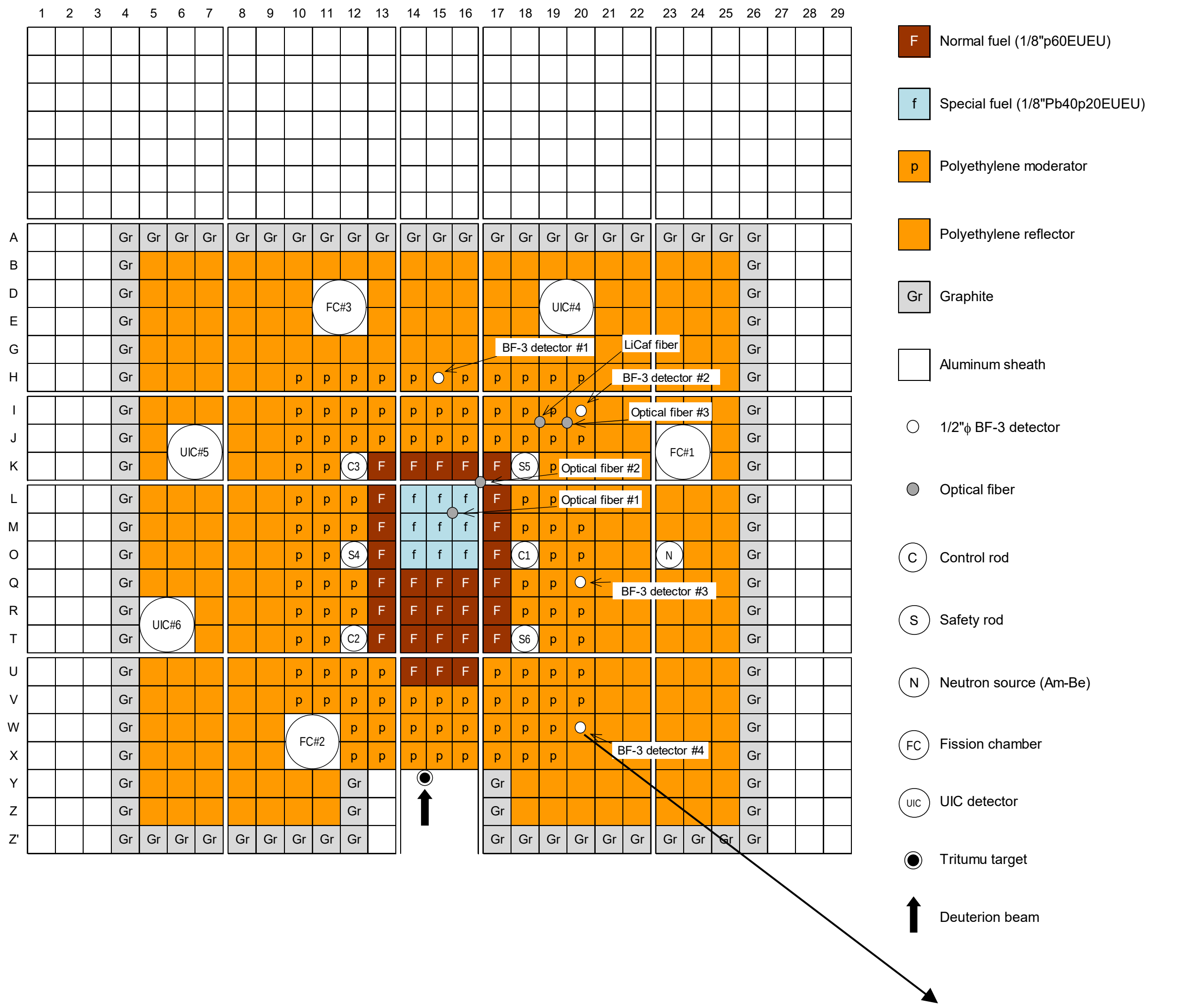

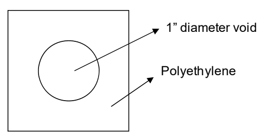

Fig. 1-1 The general view of U-Pb zoned core configuration

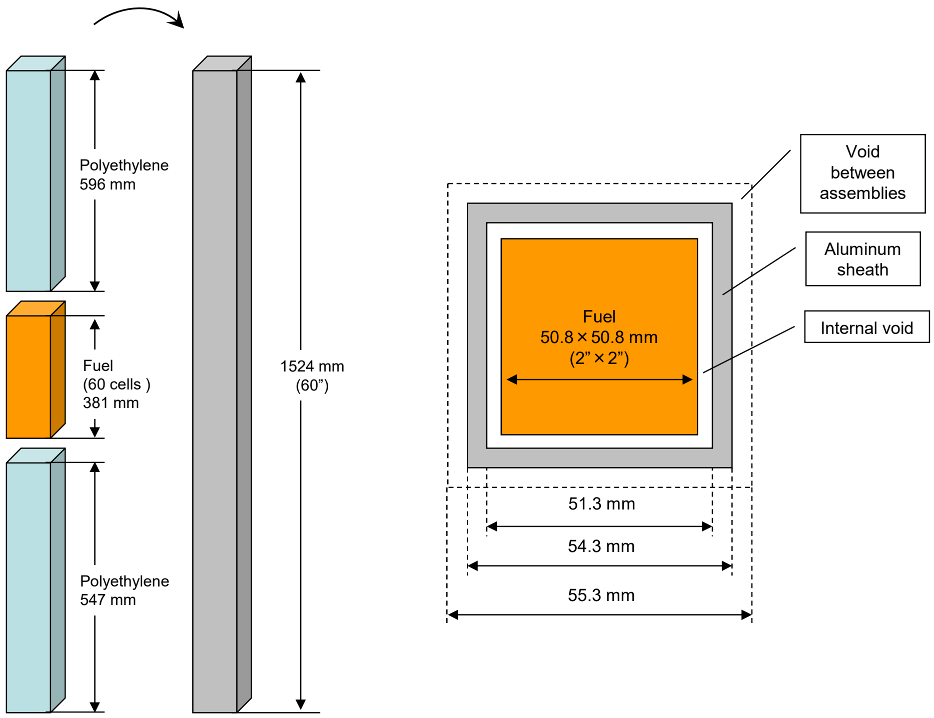

Fig. 1-2 Description of fuel assembly at KUCA

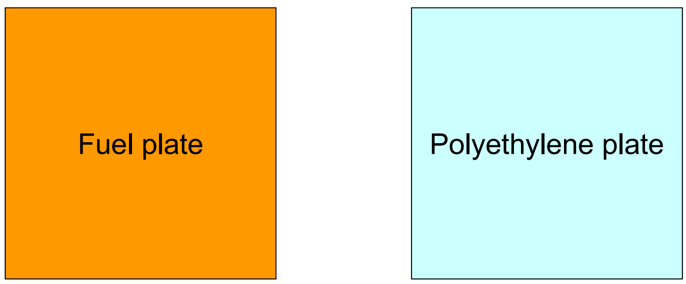

Fig. 1-3 Description of fuel (HEU; 2"×2") and polyethylene plates (2"×2")

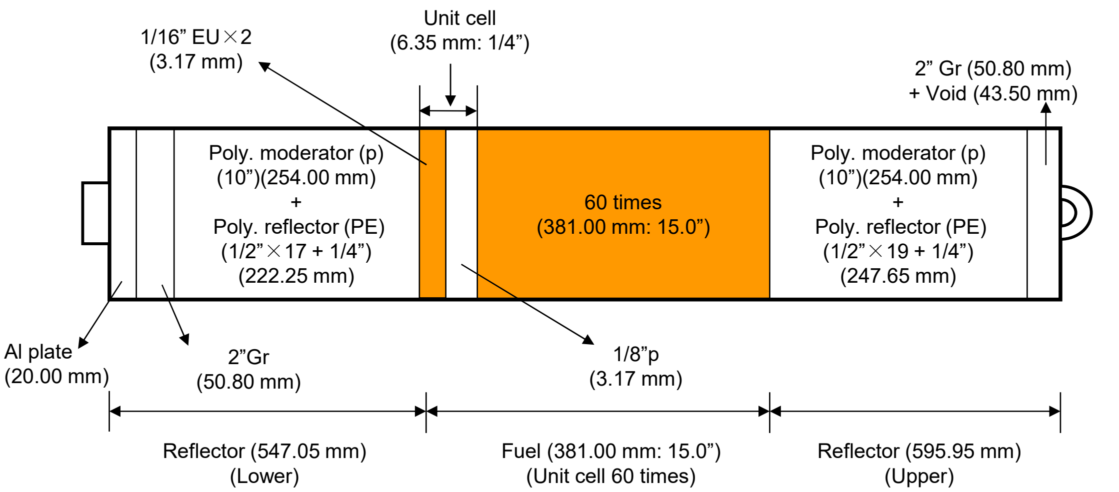

(a) Fuel assembly "F"

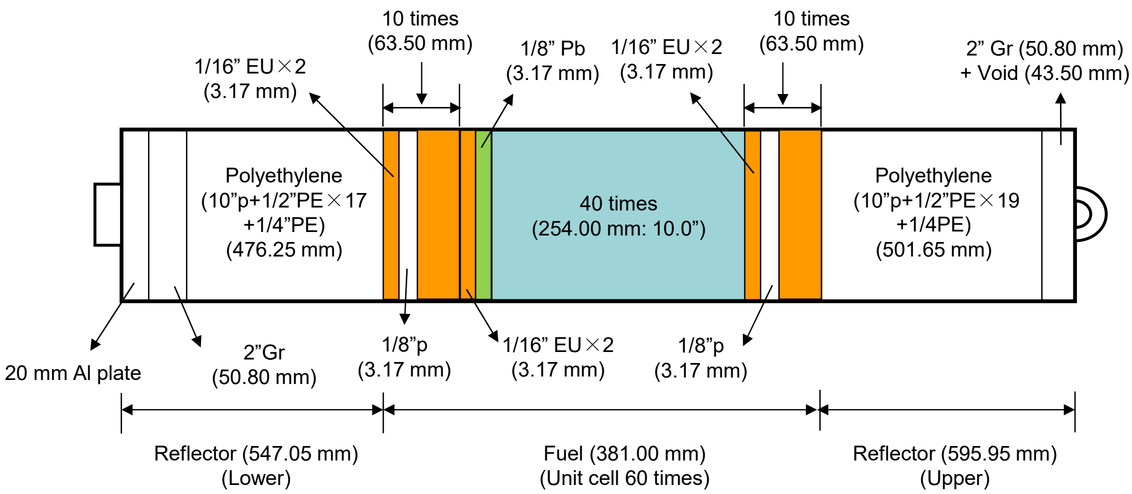

(b) Fuel assembly "f"

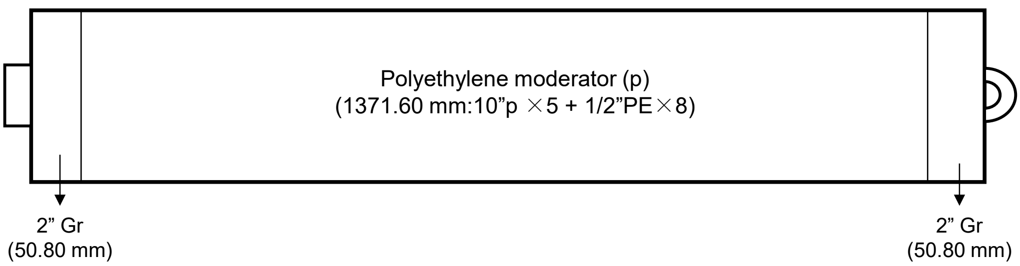

(c) Polyethylene moderator "p"

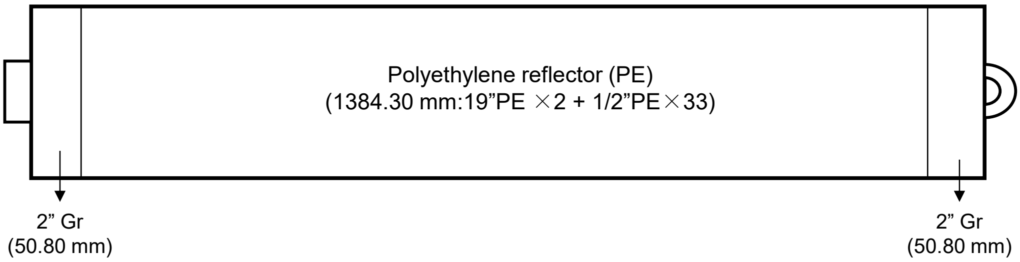

(d) Polyethylene reflector

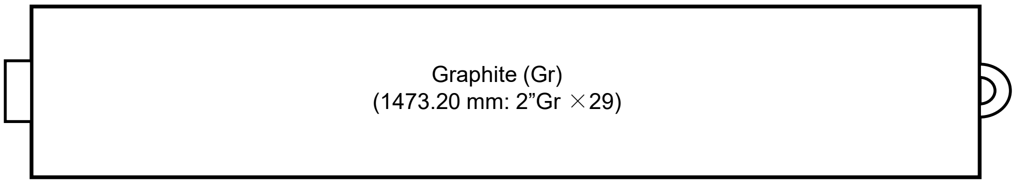

(e) Graphite “Gr”

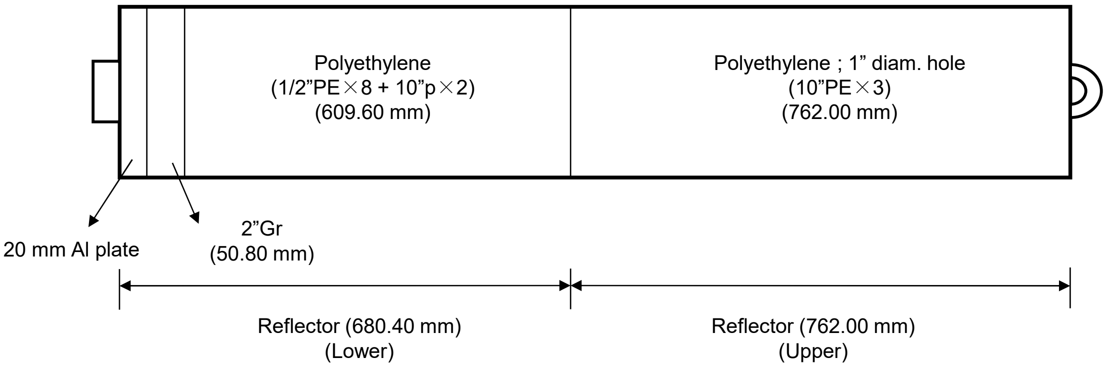

(f) Polyethylene with 1” diameter hole

Fig. 1-4 Fall sideways view of fuel and polyethylene rods shown in Fig. 1-1

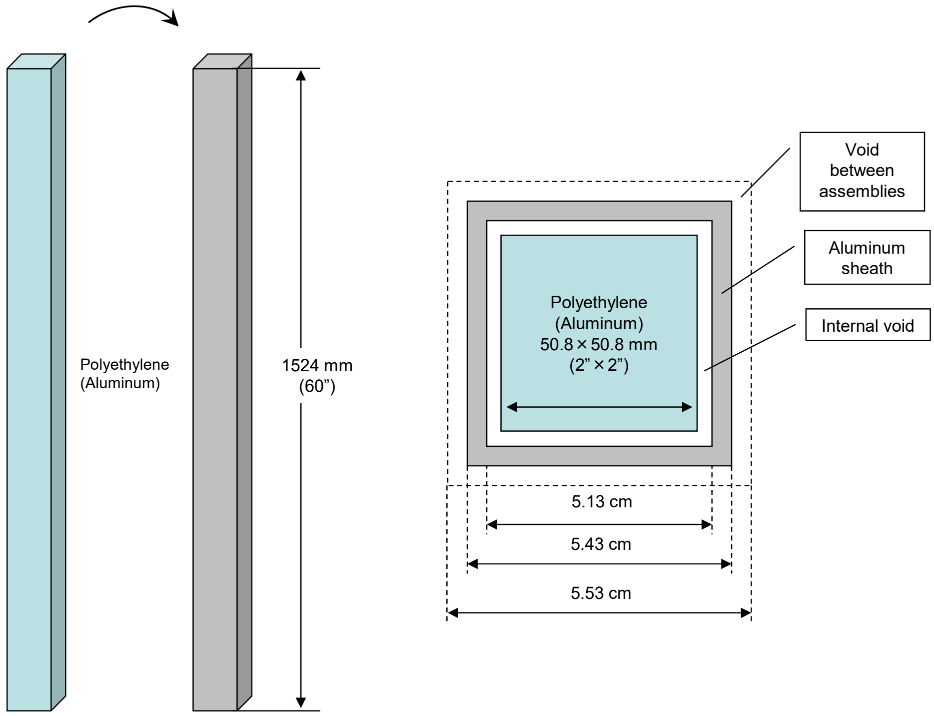

Fig. 1-5　Description of polyethylene reflector at KUCA

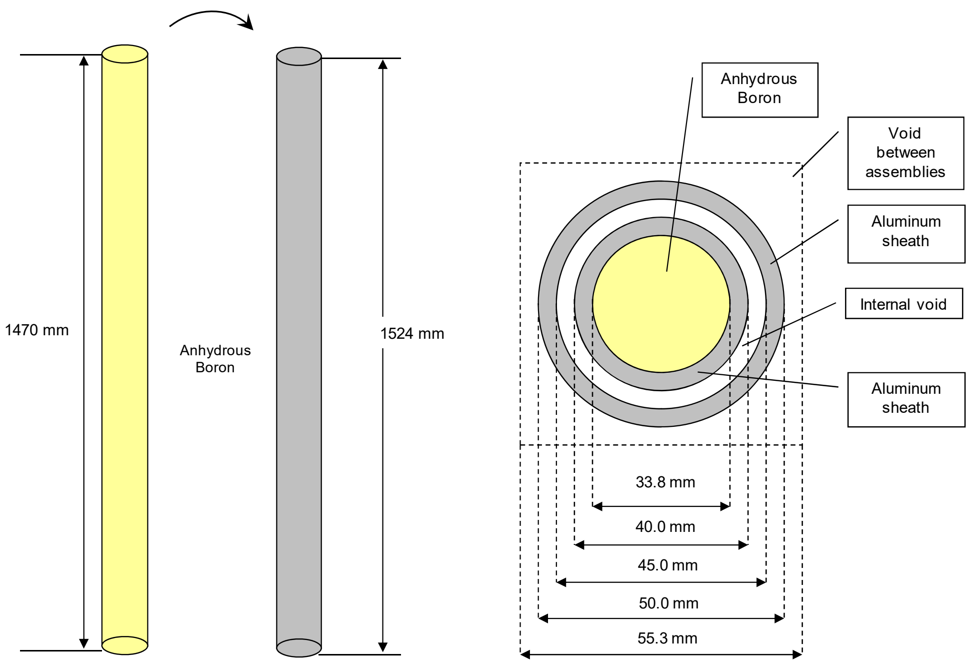

Fig. 1-6　Description of control (safety) rod at KUCA

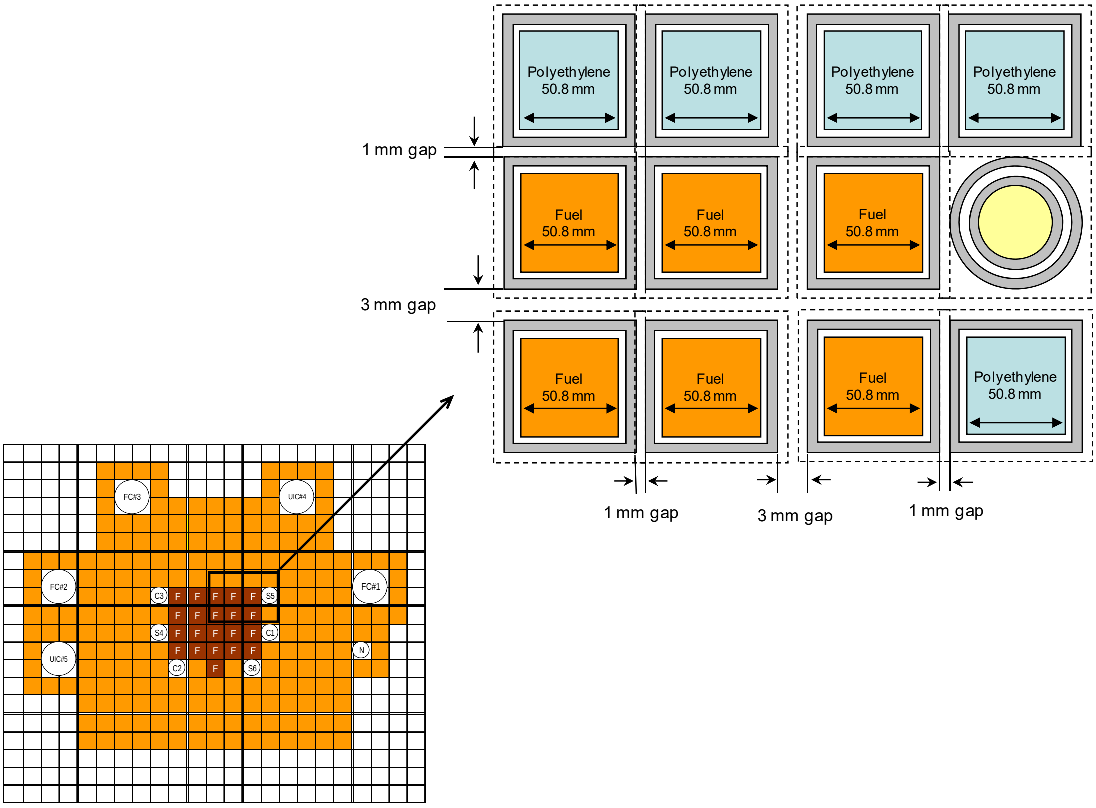

Fig. 1-7 Description of fuel assembly, polyethylene reflector and control rod at KUCA

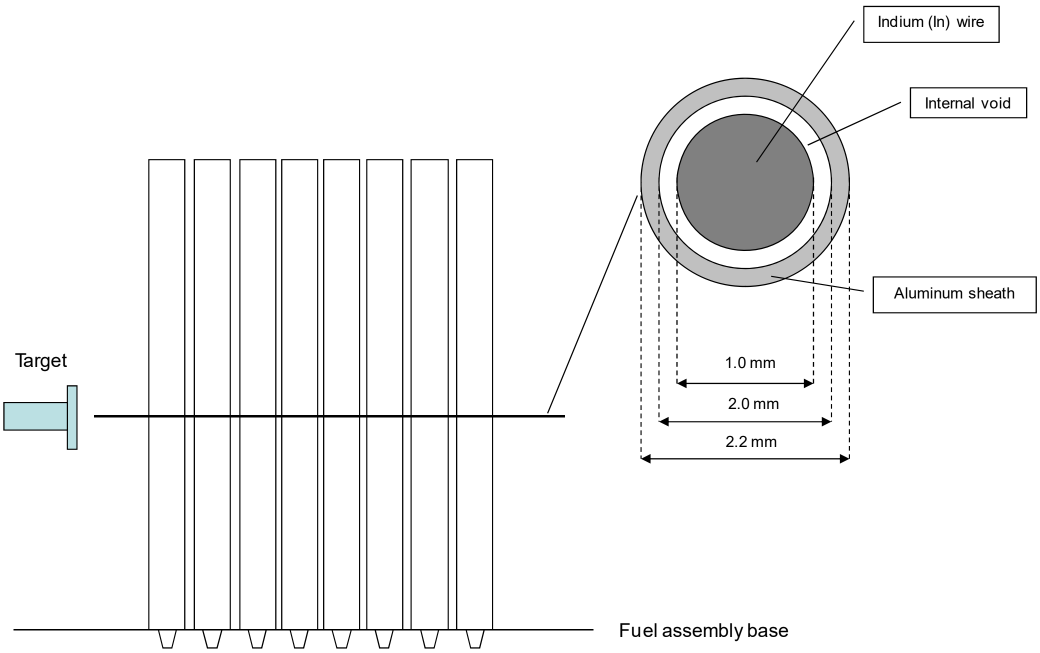

Fig. 1-8 Setting of Indium (In) wire

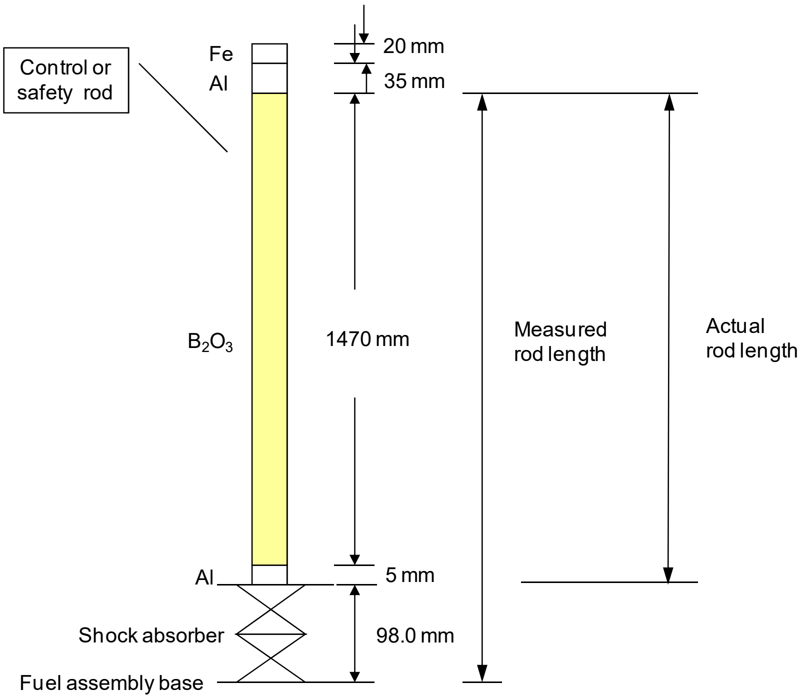

Fig. 1-9 Actual position of control (safety) rod
(Actual position = Measured position – 97.5 mm)

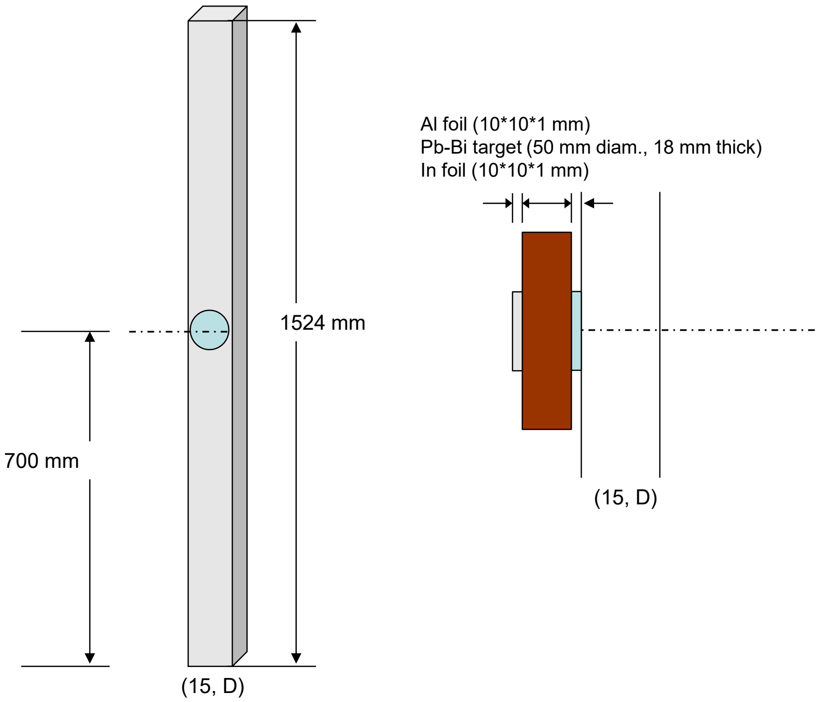

Fig. 1-10 Attachment of target, Al and In foils at the location of core target

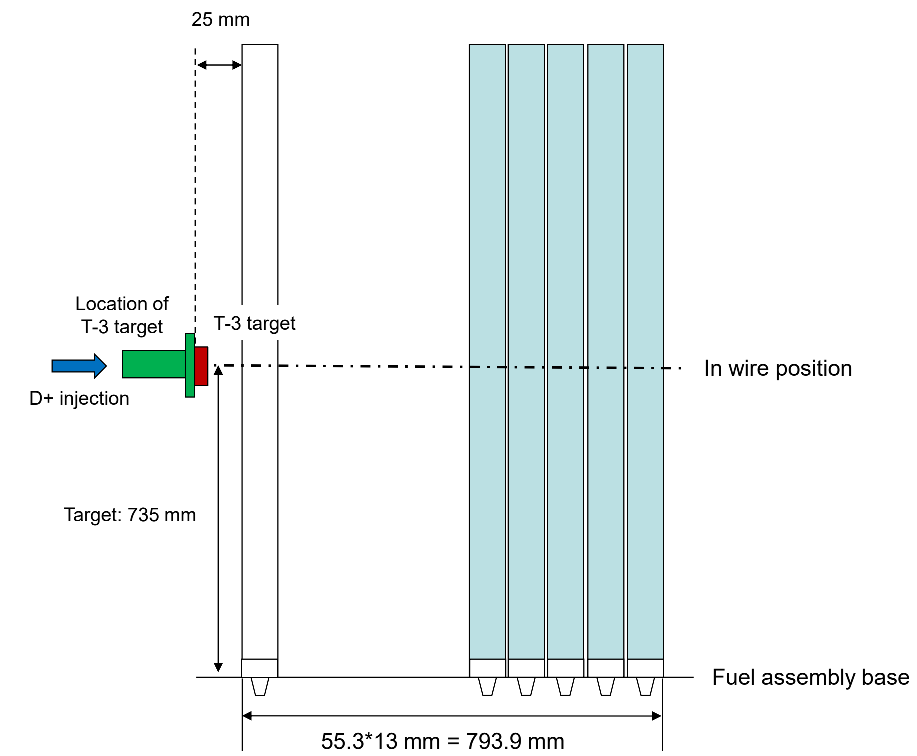

Fig. 1-11　Side view of target and core configuration with 14 MeV neutrons

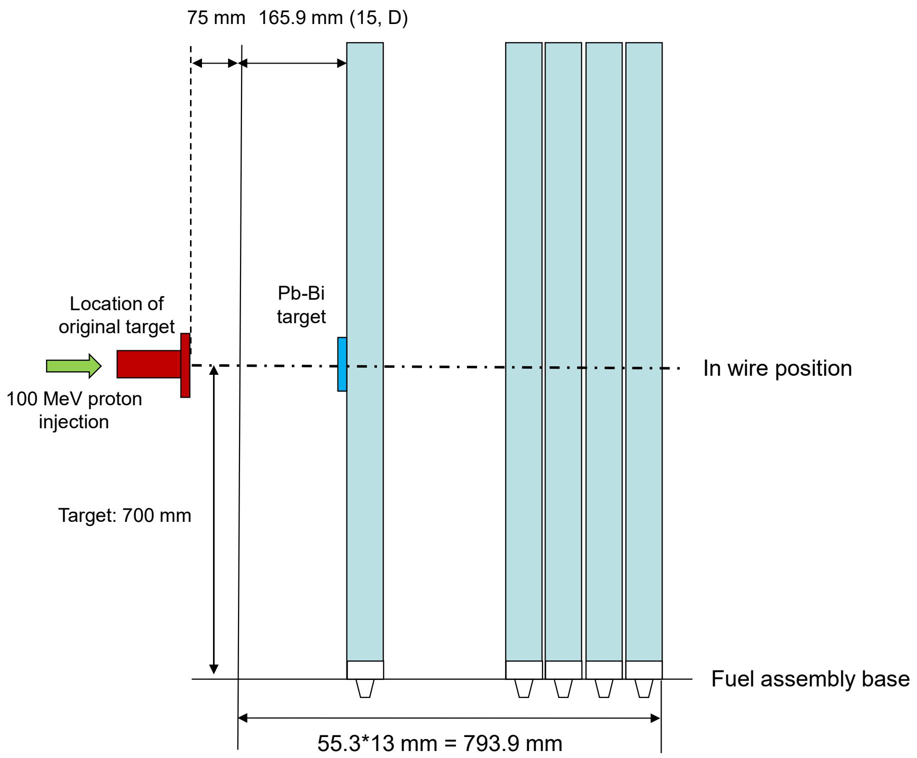

Fig. 1-12　Side view of target and core configuration with 100 MeV protons

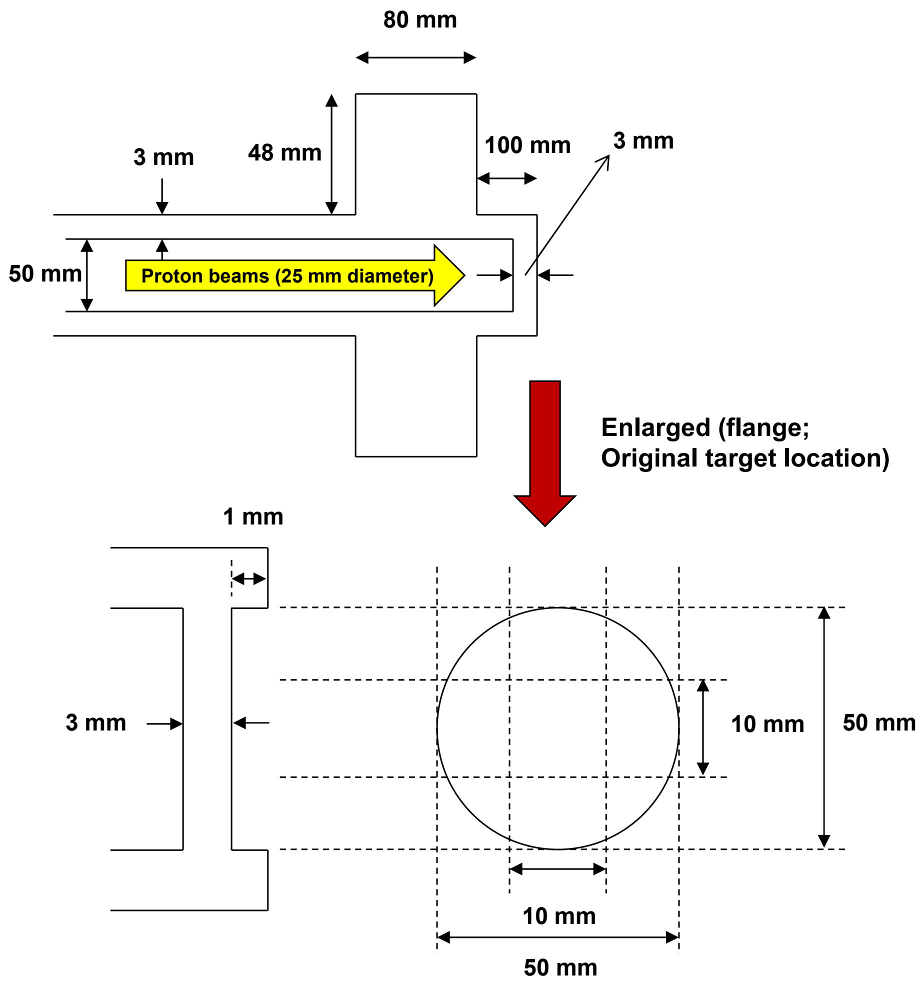

Fig. 1-13　Target configuration of the location of original target

Table 1-1 Atomic density of 1/16” thick highly-enriched uranium (HEU) fuel plate (U-Al alloy)

Isotope	Atomic density [$\times10^{24}$/cm^3]
^{234}U	1.13659E-05
^{235}U	1.50682E-03
^{236}U	4.82971E-06
^{238}U	9.25879E-05
Al	5.56436E-02

Table 1-2 Atomic density of polyethylene (p) moderator

Isotope	Atomic density [$\times10^{24}$/cm^3]	
	1/8” thick plate	10” long rod
^{1}H	7.77938E-02	7.97990E-02
^{12}C	3.95860E-02	4.08960E-02

Table 1-3 Atomic density of polyethylene (PE) reflector

Isotope	Atomic density [$\times10^{24}$/cm^3]		
	1/2” thick plate	1/4” thick plate	1/8” thick plate
H	8.06560E-02	8.08711E-02	8.02167E-02
C	4.03280E-02	4.04356E-02	4.01084E-02

Table 1-4 Atomic density of control and safety rods

Isotope	Atomic density [$\times10^{24}/cm^3$]
^{10}B	3.87448E-03
^{11}B	1.68447E-02
^{16}O	3.10787E-02

Table 1-5 Atomic density of aluminum sheath for the core element

Isotope	Atomic density [$\times10^{24}/cm^3$]
Al	6.00385E-02

Table 1-6 Atomic density of Cd, In and Au

Foil (wire)	Isotope	Abundance (%)	Purity (%)	Atomic density [$\times10^{24}/cm^3$]
In	^{113}In	4.29	99.99	1.64406E-03
	^{115}In	95.71	99.99	3.66790E-02
Au	^{197}Au	100	99.95	5.90403E-02

Table 1-7 Atomic density of Pb-Bi target

Target	Isotope	Abundance (%)	Atomic density [$\times 10^{24}/cm^3$]
Pb-Bi (44.5/55.5)	^{204}Pb	1.4	1.87461E-04
	^{206}Pb	24.1	3.25860E-03
	^{207}Pb	22.1	3.00266E-03
	^{208}Pb	52.4	7.15378E-03
	^{209}Bi	100	1.67670E-02

Table 1-8 Dimension of target

Target	Diameter [mm]	Thickness [mm]
Pb-Bi	50.0	18.0

Table 1-9 Atomic density of beam tube component (SUS304) shown in Fig. 1-13

Isotope	Atomic density [$\times 10^{24}/cm^3$]
^{54}Fe	3.55712E-03
^{56}Fe	5.58391E-02
^{57}Fe	1.28957E-03
^{58}Fe	1.71618E-04
^{50}Cr	7.51530E-04
^{52}Cr	1.44925E-02
^{53}Cr	1.64333E-03
^{54}Cr	4.09060E-04
^{58}Ni	5.10587E-03
^{60}Ni	1.96674E-03
^{61}Ni	8.54932E-05
^{62}Ni	2.72597E-04
^{64}Ni	6.94130E-05

2. Core Configuration

2.1 ADS cores with 14 MeV Neutrons

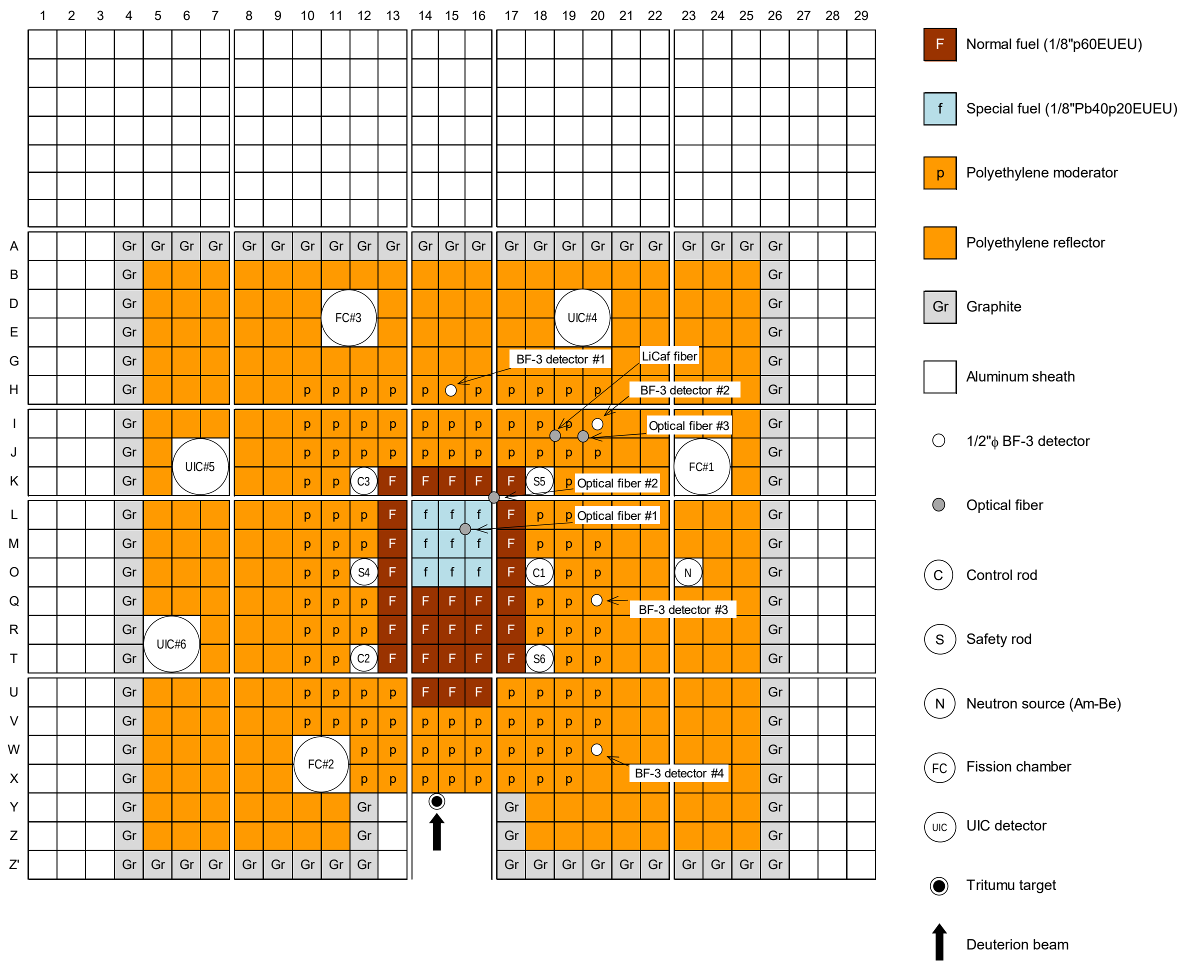

Fig. 2-1 U-Pb zoned core configuration of ADS with 14 MeV neutrons

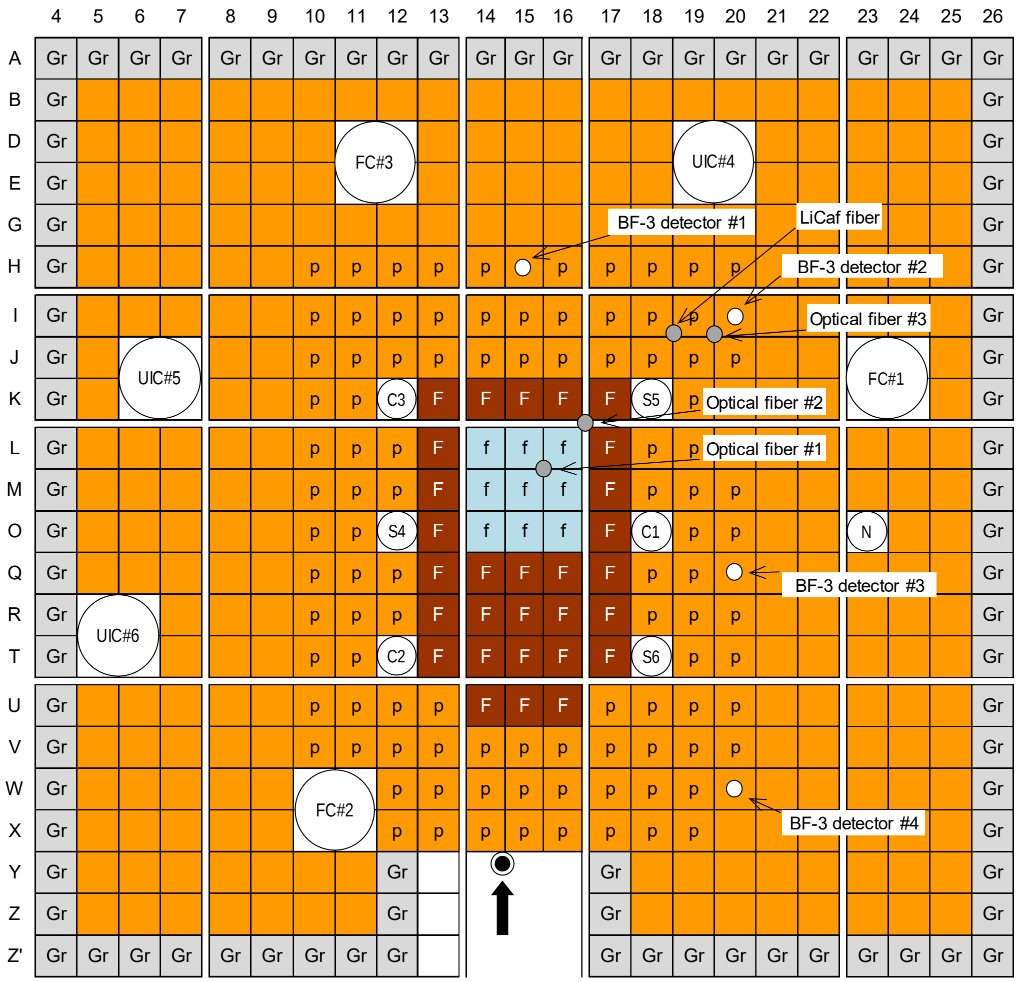

(a) Case D1 (Reference core; Number of fuel plates: 4560)

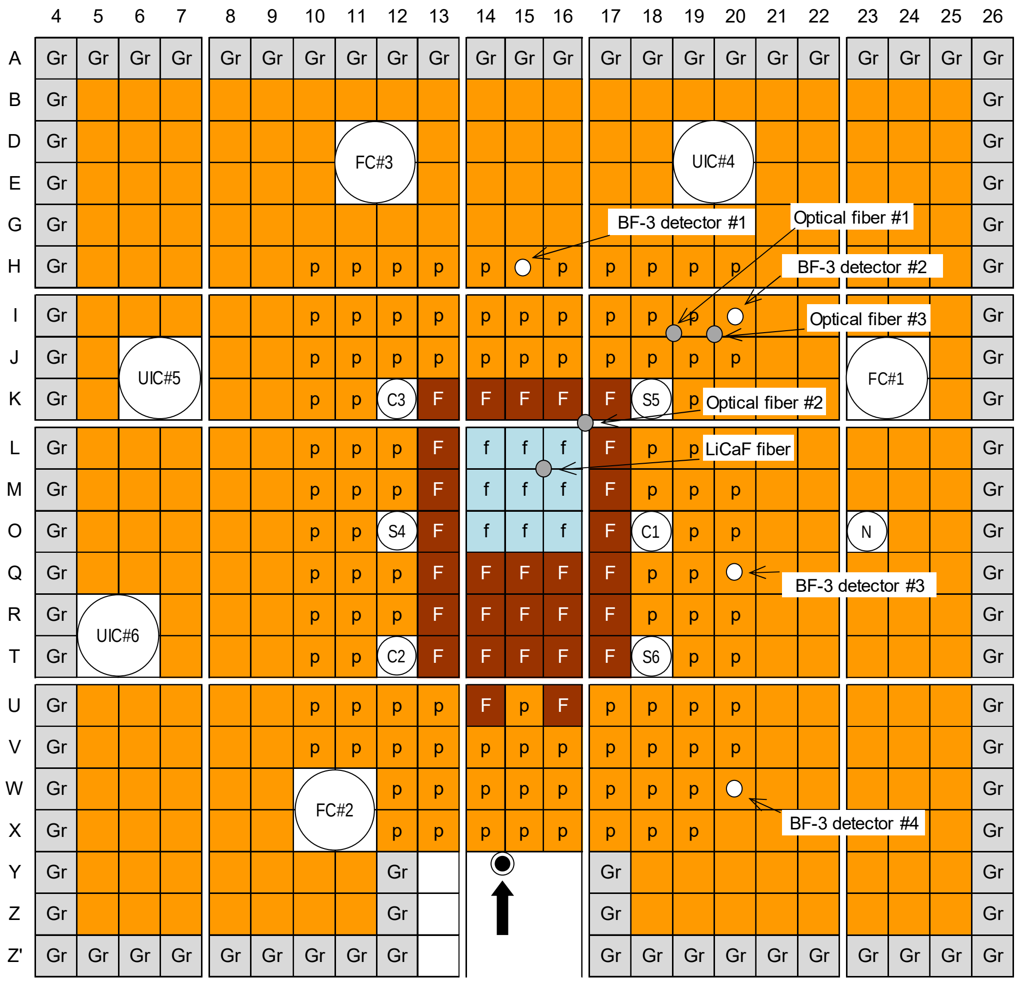

(b) Case D2 (Number of fuel plates: 4400)

Note: Change of location of detectors (comparing Case I with Case II, III, IV, V and VI)

Optical fiber #1: (15-16, L- M) ---> (18-19, I-J)

LiCaF fiber: (18-19, I-J) ---> (15-16, L-M)

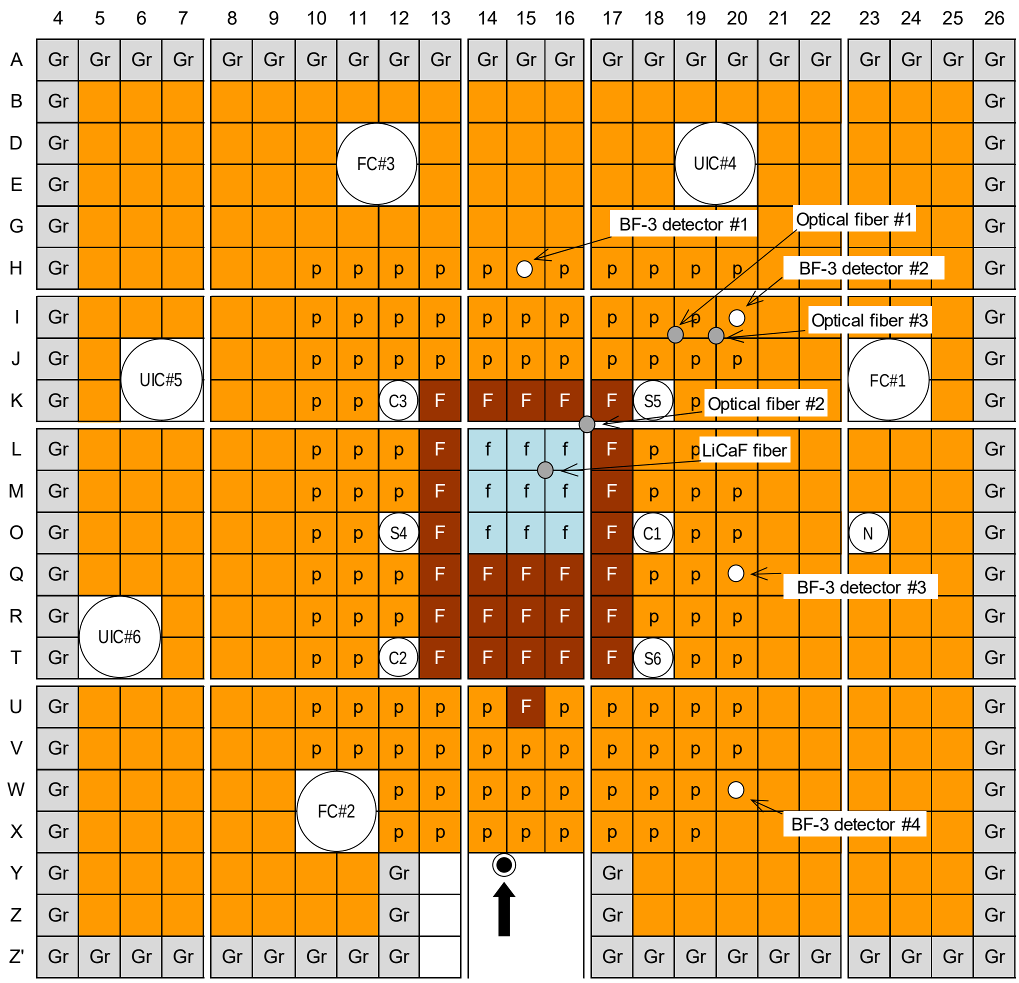

(c) Case D3 (Number of fuel plates: 4320)

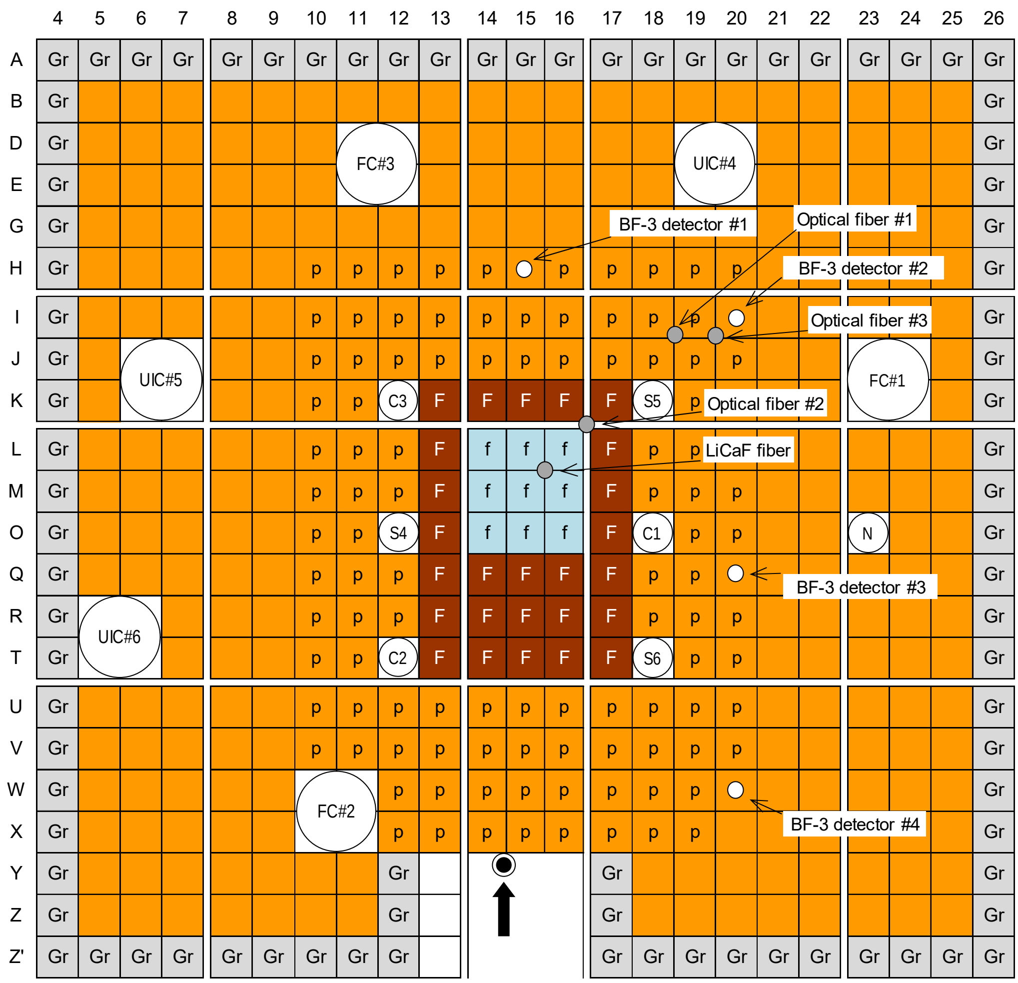

(d) Case D4 (Number of fuel plates: 4200)

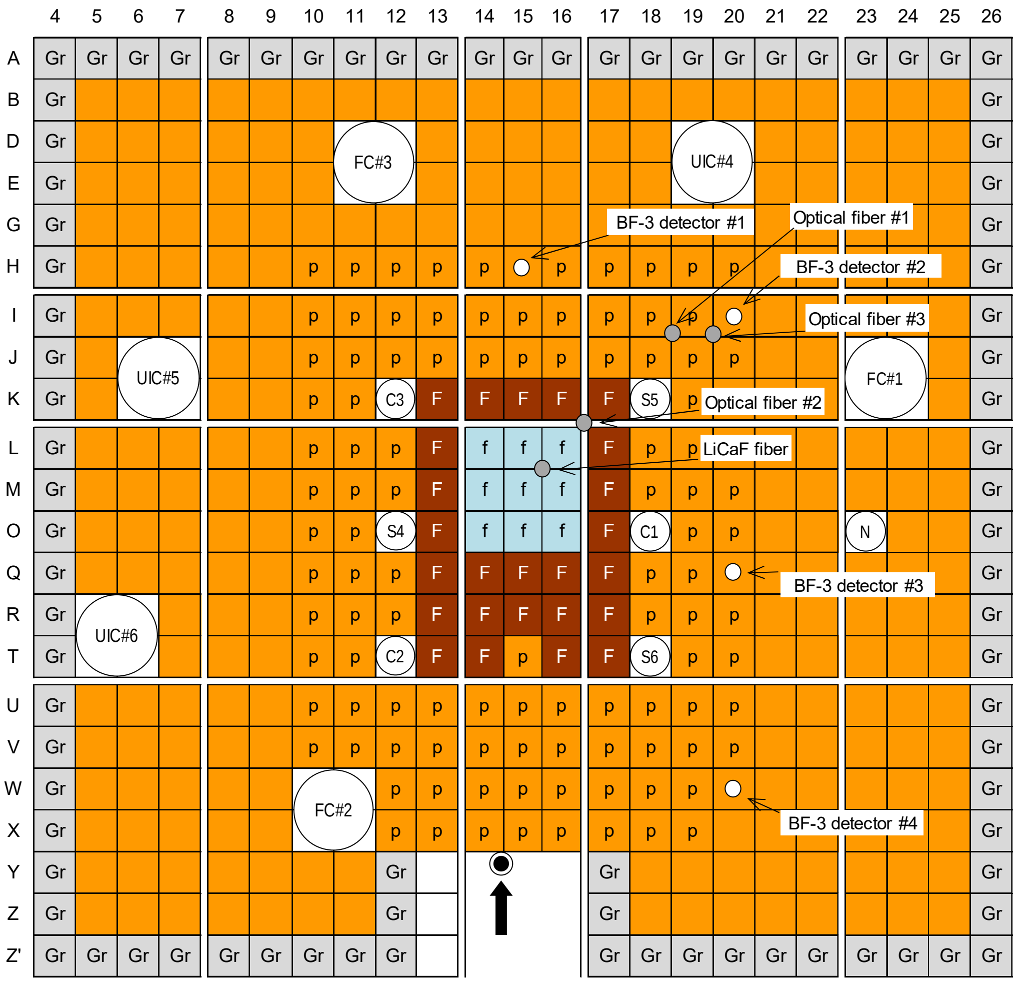

(e) Case D5 (Number of fuel plates: 4080)

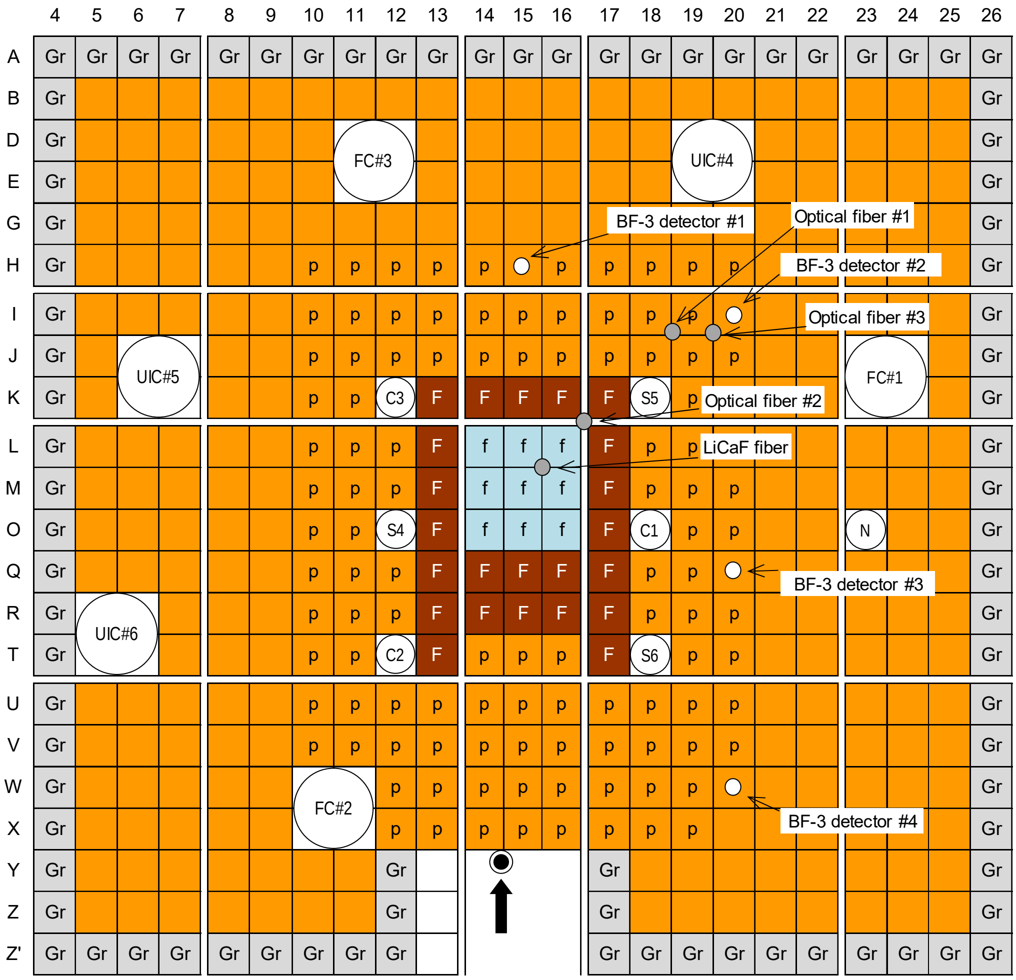

(f) Case D6 (Number of fuel plates: 3840)

Fig. 2-2 Subcritical core configurations of ADS with 14 MeV neutrons

2.2 ADS cores with 100 MeV Protons (with Pb-Bi target)

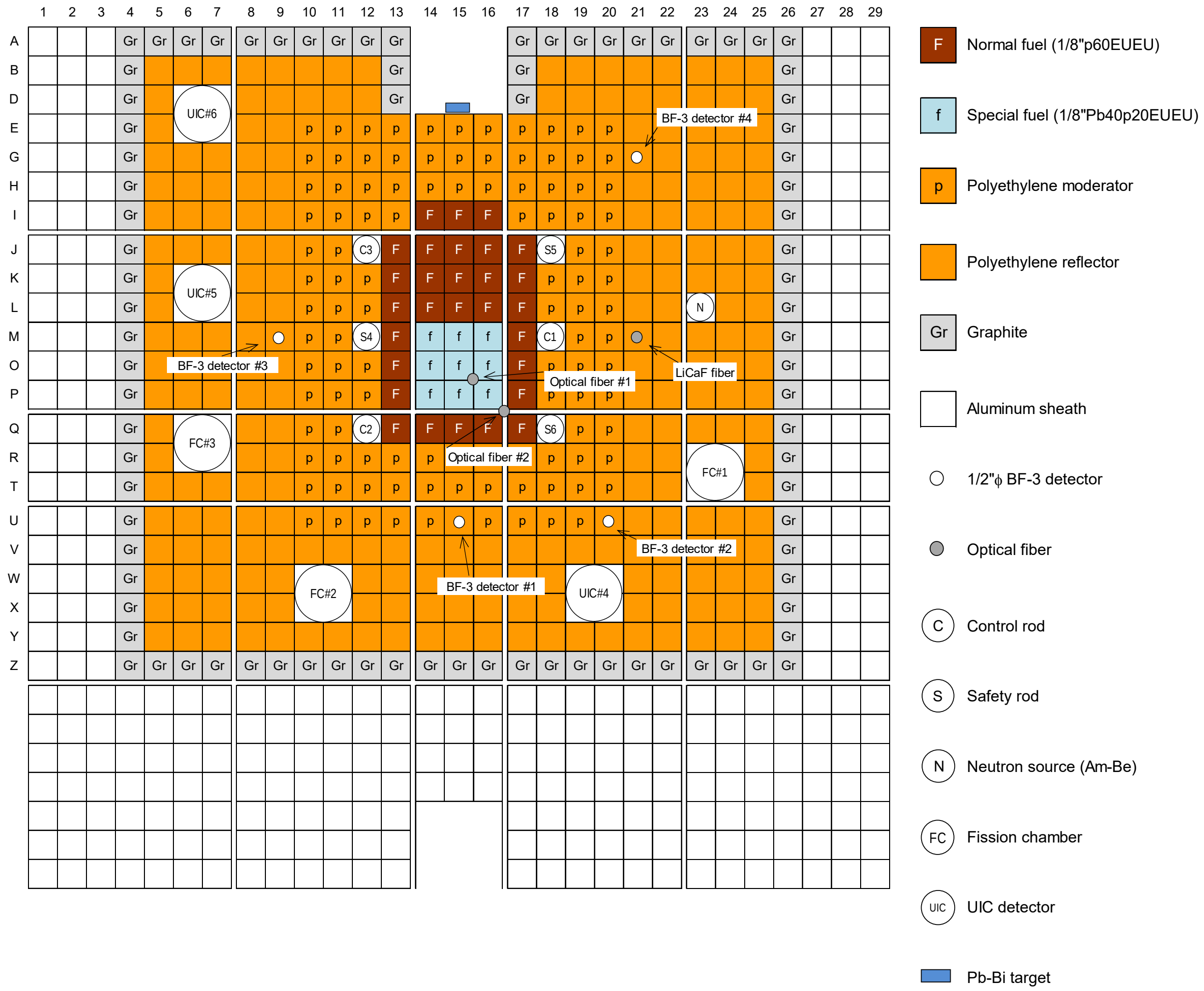

Fig. 2-3 U-Pb zoned core configuration of ADS with 100 MeV protons

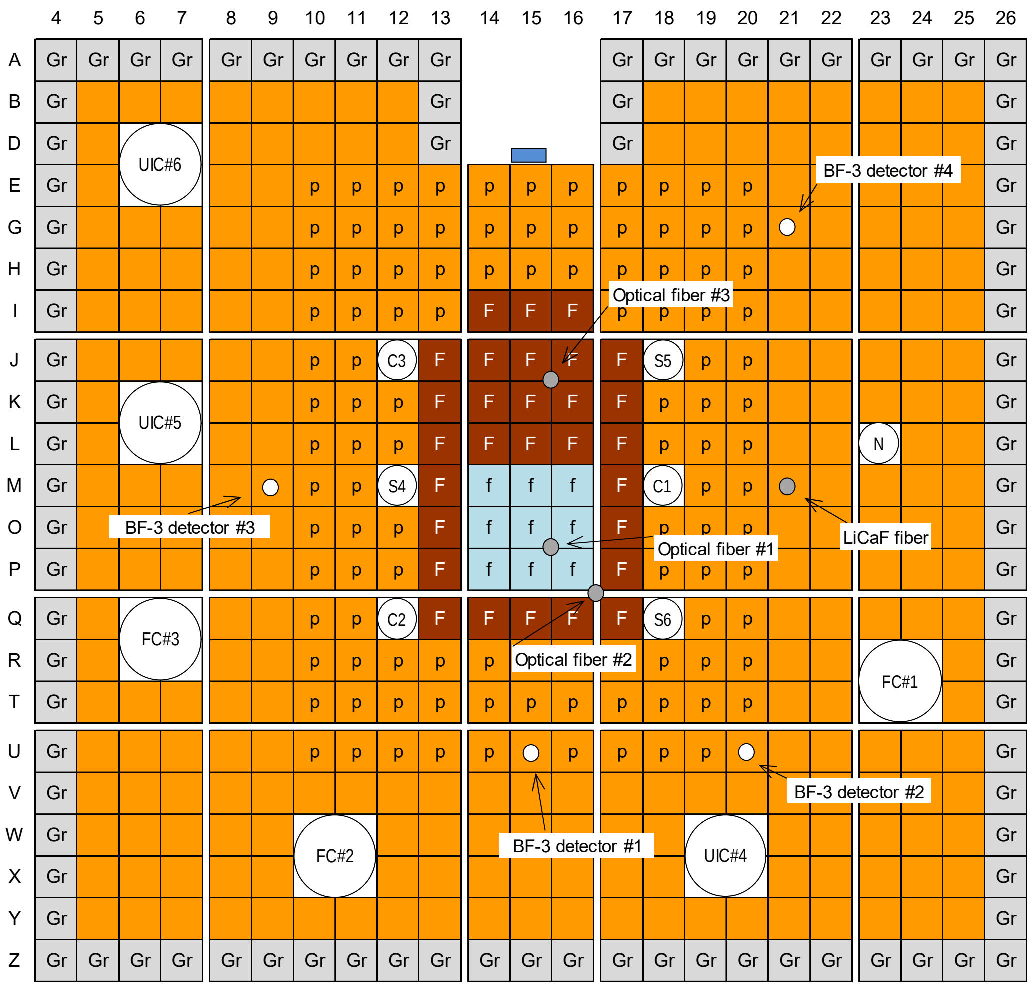

(a) Case F1 (Reference core; Number of fuel plates: 4560)

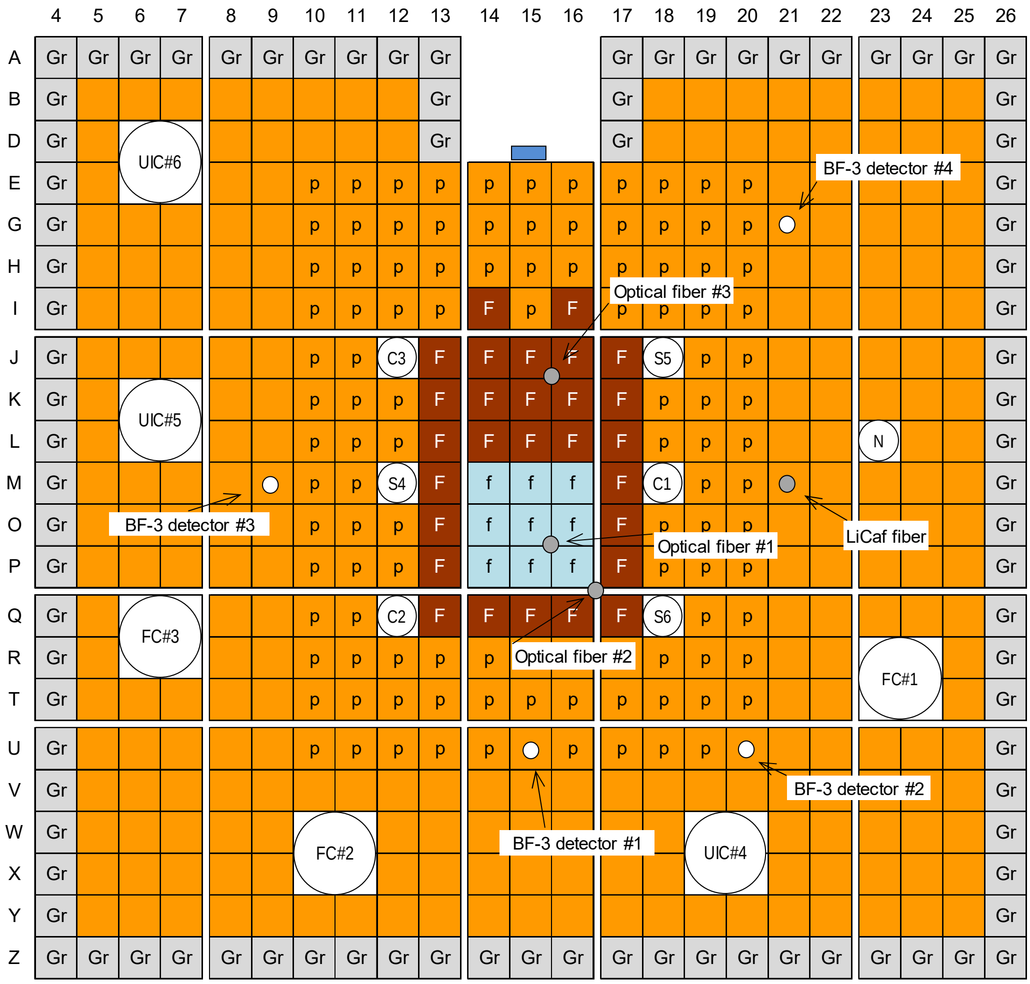

(b) Case F2 (Number of fuel plates: 4440)

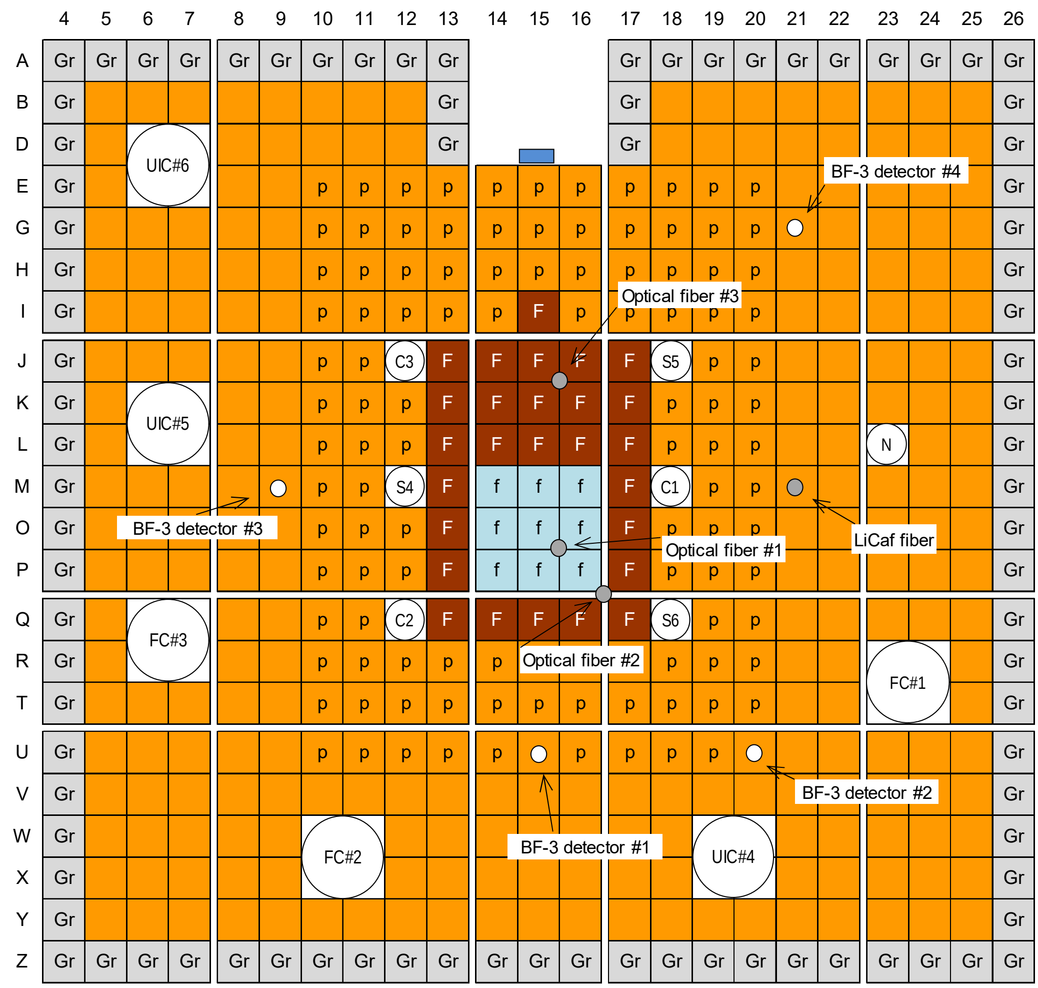

(c) Case F3 (Number of fuel plates: 4320)

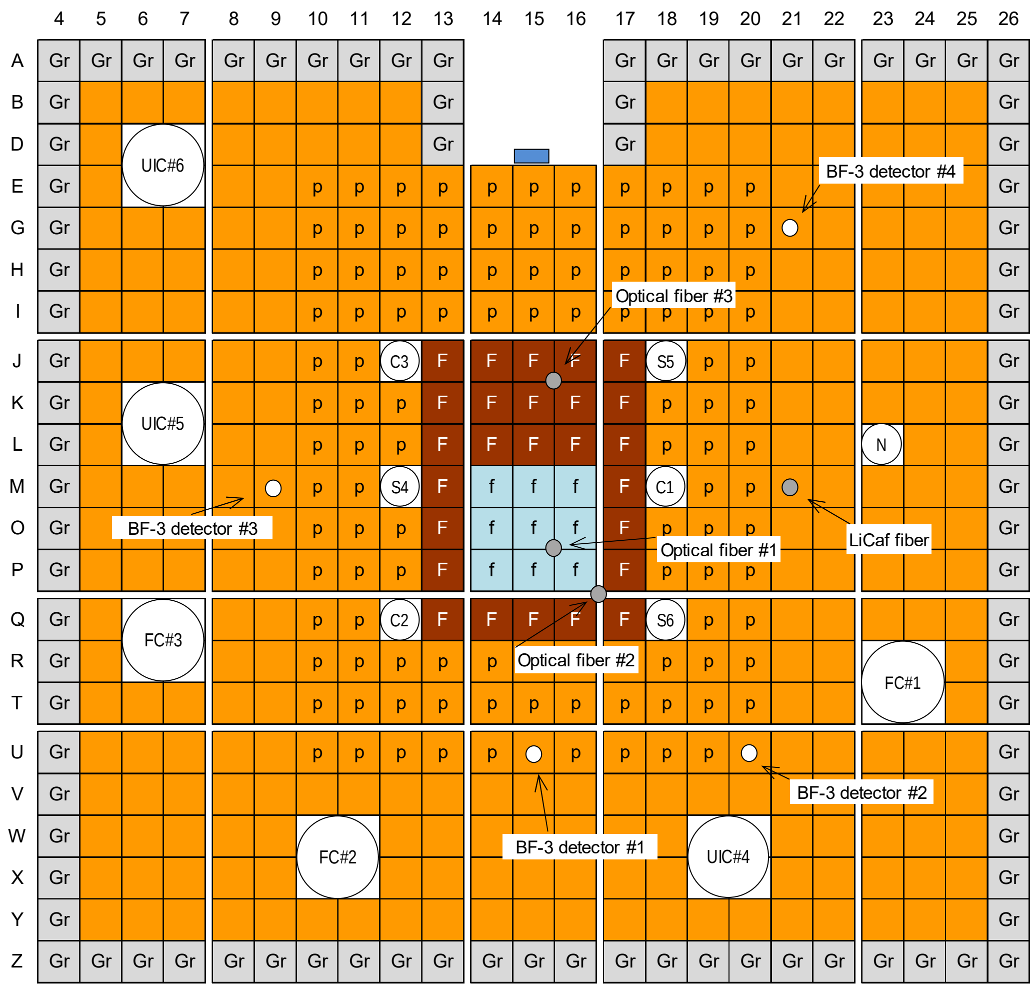

(d) Case F4 (Number of fuel plates: 4200)

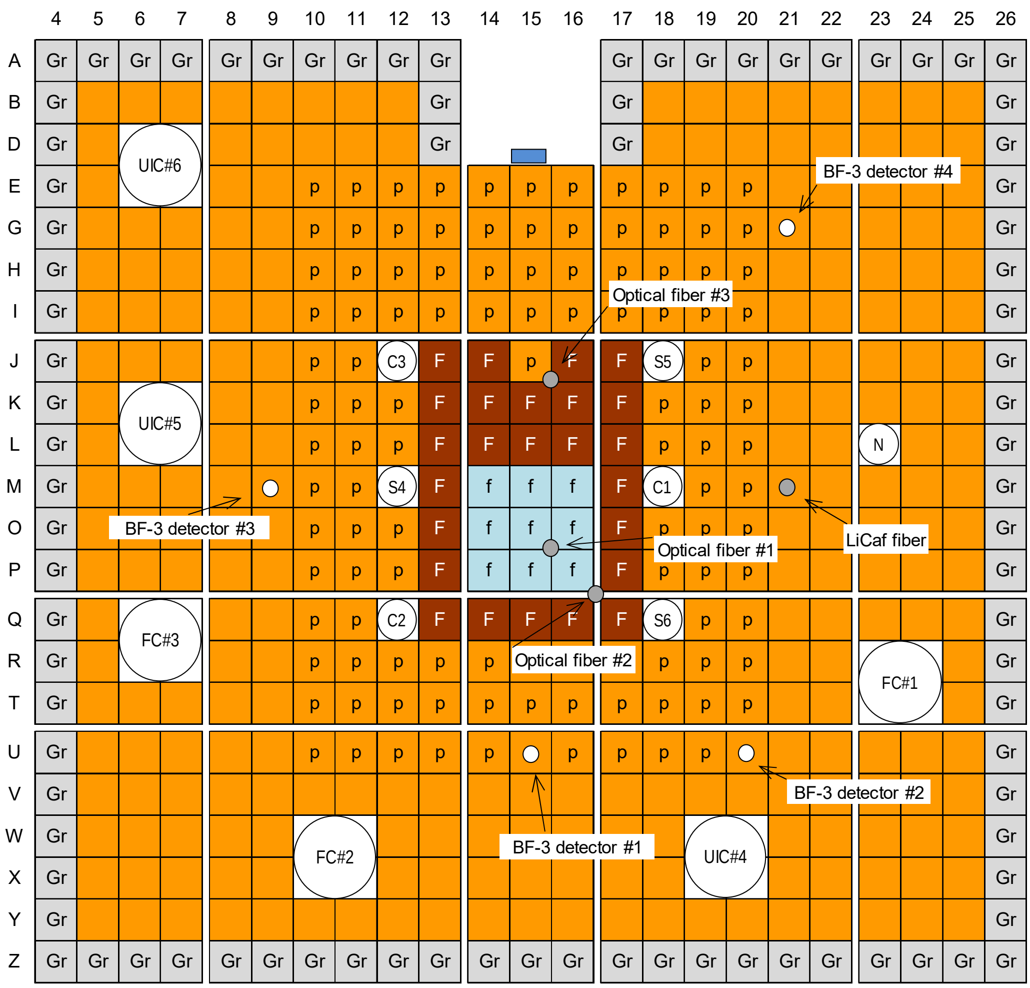

(e) Case F5 (Number of fuel plates: 4080)

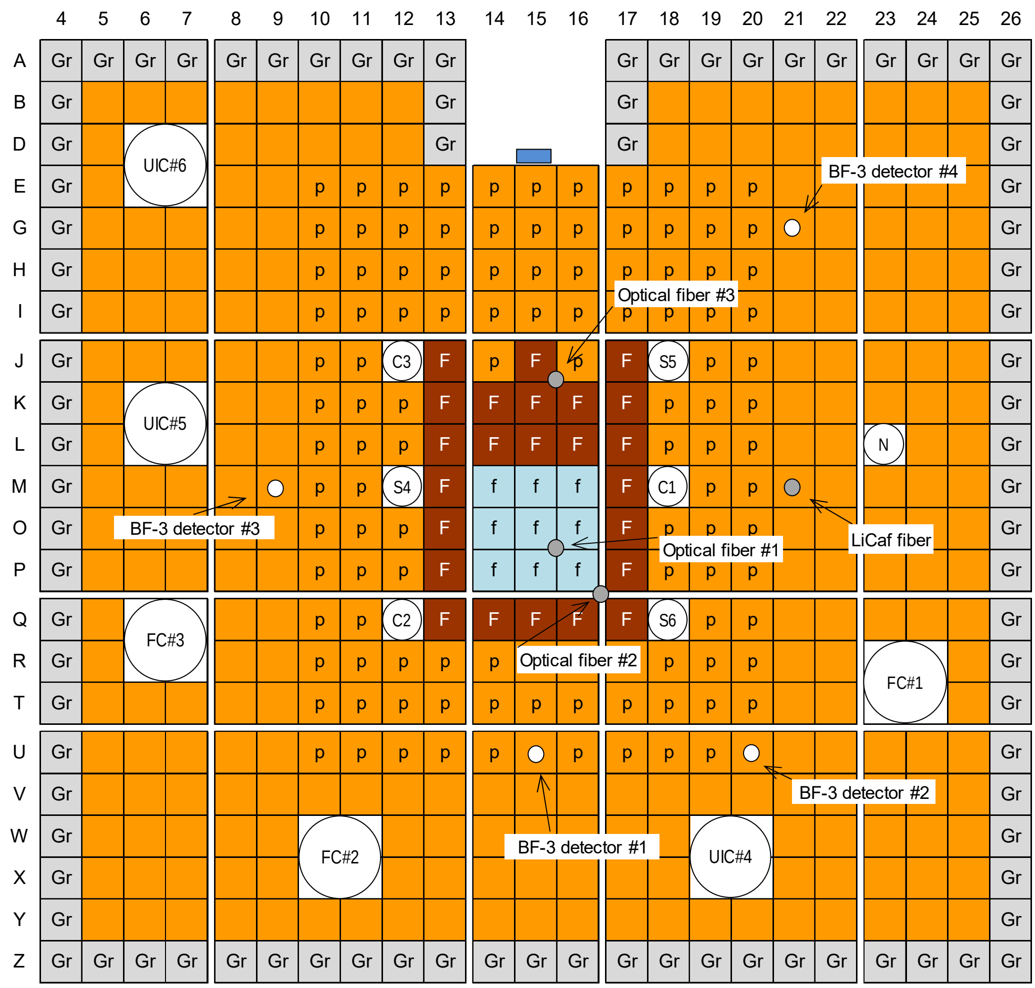

(f) Case F6 (Number of fuel plates: 3960)

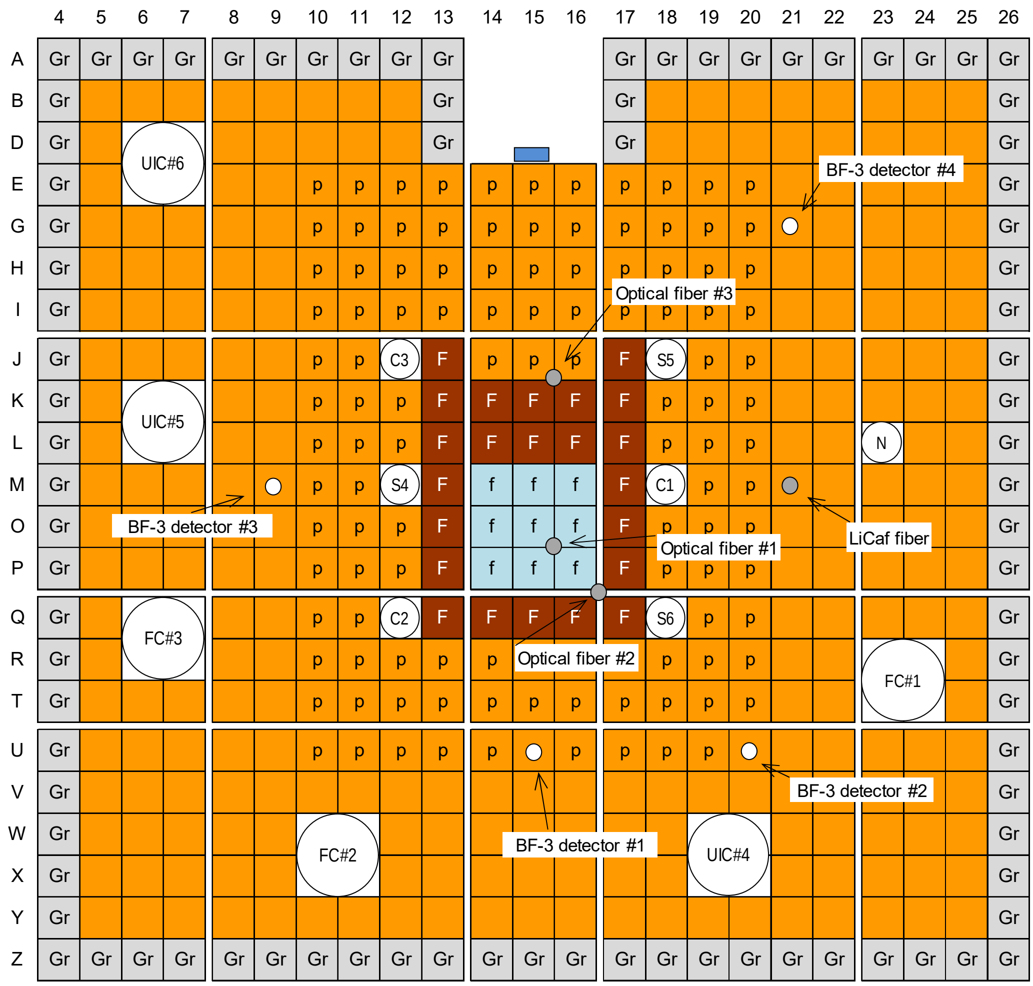

(g) Case F7 (Number of fuel plates: 3840)

Fig. 2-4 Subcritical core configurations of ADS with 100 MeV protons

3. Results of Experiments

3-1. ADS with 14 MeV Neutrons

3-1-1. Core condition at critical state (Fig. 2-1)

Table 3-1-1-1 Control rod positions at critical state in reference core (# of HEU plates: 4560; Case D1)

Rod	Rod position [mm]
C1	766.56
C2	1200.00
C3	1200.00
S4	1200.00
S5	1200.00
S6	1200.00
Excess reactivity [pcm]	80 ± 2

Table 3-1-1-2 Control rod (reactivity) worth

Rod	Rod worth [pcm]
C1 (S4)	902 ± 27
C2 (S6)	696 ± 21
C3 (S5)	232 ± 7

Table 3-1-1-3 Kinetic parameters by MCNP6.1 with JENDL-4.0

β_{eff}	853 ± 3 [pcm]
Λ	$(3.24 \pm 0.03)\times10^{-5}$ [s]

3-1-2. Case D1 (# of fuel plates: 4560 in Fig. 2-2(a))

Table 3-1-2-1 Core condition in Case D1-1 to Case D1-5 (# of fuel plates: 4560)

Case	C1	C2	C3	S4	S5	S6	k_{eff}
D1-1	0.00	1200.00	1200.00	1200.00	1200.00	1200.00	0.99178
D1-2	0.00	1200.00	1200.00	1200.00	1200.00	1200.00	0.99178
D1-3	0.00	1200.00	1200.00	1200.00	1200.00	1200.00	0.99178
D1-4	0.00	1200.00	0.00	1200.00	1200.00	1200.00	0.98947
D1-5	0.00	0.00	0.00	1200.00	1200.00	1200.00	0.98225

Table 3-1-2-2 Beam characteristics of 14 MeV neutrons in Case D1-1 to Case D1-5

Case	Frequency [Hz]	Width [μs]	Current [mA]
D1-1	20	80	0.20
D1-2	50	80	0.20
D1-3	100	80	0.20
D1-4	20	80	0.20
D1-5	20	80	0.20

Table 3-1-2-3 Measured results of α [1/s] and ρ [$] in Case D1-1

	α [1/s]		ρ [$]	
Detector	Feynman-α	α-fitting	Area (Sjostrand)	Area (Gozani)
BF-3 #1 (Ch#1)	422.96 ± 12.93	426.81 ± 28.34	0.846 ± 0.033	0.857 ± 0.120
BF-3 #2 (Ch#2)	497.90 ± 14.80	493.62 ± 31.92	0.868 ± 0.015	1.069 ± 0.119
BF-3 #3 (Ch#3)	486.88 ± 11.37	494.12 ± 21.71	0.902 ± 0.009	1.064 ± 0.079
BF-3 #4 (Ch#4)	562.18 ± 18.08	448.21 ± 53.07	0.915 ± 0.004	0.857 ± 0.141
Fiber #1 (Ch#5)	-	-	-	-
Fiber #2 (Ch#6)	-	402.58 ± 57.99	0.913 ± 0.001	0.744 ± 0.134
Fiber #3 (Ch#7)	-	-	-	-

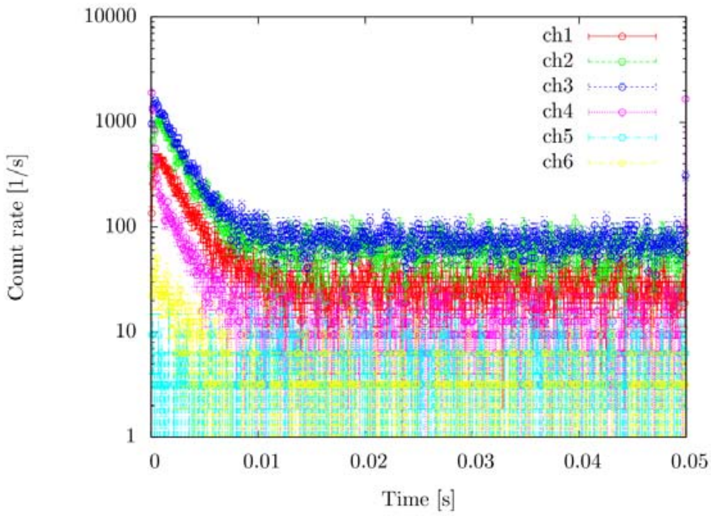

(a) PNS histogram in Case D1-1

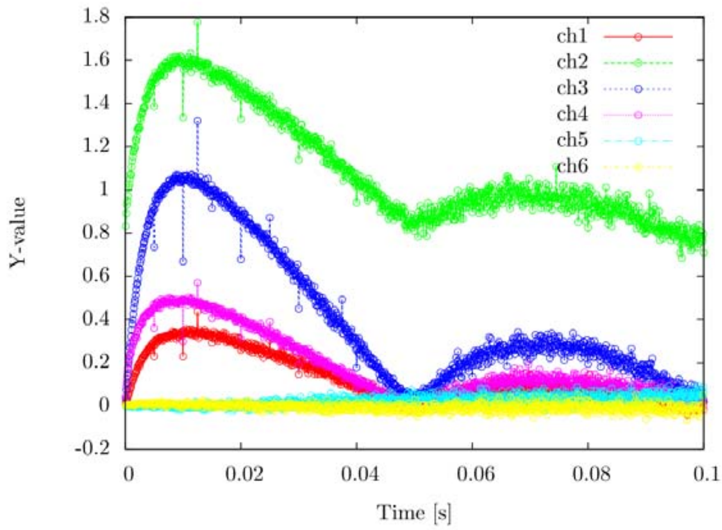

(b) Y-value distribution by Feynman-α method in Case D1-1

Fig. 3-1-2-1 Experimental resutls by PNS and Noise methods in Case D1-1

Table 3-1-2-4 Measured results of α [1/s] and ρ [$] in Case D1-2

	α [1/s]		ρ [$]	
Detector	Feynman-α	α-fitting	Area (Sjostrand)	Area (Gozani)
BF-3 #1 (Ch#1)	458.03 ± 15.40	476.24 ± 6.51	0.853 ± 0.020	1.018 ± 0.030
BF-3 #2 (Ch#2)	494.00 ± 14.20	484.22 ± 6.17	0.887 ± 0.010	1.070 ± 0.016
BF-3 #3 (Ch#3)	481.88 ± 8.95	484.81 ± 4.34	0.850 ± 0.006	0.970 ± 0.009
BF-3 #4 (Ch#4)	835.59 ± 29.96	511.58 ± 11.18	0.776 ± 0.003	0.808 ± 0.011
Fiber #1 (Ch#5)	-	-	-	-
Fiber #2 (Ch#6)	501.50 ± 146.80	384.68 ± 53.93	0.776 ± 0.003	0.704 ± 0.042
Fiber #3 (Ch#7)	-	-	-	-

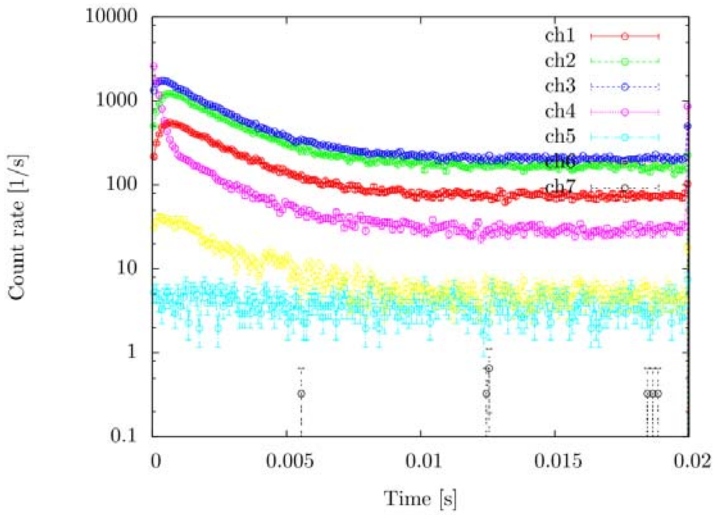

(a) PNS histogram in Case D1-2

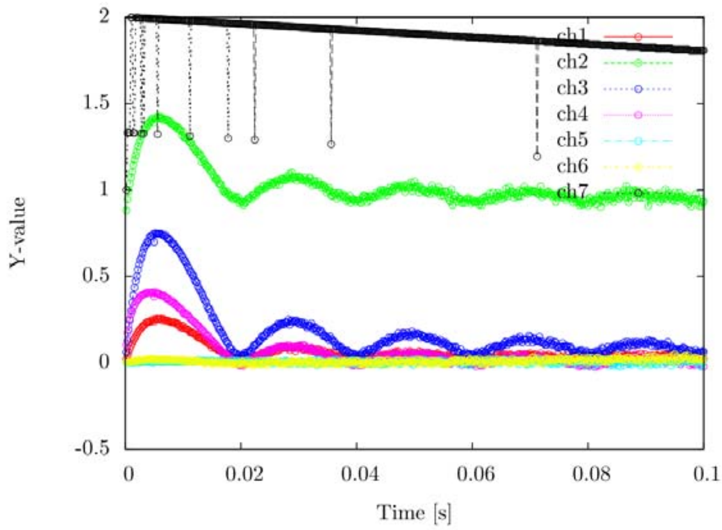

(b) Y-value distribution by Feynman-α method in Case D1-2

Fig. 3-1-2-2 Experimental resutls by PNS and Noise methods in Case D1-2

Table 3-1-2-5 Measured results of α [1/s] and ρ [$] in Case D1-3

	α [1/s]		ρ [$]	
Detector	Feynman-α	α-fitting	Area (Sjostrand)	Area (Gozani)
BF-3 #1 (Ch#1)	434.36 ± 123.56	521.50 ± 26.53	0.739 ± 0.014	0.918 ± 0.034
BF-3 #2 (Ch#2)	643.90 ± 99.97	511.42 ± 26.28	0.769 ± 0.007	0.939 ± 0.029
BF-3 #3 (Ch#3)	502.81 ± 92.37	544.23 ± 48.33	0.763 ± 0.004	0.918 ± 0.049
BF-3 #4 (Ch#4)	1639.61±131.63	677.76±359.00	0.698 ± 0.002	0.861 ±0.340
Fiber #1 (Ch#5)	-	-	-	-
Fiber #2 (Ch#6)	-	508.13 ± 88.37	0.696 ± 0.001	0.713 ± 0.069
LiCaF (Ch#7)	538.30 ± 16.81	-	0.604 ± 0.002	0.632 ± 0.012

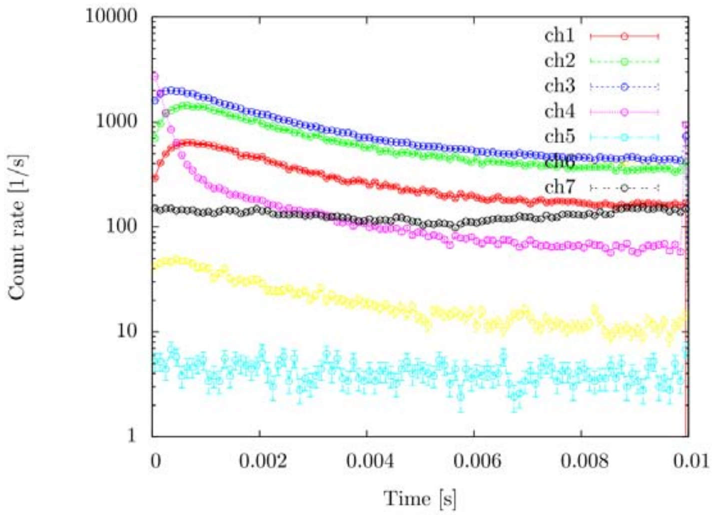

(a) PNS histogram in Case D1-3

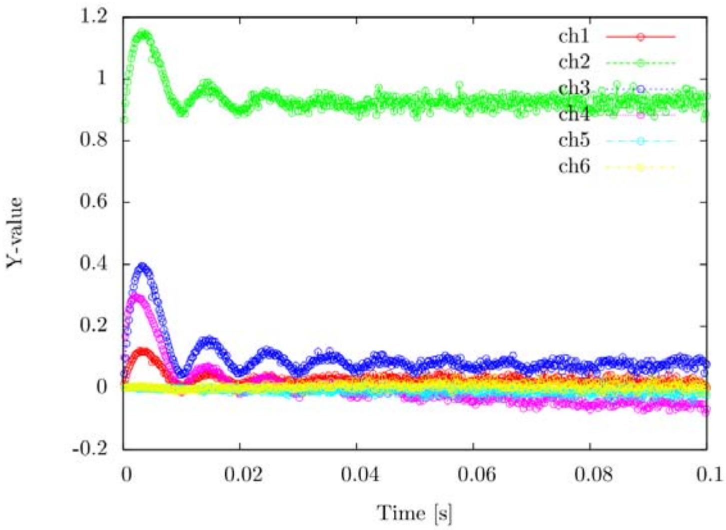

(b) Y-value distribution by Feynman-α method in Case D1-3

Fig. 3-1-2-3 Experimental resutls by PNS and Noise methods in Case D1-3

Table 3-1-2-6 Measured results of α [1/s] and ρ [$] in Case D1-4

	α [1/s]		ρ [$]	
Detector	Feynman-α	α-fitting	Area (Sjostrand)	Area (Gozani)
BF-3 #1 (Ch#1)	565.29 ± 4.61	568.41 ± 9.41	1.118 ± 0.012	1.400 ± 0.024
BF-3 #2 (Ch#2)	589.68 ± 5.40	559.85 ± 9.51	1.130 ± 0.006	1.403 ± 0.018
BF-3 #3 (Ch#3)	555.32 ± 2.11	570.25 ± 9.56	1.158 ± 0.013	1.306 ± 0.024
BF-3 #4 (Ch#4)	-	514.20 ± 21.79	1.212 ± 0.005	1.076 ± 0.027
Fiber #1 (Ch#5)	-	-	-	-
Fiber #2 (Ch#6)	490.46 ± 41.67	521.64 ± 35.67	1.049 ± 0.001	1.245 ± 0.049
LiCaF (Ch#7)	1023.42±277.51	-	1.022 ± 0.001	2.107 ± 0.643

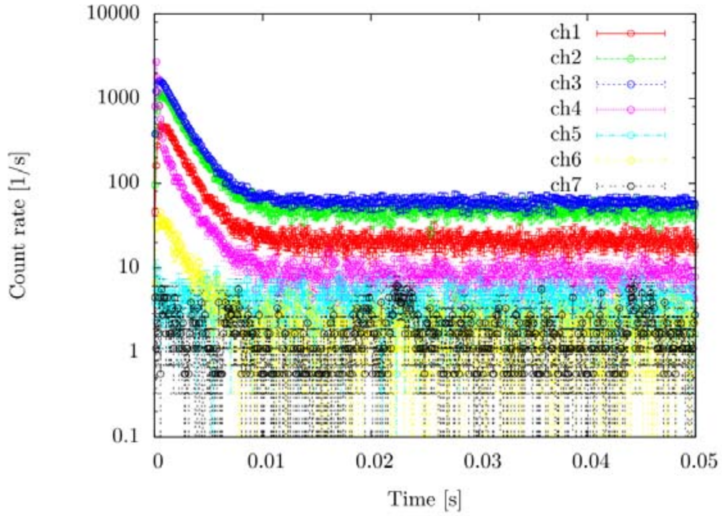

(a) PNS histogram in Case D1-4

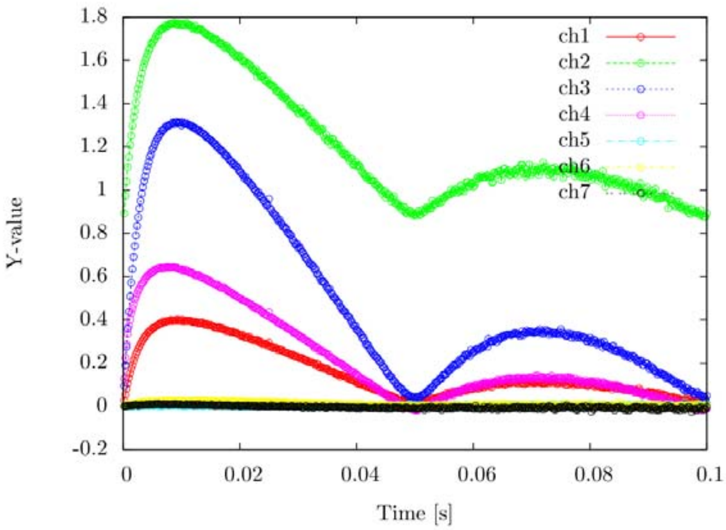

(b) Y-value distribution by Feynman-α method in Case D1-4

Fig. 3-1-2-4 Experimental resutls by PNS and Noise methods in Case D1-4

Table 3-1-2-7 Measured results of α [1/s] and ρ [$] in Case D1-5

	α [1/s]		ρ [$]	
Detector	Feynman-α	α-fitting	Area (Sjostrand)	Area (Gozani)
BF-3 #1 (Ch#1)	498.46 ± 7.46	480.22 ± 5.36	0.899 ± 0.018	1.090 ± 0.028
BF-3 #2 (Ch#2)	489.43 ± 6.55	483.02 ± 5.09	0.887 ± 0.008	1.068 ± 0.014
BF-3 #3 (Ch#3)	488.59 ± 3.46	483.93 ± 3.76	0.890 ± 0.005	1.024 ± 0.009
BF-3 #4 (Ch#4)	-	497.04 ± 9.23	0.891 ± 0.002	0.951 ± 0.010
Fiber #1 (Ch#5)	-	-	-	-
Fiber #2 (Ch#6)	541.11 ± 127.67	709.57 ± 185.61	0.872 ± 0.001	1.181 ± 0.241
LiCaF (Ch#7)	-	-	-	-

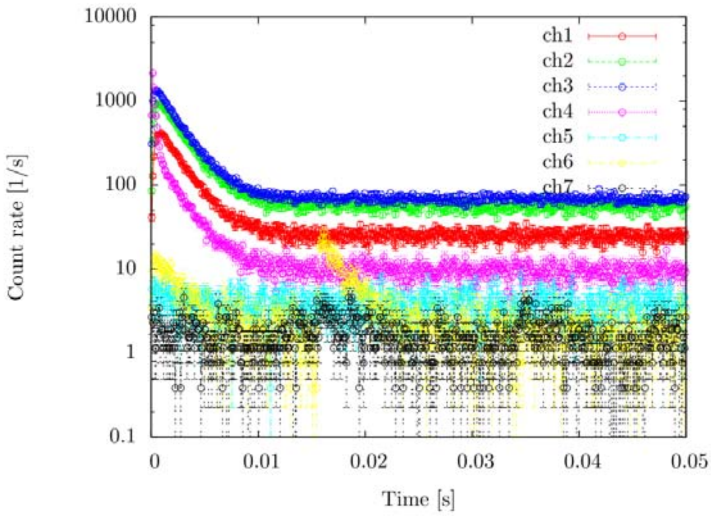

(a) PNS histogram in Case D1-5

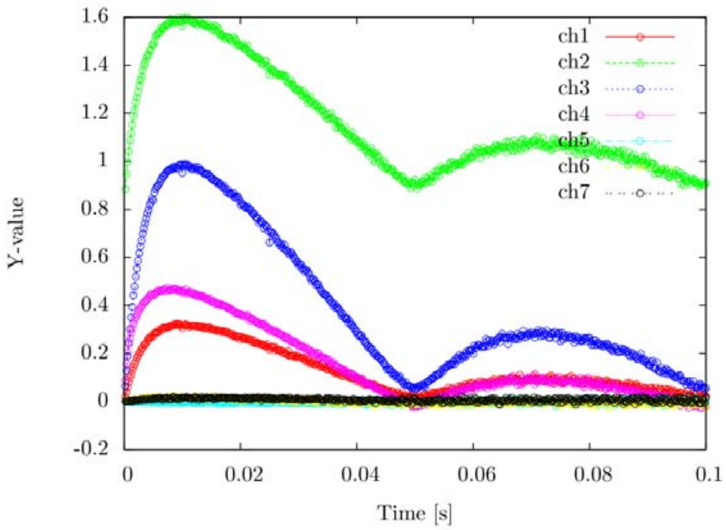

(b) Y-value distribution by Feynman-α method in Case D1-5

Fig. 3-1-2-5 Experimental resutls by PNS and Noise methods in Case D1-5

3-1-3. Case D2 (# of fuel plates: 4400 in Fig. 2-2(b))

Table 3-1-3-1 Core condition in Case D2-1 to Case D2-3 (# of fuel plates: 4400)

Case	C1	C2	C3	S4	S5	S6	k_{eff}
D2-1	1200.00	1200.00	1200.00	1200.00	1200.00	1200.00	0.99328
D2-2	1200.00	1200.00	1200.00	1200.00	1200.00	1200.00	0.99328
D2-3	1200.00	1200.00	1200.00	1200.00	1200.00	1200.00	0.99328

Table 3-1-3-2 Beam characteristics of 14 MeV neutrons in Case D2-1 to Case D2-3

Case	Frequency [Hz]	Width [μs]	Current [mA]
D2-1	20	75	0.10
D2-2	50	80	0.20
D2-3	100	80	0.15

Table 3-1-3-3 Measured results of α [1/s] and ρ [$] in Case D2-1

	α [1/s]		ρ [$]	
Detector	Feynman-α	α-fitting	Area (Sjostrand)	Area (Gozani)
BF-3 #1 (Ch#1)	376.67 ± 8.46	370.33 ± 4.94	0.565 ± 0.010	0.652 ± 0.014
BF-3 #2 (Ch#2)	389.96 ± 7.21	370.56 ± 4.21	0.578 ± 0.004	0.665 ± 0.007
BF-3 #3 (Ch#3)	370.68 ± 2.88	369.87 ± 2.84	0.587 ± 0.003	0.437 ± 0.002
BF-3 #4 (Ch#4)	501.71 ± 11.71	376.97 ± 8.13	0.612 ± 0.001	0.647 ± 0.006
Fiber #1 (Ch#5)	-	-	0.585 ± 0.001	-
Fiber #2 (Ch#6)	703.56 ± 71.90	-	0.570 ± 0.001	0.861 ± 0.068
Fiber #3 (Ch#7)	-	-	-	-

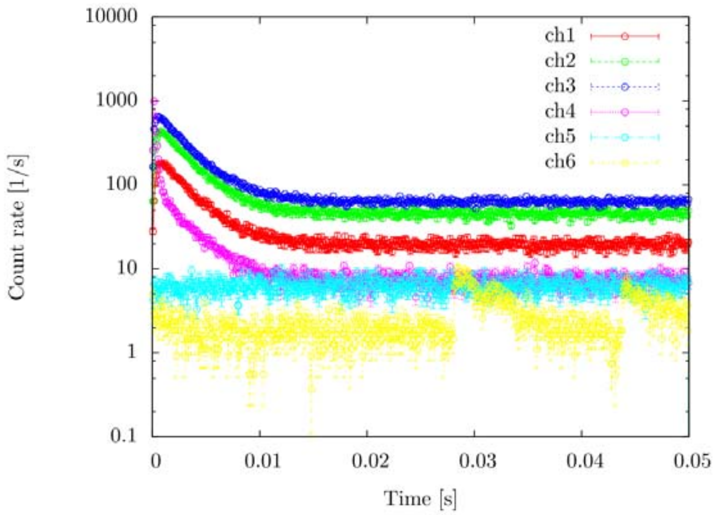

(a) PNS histogram in Case D2-1

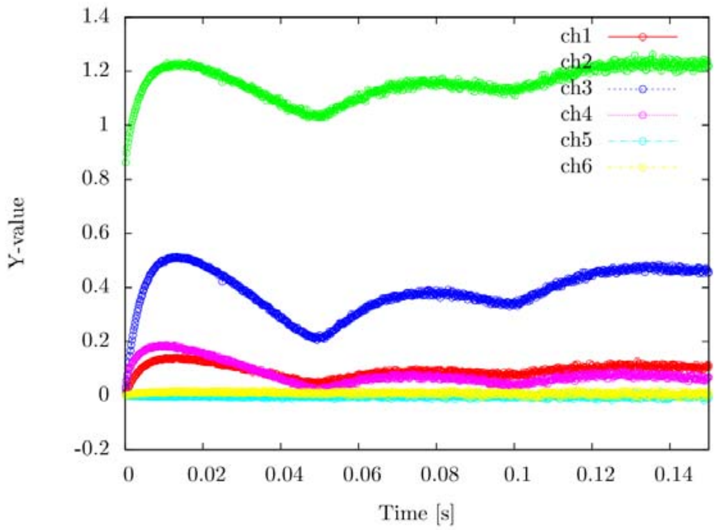

(b) Y-value distribution by Feynman-α method in Case D2-1

Fig. 3-1-3-1 Experimental resutls by PNS and Noise methods in Case D2-1

Table 3-1-3-4 Measured results of α [1/s] and ρ [$] in Case D2-2

	α [1/s]		ρ [$]	
Detector	Feynman-α	α-fitting	Area (Sjostrand)	Area (Gozani)
BF-3 #1 (Ch#1)	370.30 ± 15.26	378.35 ± 5.69	0.589 ± 0.006	0.691 ± 0.009
BF-3 #2 (Ch#2)	431.86 ± 12.01	376.62 ± 4.97	0.582 ± 0.003	0.676 ± 0.005
BF-3 #3 (Ch#3)	367.38 ± 7.31	369.18 ± 3.58	0.595 ± 0.002	0.666 ± 0.003
BF-3 #4 (Ch#4)	-	365.64 ± 12.33	0.637 ± 0.001	0.689 ± 0.009
Fiber #1 (Ch#5)	-	-	0.630 ± 0.001	0.455 ± 0.001
Fiber #2 (Ch#6)	-	386.76 ± 22.42	0.629 ± 0.001	0.696 ± 0.017
Fiber #3 (Ch#7)	-	-	-	-

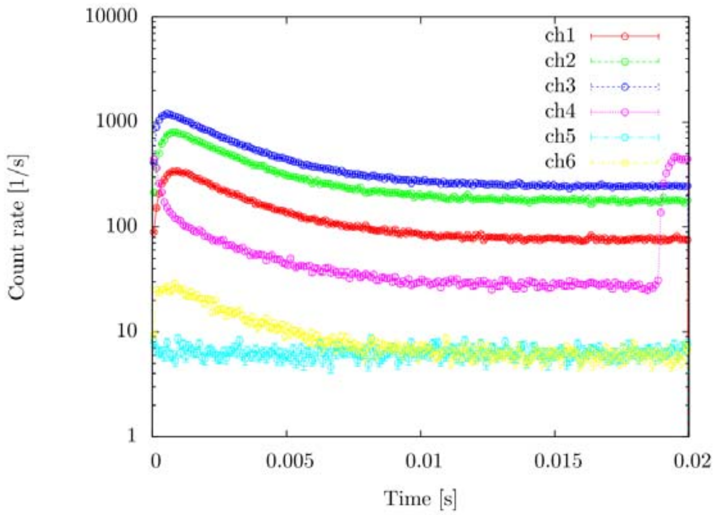

(a) PNS histogram in Case D2-2

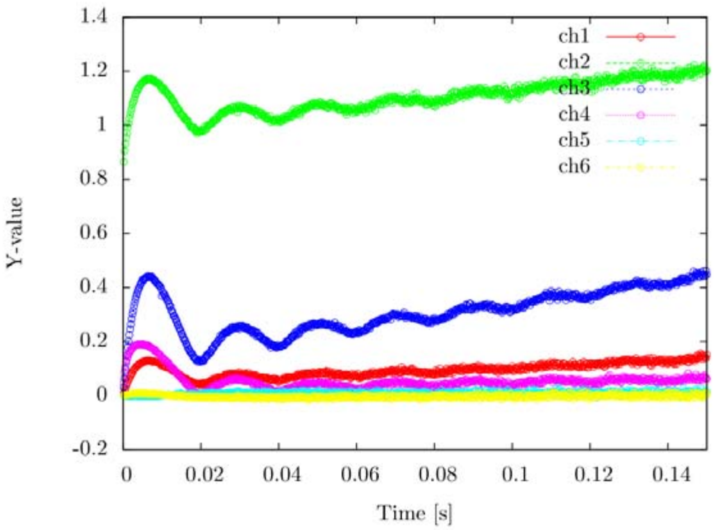

(b) Y-value distribution by Feynman-α method in Case D2-2

Fig. 3-1-3-2　Experimental resutls by PNS and Noise methods in Case D2-2

Table 3-1-3-5 Measured results of α [1/s] and ρ [$] in Case D2-3

	α [1/s]		ρ [$]	
Detector	Feynman-α	α-fitting	Area (Sjostrand)	Area (Gozani)
BF-3 #1 (Ch#1)	249.68 ± 154.15	367.36 ± 9.62	0.484 ± 0.009	0.550 ± 0.014
BF-3 #2 (Ch#2)	789.84 ± 57.23	359.50 ± 8.38	0.479 ± 0.004	0.536 ± 0.007
BF-3 #3 (Ch#3)	384.44 ± 37.91	372.34 ± 4.49	0.466 ± 0.003	0.506 ± 0.004
BF-3 #4 (Ch#4)	-	398.44 ± 15.90	0.507 ± 0.001	0.558 ± 0.010
Fiber #1 (Ch#5)	-	-	0.504 ± 0.001	0.358 ± 0.0001
Fiber #2 (Ch#6)	-	384.18 ± 29.34	0.503 ± 0.001	0.546 ± 0.018
Fiber #3 (Ch#7)	-	-	-	-

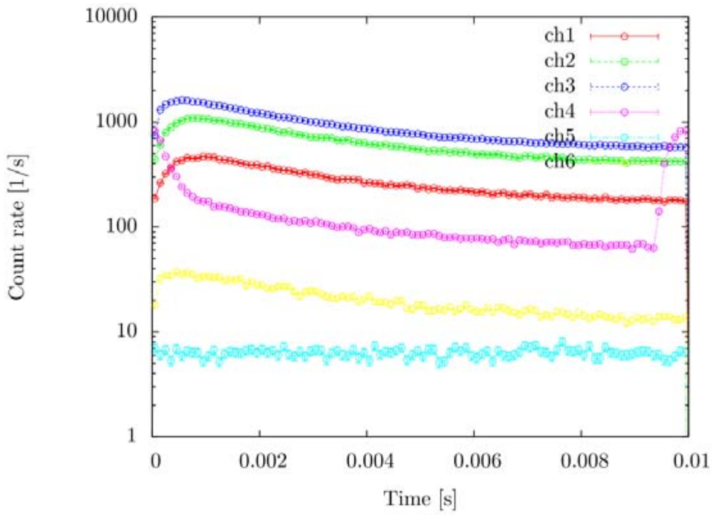

(a) PNS histogram in Case D2-3

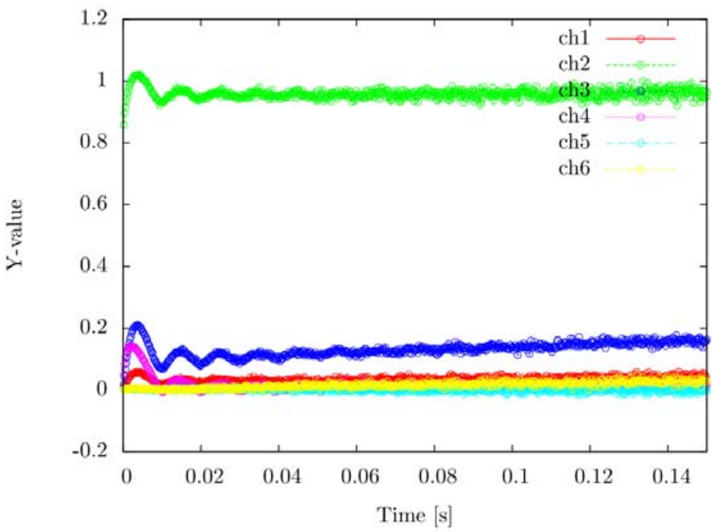

(b) Y-value distribution by Feynman-α method in Case D2-3

Fig. 3-1-3-3 Experimental resutls by PNS and Noise methods in Case D2-3

3-1-4. Case D3 (# of fuel plates: 4320 in Fig. 2-2(c))

Table 3-1-4-1 Core condition in Case D3-1 (# of fuel plates: 4320)

Case	C1	C2	C3	S4	S5	S6	k_{eff}
D3-1	1200.00	1200.00	1200.00	1200.00	1200.00	1200.00	0.98004

Table 3-1-4-2 Beam characteristics of 14 MeV neutrons in Case D3-1

Case	Frequency [Hz]	Width [μs]	Current [mA]
D3-1	20	80	0.20

Table 3-1-4-3 Measured results of α [1/s] and ρ [$] in Case D3-1

	α [1/s]		ρ [$]	
Detector	Feynman-α	α-fitting	Area (Sjostrand)	Area (Gozani)
BF-3 #1 (Ch#1)	669.23 ± 5.43	678.46 ± 4.75	1.911 ± 0.024	2.589 ± 0.041
BF-3 #2 (Ch#2)	693.11 ± 4.60	681.85 ± 4.28	1.880 ± 0.011	2.610 ± 0.022
BF-3 #3 (Ch#3)	684.25 ± 1.93	686.16 ± 2.50	1.972 ± 0.007	2.663 ± 0.013
BF-3 #4 (Ch#4)	1296.59 ± 35.04	715.47 ± 9.24	2.244 ± 0.002	2.757 ± 0.028
Fiber #1 (Ch#5)	-	-	-	-
Fiber #2 (Ch#6)	703.56 ± 71.90	-	1.916 ± 0.001	2.323 ± 0.184
LiCaF (Ch#7)	-	-	-	-

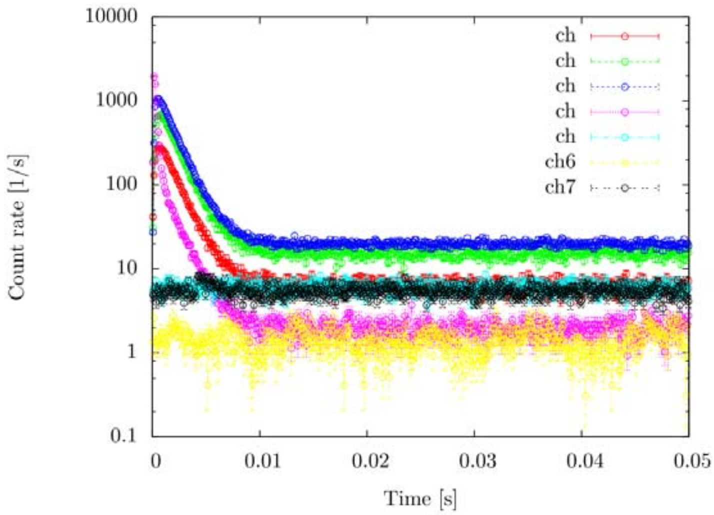

(a) PNS histogram in Case D3-1

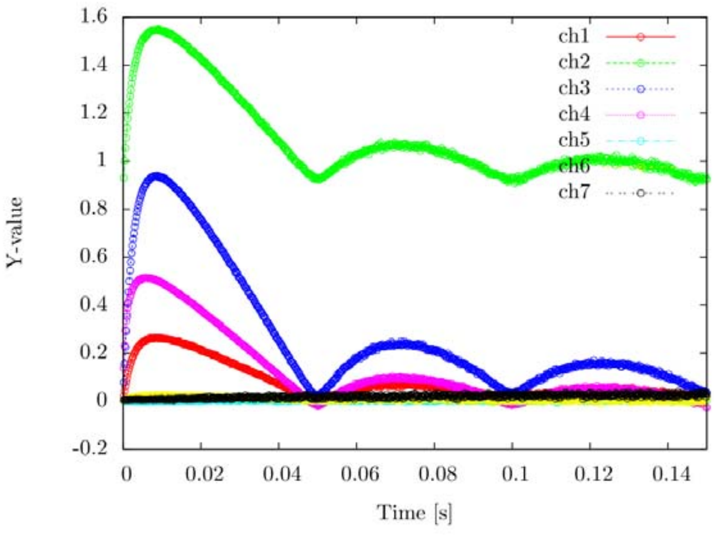

(b) Y-value distribution by Feynman-α method in Case D3-1

Fig. 3-1-4-1 Experimental resutls by PNS and Noise methods in Case D3-1

3-1-4. Case D4 (# of fuel plates: 4200 in Fig. 2-2(d))

Table 3-1-4-1 Core condition in Case D4-1 (# of fuel plates: 4200)

Case	C1	C2	C3	S4	S5	S6	k_{eff}
D4-1	1200.00	1200.00	1200.00	1200.00	1200.00	1200.00	0.96603

Table 3-1-4-2 Beam characteristics of 14 MeV neutrons in Case D4-1 and Case D4-2

Case	Frequency [Hz]	Width [μs]	Current [mA]
D4-1	10	80	0.20

Table 3-1-4-3 Measured results of α [1/s] and ρ [$] in Case D4-1

	α [1/s]		ρ [$]	
Detector	Feynman-α	α-fitting	Area (Sjostrand)	Area (Gozani)
BF-3 #1 (Ch#1)	878.01 ± 26.55	969.40 ± 33.08	2.687 ± 0.116	3.618 ± 0.242
BF-3 #2 (Ch#2)	979.74 ± 27.61	970.87 ± 26.68	2.785 ± 0.055	3.789 ± 0.147
BF-3 #3 (Ch#3)	997.15 ± 13.85	1045.50 ± 14.28	2.843 ± 0.034	3.793 ± 0.084
BF-3 #4 (Ch#4)	2345.71 ± 86.12	1265.82 ± 92.59	2.924 ± 0.019	3.929 ± 0.402
Fiber #1 (Ch#5)	-	-	-	-
Fiber #2 (Ch#6)	-	-	-	-
LiCaF (Ch#7)	-	-	-	-

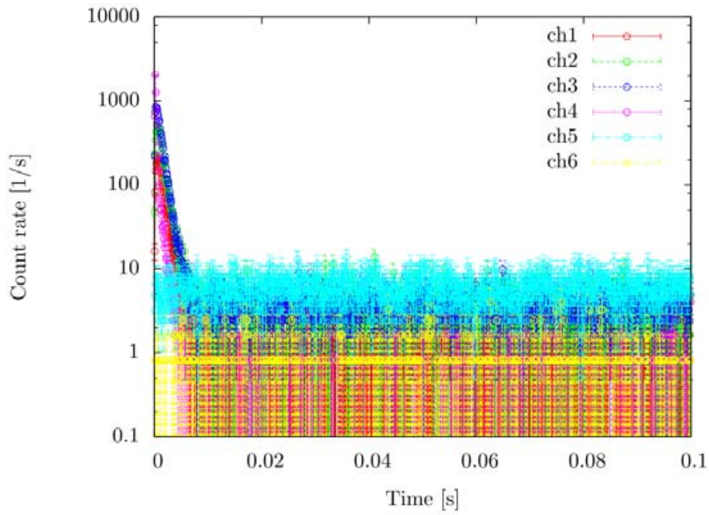

(a) PNS histogram in Case D4-1

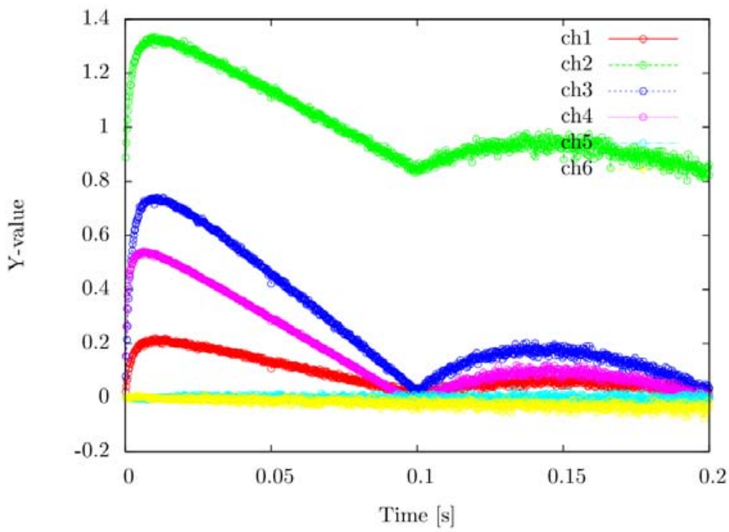

(b) Y-value distribution by Feynman-α method in Case D4-1

Fig. 3-1-4-1 Experimental resutls by PNS and Noise methods in Case D4-1

3-1-5. Case D5 (# of fuel plates: 4080 in Fig. 2-2(e))

Table 3-1-5-1 Core condition in Case D5-1 to Case D5-3 (# of fuel plates: 4080)

Case	C1	C2	C3	S4	S5	S6	k_{eff}
D5-1	1200.00	1200.00	1200.00	1200.00	1200.00	1200.00	0.95560
D5-2	1200.00	1200.00	1200.00	1200.00	1200.00	1200.00	0.95560
D5-3	1200.00	1200.00	1200.00	1200.00	1200.00	1200.00	0.95560

Table 3-1-5-2 Beam characteristics of 14 MeV neutrons in Case D5-1 to Case D5-3

Case	Frequency [Hz]	Width [μs]	Current [mA]
D5-1	20	90	0.20
D5-2	50	90	0.20
D5-3	100	90	0.20

Table 3-1-5-3 Measured results of α [1/s] and ρ [$] in Case D5-1

	α [1/s]		ρ [$]	
Detector	Feynman-α	α-fitting	Area (Sjostrand)	Area (Gozani)
BF-3 #1 (Ch#1)	1143.72 ± 17.67	1150.34 ± 15.00	3.641 ± 0.084	5.436 ± 0.178
BF-3 #2 (Ch#2)	1203.76 ± 15.21	1148.70 ± 13.09	3.642 ± 0.038	5.329 ± 0.103
BF-3 #3 (Ch#3)	1188.02 ± 6.15	1186.95 ± 9.38	3.608 ± 0.023	4.849 ± 0.064
BF-3 #4 (Ch#4)	2957.04 ± 86.78	1291.39 ± 30.21	2.618 ± 0.012	2.543 ± 0.087
Fiber #1 (Ch#5)	-	-	1.948 ± 0.006	0.457 ± 0.003
Fiber #2 (Ch#6)	-	-	1.900 ± 0.002	0.449 ± 0.001
Fiber #3 (Ch#7)	-	-	-	-

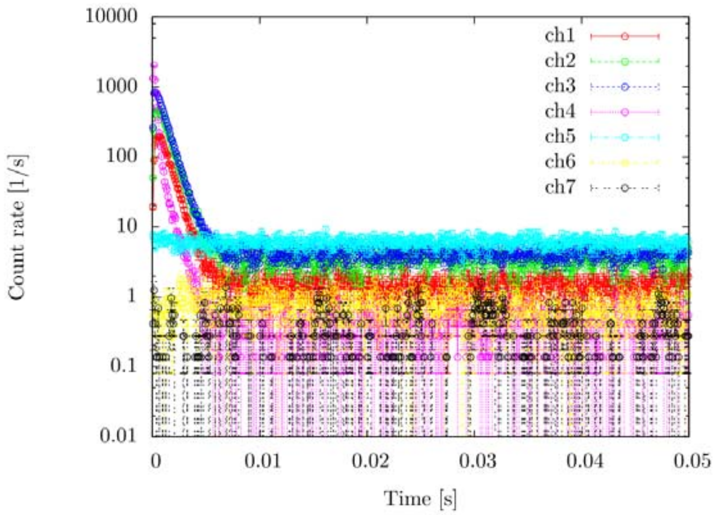

(a) PNS histogram in Case D5-1

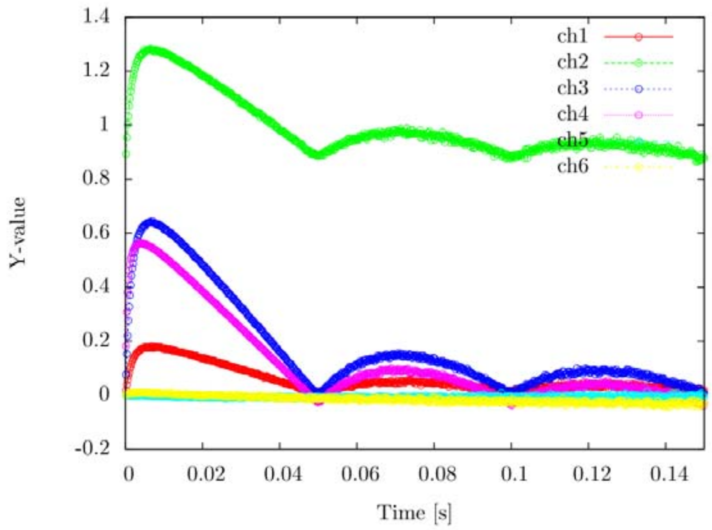

(b) Y-value distribution by Feynman-α method in Case D5-1

Fig. 3-1-5-1　Experimental resutls by PNS and Noise methods in Case D5-1

Table 3-1-5-4 Measured results of α [1/s] and ρ [$] in Case D5-2

	α [1/s]		ρ [$]	
Detector	Feynman-α	α-fitting	Area (Sjostrand)	Area (Gozani)
BF-3 #1 (Ch#1)	1093.68 ± 23.47	1167.71 ± 14.40	3.957 ± 0.093	6.047 ± 0.192
BF-3 #2 (Ch#2)	1193.46 ± 17.93	1162.44 ± 12.44	4.073 ± 0.044	6.133 ± 0.114
BF-3 #3 (Ch#3)	1138.36 ± 8.72	1185.21 ± 9.52	3.596 ± 0.024	4.733 ± 0.063
BF-3 #4 (Ch#4)	-	1337.28 ± 29.46	2.558 ± 0.011	2.303 ± 0.077
Fiber #1 (Ch#5)	-	-	2.260 ± 0.005	-
Fiber #2 (Ch#6)	823.99 ± 179.48	-	2.187 ± 0.003	0.451 ± 0.001
Fiber #3 (Ch#7)	-	-	-	-

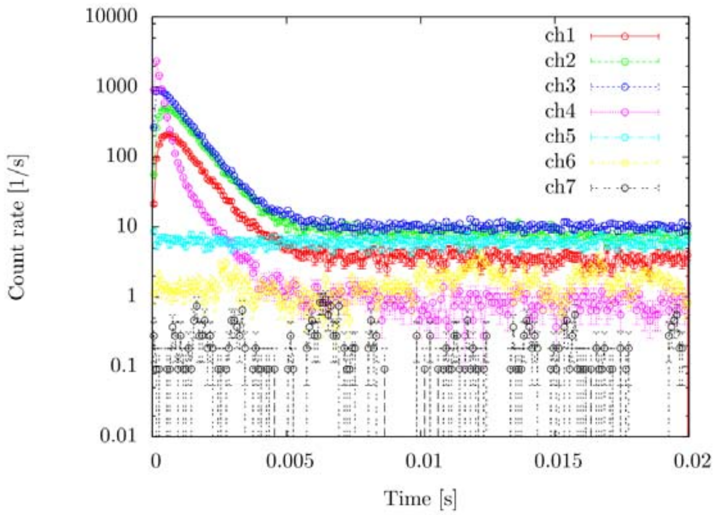

(a) PNS histogram in Case D5-2

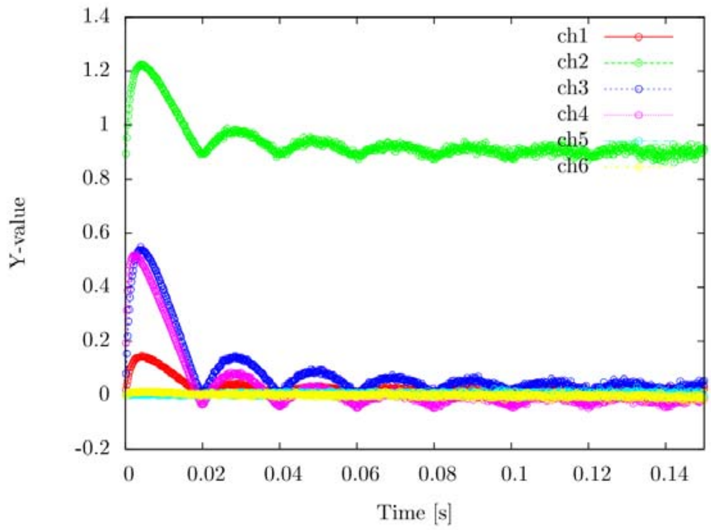

(b) Y-value distribution by Feynman-α method in Case D5-2

Fig. 3-1-5-2 Experimental resutls by PNS and Noise methods in Case D5-2

Table 3-1-5-5 Measured results of α [1/s] and ρ [$] in Case D5-3.

	α [1/s]		ρ [$]	
Detector	Feynman-α	α-fitting	Area (Sjostrand)	Area (Gozani)
BF-3 #1 (Ch#1)	959.79 ± 48.45	1160.10 ± 17.13	2.710 ± 0.123	3.766 ± 0.224
BF-3 #2 (Ch#2)	1215.05 ± 44.44	1166.86 ± 14.88	2.585 ± 0.053	3.460 ± 0.108
BF-3 #3 (Ch#3)	1105.17 ± 16.49	1174.34 ± 10.96	1.493 ± 0.020	1.086 ± 0.040
BF-3 #4 (Ch#4)	3583.95±186.81	1352.44 ± 42.55	0.333 ± 0.007	-
Fiber #1 (Ch#5)	-	-	0.324 ± 0.001	-
Fiber #2 (Ch#6)	-	1157.06 ± 80.98	0.328 ± 0.001	-
Fiber #3 (Ch#7)	-	-	-	-

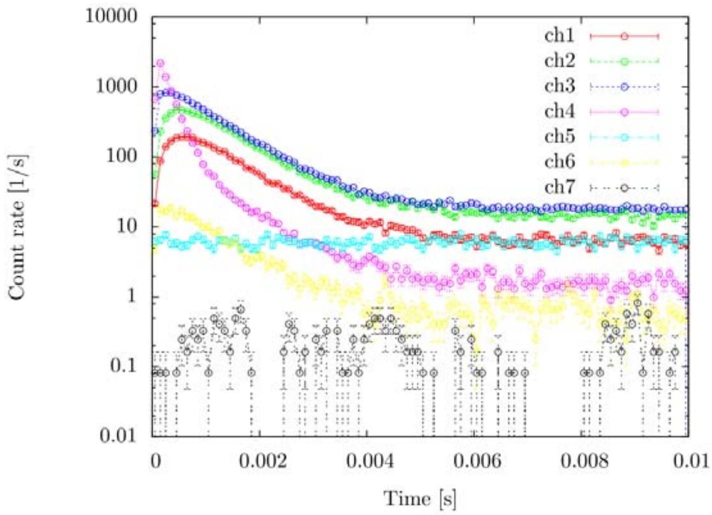

(a) PNS histogram in Case D5-3

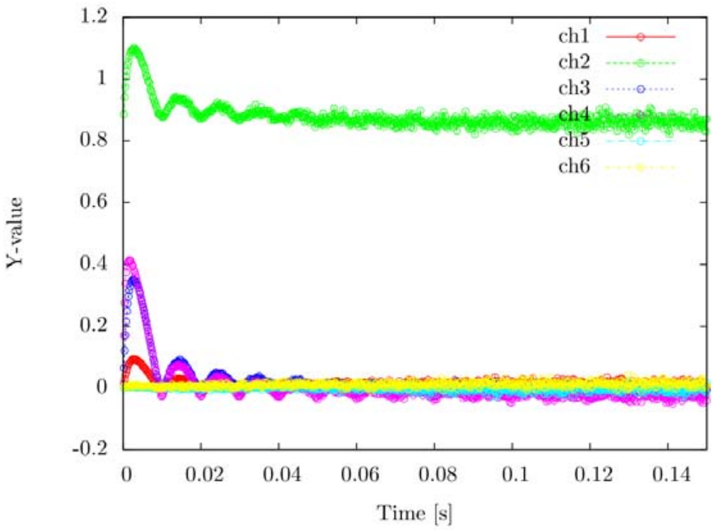

(b) Y-value distribution by Feynman-α method in Case D5-3

Fig. 3-1-5-3 Experimental resutls by PNS and Noise methods in Case D5-3

3-1-6. Case D6 (# of fuel plates: 3840 in Fig. 2-2(f))

Table 3-1-6-1 Core condition in Case D6-1 to Case D6-3 (# of fuel plates: 3840)

Case	C1	C2	C3	S4	S5	S6	k_{eff}
D6-1	1200.00	1200.00	1200.00	1200.00	1200.00	1200.00	0.93000
D6-2	1200.00	1200.00	1200.00	1200.00	1200.00	1200.00	0.93000
D6-3	1200.00	1200.00	1200.00	1200.00	1200.00	1200.00	0.93000

Table 3-1-6-2 Beam characteristics of 14 MeV neutrons in Case D6-1 to Case D6-3

Case	Frequency [Hz]	Width [μs]	Current [mA]
D6-1	20	90	0.20
D6-2	50	90	0.20
D6-3	100	80	0.15

Table 3-1-6-3 Measured results of α [1/s] and ρ [$] in Case D6-1

	α [1/s]		ρ [$]	
Detector	Feynman-α	α-fitting	Area (Sjostrand)	Area (Gozani)
BF-3 #1 (Ch#1)	1493.13 ± 25.33	1604.09 ± 19.04	4.797 ± 0.122	8.069 ± 0.315
BF-3 #2 (Ch#2)	1635.64 ± 42.06	1734.05 ± 63.78	2.622 ± 0.033	5.053 ± 0.336
BF-3 #3 (Ch#3)	1641.15 ± 8.91	1686.35 ± 13.28	3.182 ± 0.024	3.992 ± 0.082
BF-3 #4 (Ch#4)	4166.57 ± 77.36	2118.77 ± 64.65	2.431 ± 0.012	-
Fiber #1 (Ch#5)	-	-	1.449 ± 0.006	-
Fiber #2 (Ch#6)	-	-	1.410 ± 0.001	-
Fiber #3 (Ch#7)	-	-	-	-

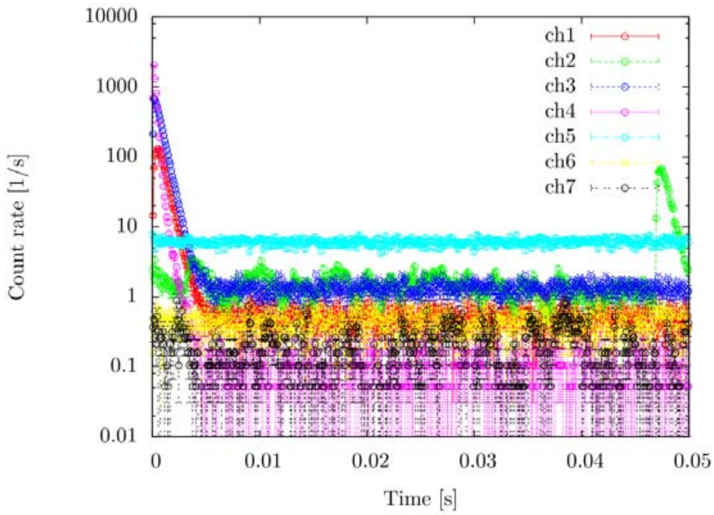

(a) PNS histogram in Case D6-1

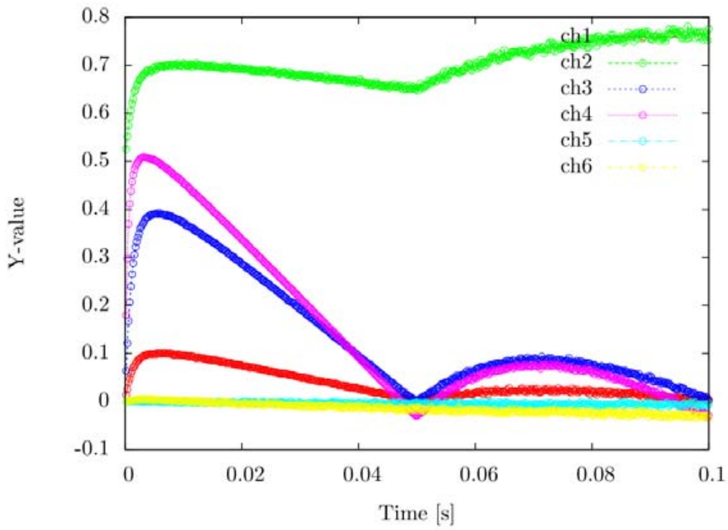

(b) Y-value distribution by Feynman-α method in Case D6-1

Fig. 3-1-6-1 Experimental resutls by PNS and Noise methods in Case D6-1

Table 3-1-6-4 Measured results of α [1/s] and ρ [$] in Case D6-2

	α [1/s]		ρ [$]	
Detector	Feynman-α	α-fitting	Area (Sjostrand)	Area (Gozani)
BF-3 #1 (Ch#1)	1671.52 ± 79.63	1672.67 ± 58.63	5.067 ± 0.289	9.059 ± 0.871
BF-3 #2 (Ch#2)	1790.58±101.01	1694.67 ± 43.44	4.847 ± 0.125	8.255 ± 0.483
BF-3 #3 (Ch#3)	1621.79 ± 48.81	1695.97 ± 29.62	4.070 ± 0.062	4.920 ± 0.203
BF-3 #4 (Ch#4)	4288.55±202.00	2125.10 ± 147.31	2.562 ± 0.027	0.015 ± 0.096
Fiber #1 (Ch#5)	-	-	2.105 ± 0.012	-
Fiber #2 (Ch#6)	-	-	2.042 ± 0.005	-
Fiber #3 (Ch#7)	-	-	-	-

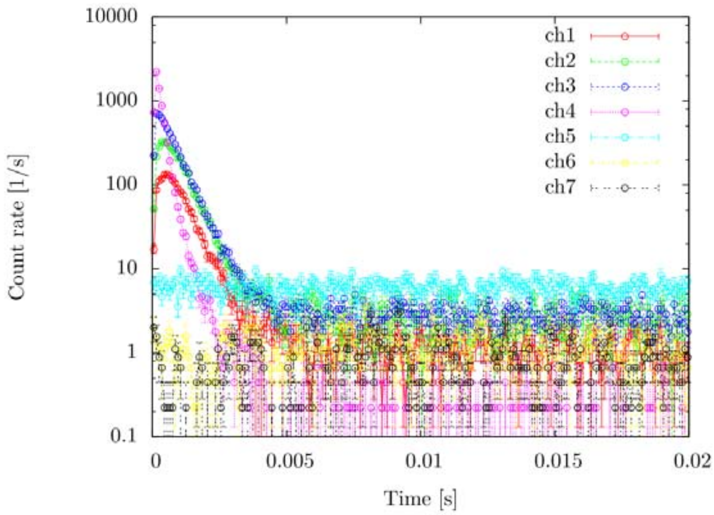

(a) PNS histogram in Case D6-2

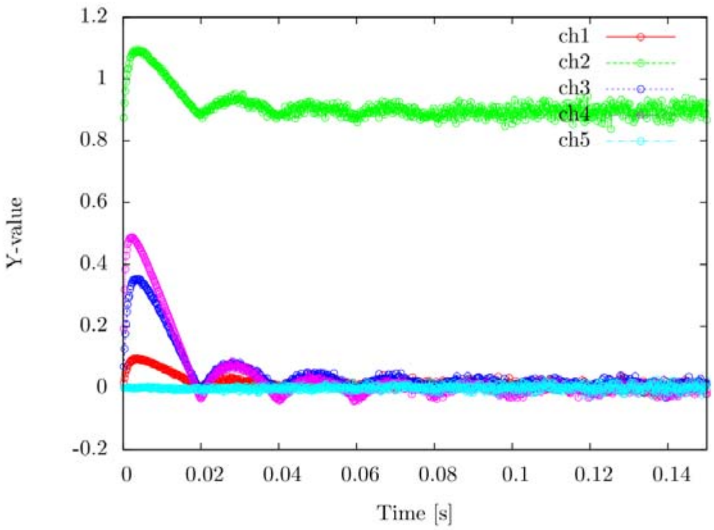

(b) Y-value distribution by Feynman-α method in Case D6-2

Fig. 3-1-6-2 Experimental resutls by PNS and Noise methods in Case D6-2

Table 3-1-6-5 Measured results of α [1/s] and ρ [$] in Case D6-3

	α [1/s]		ρ [$]	
Detector	Feynman-α	α-fitting	Area (Sjostrand)	Area (Gozani)
BF-3 #1 (Ch#1)	1409.00 ± 46.46	1640.90 ± 18.09	4.329 ± 0.132	5.762 ± 0.251
BF-3 #2 (Ch#2)	1526.97±131.68	1666.31 ± 28.51	4.163 ± 0.058	5.448 ± 0.186
BF-3 #3 (Ch#3)	1640.72 ± 12.49	1711.10 ± 12.79	1.869 ± 0.019	0.047 ± 0.054
BF-3 #4 (Ch#4)	4356.49±139.02	2083.91 ± 46.16	0.596 ± 0.005	-
Fiber #1 (Ch#5)	-	-	0.557 ± 0.002	-
Fiber #2 (Ch#6)	-	-	0.553 ± 0.001	-
Fiber #3 (Ch#7)	-	-	-	-

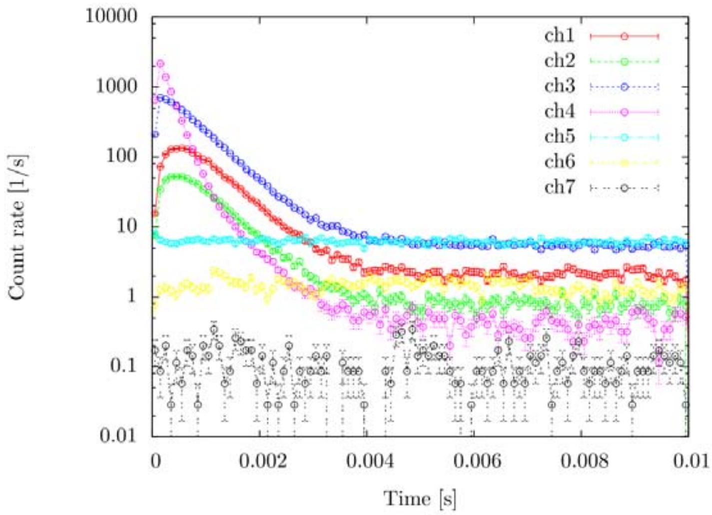

(a) PNS histogram in Case D6-3

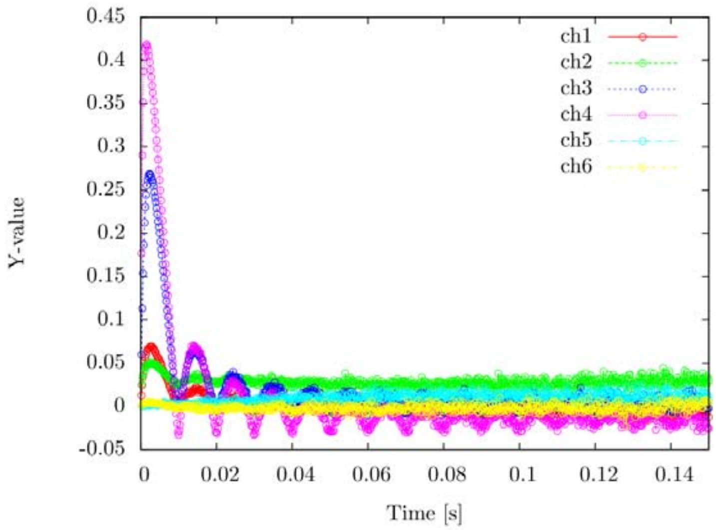

(b) Y-value distribution by Feynman-α method in Case D6-3

Fig. 3-1-6-3 Experimental resutls by PNS and Noise methods in Case D6-3

3-2. ADS with 100 MeV Protons

3-2-1. Core condition at critical state (Fig. 2-3)

Table 3-2-1-1 Control rod positions at the critical state in reference core
(# of HEU plates: 4560; Case F1)

Rod	Rod position [mm]
C1	786.14
C2	1200.00
C3	1200.00
S4	1200.00
S5	1200.00
S6	1200.00
Excess reactivity [pcm]	37 ± 1

Table 3-2-1-2 Control rod worth

Rod	Rod worth [pcm]
C1 (S4)	902 ± 27
C2 (S6)	696 ± 21
C3 (S5)	232 ± 7

Table 3-2-1-3 Kinetic parameters by MCNP6.1 with JENDL-4.0

β_{eff}	853 ± 3 [pcm]
Λ	$(3.24 \pm 0.03)\times10^{-5}$ [s]

Table 3-2-1-4 Proton beam characteristics obtained from FFAG accelerator

Energy [MeV]	Frequency [Hz]	Repetition [ns]	Current [nA]
100	20	100	0.05

3-2-2. Case F1 (# of fuel plates: 4560 in Fig. 2-4(a))

Table 3-2-2-1 Core condition in Case F1-1 to Case F1-6 (# of fuel plates: 4560)

Case	C1	C2	C3	S4	S5	S6	k_{eff}
F1-1	0.00	0.00	0.00	1200.00	1200.00	1200.00	0.98208
F1-2	0.00	1200.00	1200.00	1200.00	1200.00	1200.00	0.99135
F1-3	0.00	0.00	1200.00	1200.00	1200.00	1200.00	0.98439
F1-4	0.00	0.00	1200.00	1200.00	1200.00	1200.00	0.98208
F1-5	0.00	0.00	1200.00	1200.00	1200.00	0.00	0.97744
F1-6	0.00	0.00	1200.00	0.00	1200.00	0.00	0.96842

Table 3-2-2-2 Measured results of α [1/s] and ρ [$] in Case F1-1

	α [1/s]		ρ [$]	
Detector	Feynman-α	α-fitting	Area (Sjostrand)	Area (Gozani)
BF-3 #5 (Ch#1)	805.90 ± 7.13	775.65 ± 6.01	1.834 ± 0.004	1.529 ± 0.005
BF-3 #2 (Ch#2)	793.06 ± 7.12	791.55 ± 6.71	1.949 ± 0.018	1.921 ± 0.020
BF-3 #3 (Ch#3)	807.48 ± 3.88	803.10 ± 3.07	2.048 ± 0.012	1.952 ± 0.013
BF-3 #4 (Ch#4)	1145.43 ± 17.85	868.30 ± 11.13	1.801 ± 0.005	1.501 ± 0.008
BF-3 #1 (Ch#5)	771.43 ± 6.92	786.80 ± 6.76	1.964 ± 0.037	1.941 ± 0.040

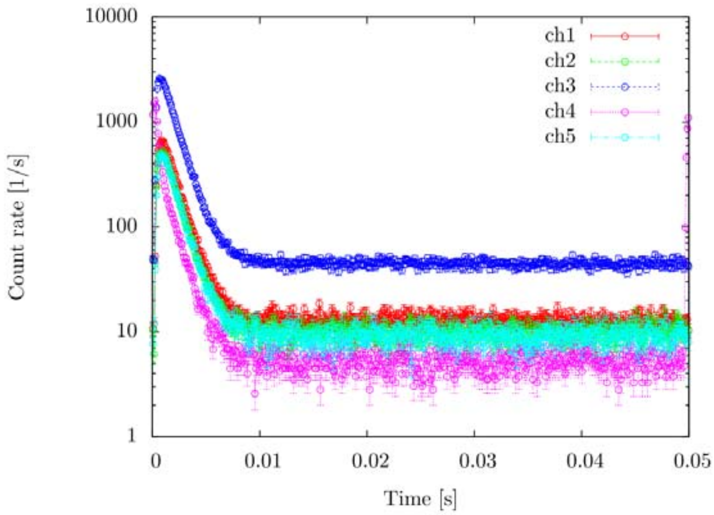

(a) PNS histogram in Case F1-1

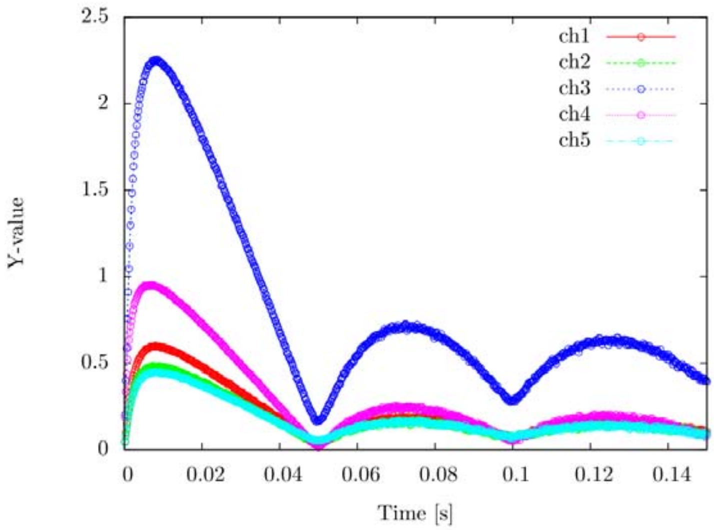

(b) Y-value distribution by Feynman-α method in Case F1-1

Fig. 3-2-2-1 Experimental resutls by PNS and Noise methods in Case F1-1

Table 3-2-2-3 Measured results of α [1/s] and ρ [$] in Case F1-2

	α [1/s]		ρ [$]	
Detector	Feynman-α	α-fitting	Area (Sjostrand)	Area (Gozani)
BF-3 #5 (Ch#1)	494.19 ± 2.79	479.32 ± 3.11	0.895 ± 0.001	0.798 ± 0.002
BF-3 #2 (Ch#2)	483.23 ± 3.19	481.73 ± 3.31	0.968 ± 0.006	0.953 ± 0.006
BF-3 #3 (Ch#3)	488.39 ± 1.90	484.30 ± 1.59	0.970 ± 0.004	0.931 ± 0.004
BF-3 #4 (Ch#4)	639.45 ± 8.43	516.73 ± 4.89	0.884 ± 0.001	0.783 ± 0.002
BF-3 #1 (Ch#5)	496.11 ± 2.97	478.76 ± 3.39	0.973 ± 0.011	0.963 ± 0.012

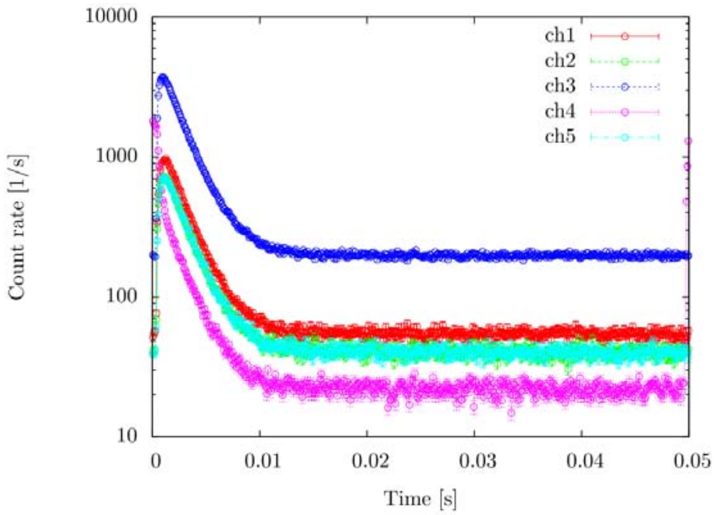

(a) PNS histogram in Case F1-2

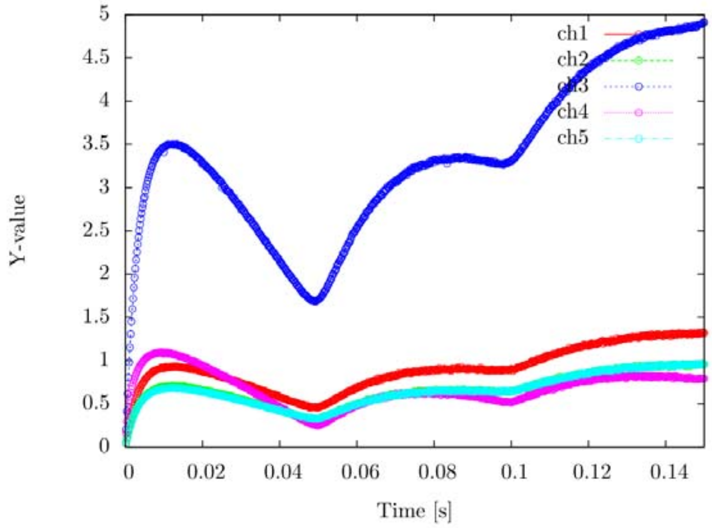

(b) Y-value distribution by Feynman-α method in Case F1-2

Fig. 3-2-2-2 Experimental resutls by PNS and Noise methods in Case F1-2

Table 3-2-2-4 Measured results of α [1/s] and ρ [$] in Case F1-3

	α [1/s]		ρ [$]	
Detector	Feynman-α	α-fitting	Area (Sjostrand)	Area (Gozani)
BF-3 #5 (Ch#1)	541.28 ± 13.64	539.51 ± 10.25	1.310 ± 0.007	1.185 ± 0.008
BF-3 #2 (Ch#2)	544.49 ± 15.24	548.34 ± 10.76	1.194 ± 0.025	1.174 ± 0.028
BF-3 #3 (Ch#3)	555.53 ± 9.39	555.50 ± 4.92	1.210 ± 0.016	1.161 ± 0.017
BF-3 #4 (Ch#4)	704.34 ± 16.18	634.24 ± 15.92	1.320 ± 0.005	1.216 ± 0.009
BF-3 #1 (Ch#5)	542.98 ± 13.16	537.86 ± 10.37	1.209 ± 0.050	1.182 ± 0.055

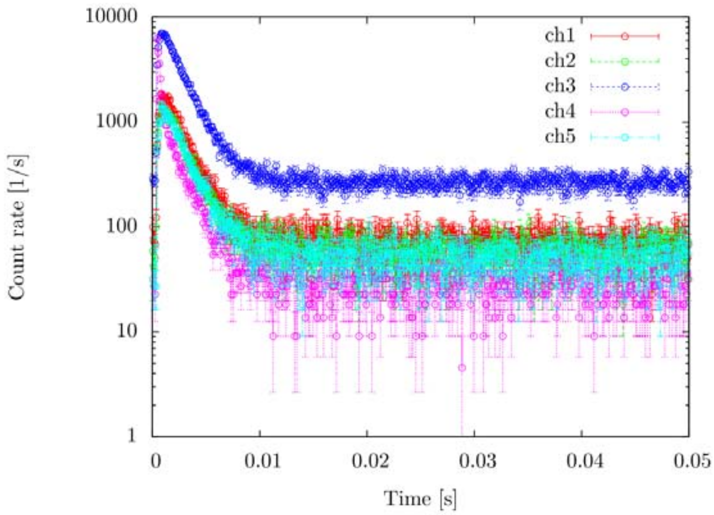

(a) PNS histogram in Case F1-3

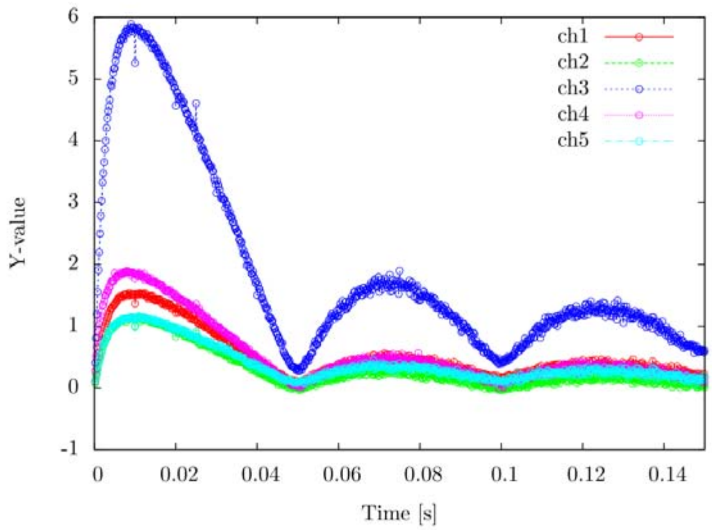

(b) Y-value distribution by Feynman-α method in Case F1-3

Fig. 3-2-2-3 Experimental resutls by PNS and Noise methods in Case F1-3

Table 3-2-2-5 Measured results of α [1/s] and ρ [$] in Case F1-4

	α [1/s]		ρ [$]	
Detector	Feynman-α	α-fitting	Area (Sjostrand)	Area (Gozani)
BF-3 #1 (Ch#1)	-	-	-	-
BF-3 #2 (Ch#2)	565.46 ± 6.56	548.85 ± 5.90	1.212 ± 0.024	1.199 ± 0.026
BF-3 #3 (Ch#3)	557.91 ± 4.08	557.84 ± 2.66	1.208 ± 0.009	1.160 ± 0.010
BF-3 #4 (Ch#4)	739.66 ± 10.29	645.39 ± 10.33	1.336 ± 0.003	1.214 ± 0.005
Fiber #1 (Ch#5)	-	-	-	-
Fiber #2 (Ch#6)	-	-	-	-
Fiber #3 (Ch#7)	541.36 ± 19.29	579.08 ± 12.96	1.314 ± 0.002	1.162 ± 0.006

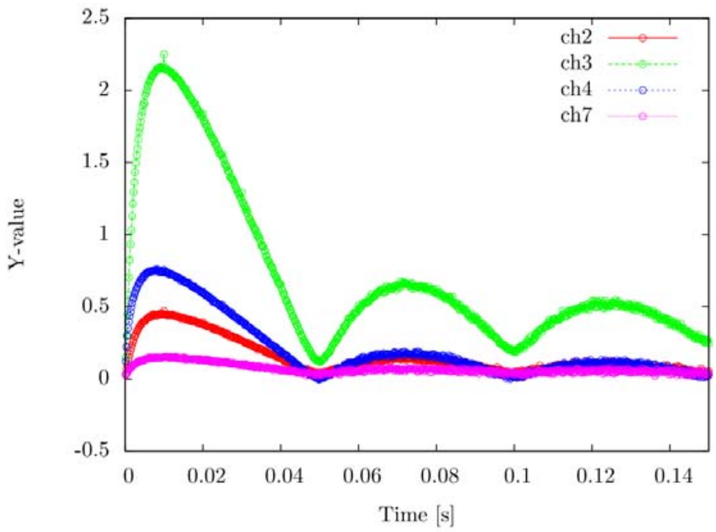

(a) PNS histogram in Case F1-4

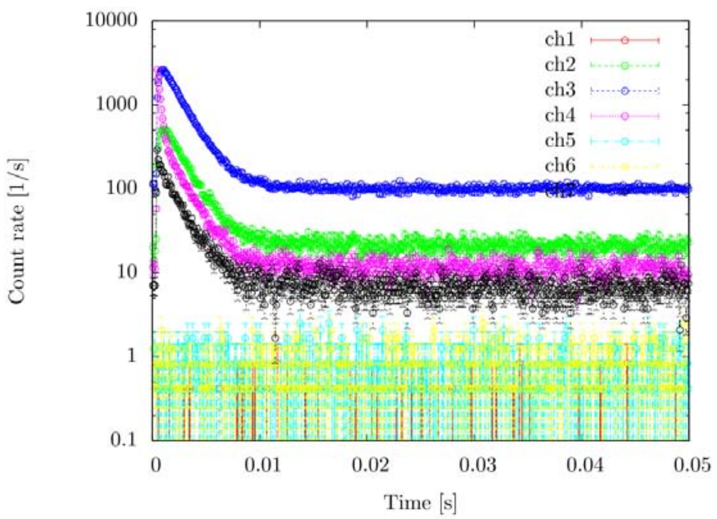

(b) Y-value distribution by Feynman-α method in Case F1-4

Fig. 3-2-2-4 Experimental resutls by PNS and Noise methods in Case F1-4

Table 3-2-2-6 Measured results of α [1/s] and ρ [$] in Case F1-5

	α [1/s]		ρ [$]	
Detector	Feynman-α	α-fitting	Area (Sjostrand)	Area (Gozani)
BF-3 #1 (Ch#1)	-	-	-	-
BF-3 #2 (Ch#2)	611.43 ± 5.24	612.90 ± 4.72	1.464 ± 0.025	1.421 ± 0.026
BF-3 #3 (Ch#3)	623.65 ± 2.41	621.46 ± 2.29	1.456 ± 0.008	1.397 ± 0.009
BF-3 #4 (Ch#4)	811.32 ± 11.35	704.50 ± 9.52	1.623 ± 0.003	1.458 ±0.006
Fiber #1 (Ch#5)	-	-	-	-
Fiber #2 (Ch#6)	-	-	-	-
Fiber #3 (Ch#7)	658.73 ± 11.57	651.85 ± 8.92	1.613 ± 0.002	1.396 ± 0.005

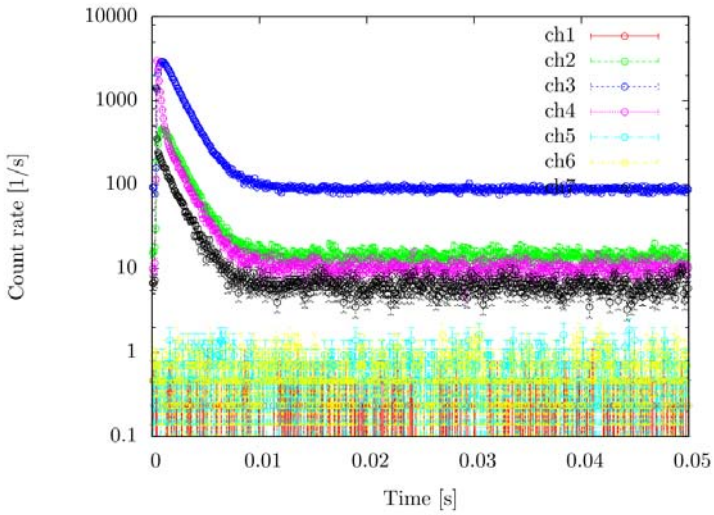

(a) PNS histogram in Case F1-5

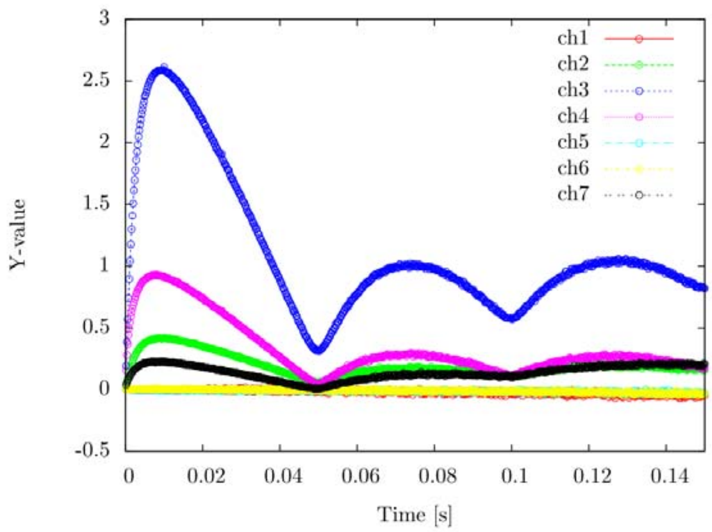

(b) Y-value distribution by Feynman-α method in Case F1-5

Fig. 3-2-2-5　Experimental resutls by PNS and Noise methods in Case F1-5

Table 3-2-2-7 Measured results of α [1/s] and ρ [$] in Case F1-6

	α [1/s]		ρ [$]	
Detector	Feynman-α	α-fitting	Area (Sjostrand)	Area (Gozani)
BF-3 #1 (Ch#1)	-	-	-	-
BF-3 #2 (Ch#2)	867.68 ± 17.35	894.89 ± 14.37	2.181 ± 0.087	2.111 ± 0.094
BF-3 #3 (Ch#3)	903.75 ± 10.95	911.20 ± 6.54	2.414 ± 0.038	2.266 ± 0.039
BF-3 #4 (Ch#4)	1351.25 ± 29.42	1041.78 ± 29.28	2.909 ± 0.016	2.441 ± 0.029
Fiber #1 (Ch#5)	-	-	-	-
Fiber #2 (Ch#6)	-	-	-	-
Fiber #3 (Ch#7)	1000.60 ± 49.77	908.43 ± 27.12	2.758 ± 0.012	2.196 ± 0.023

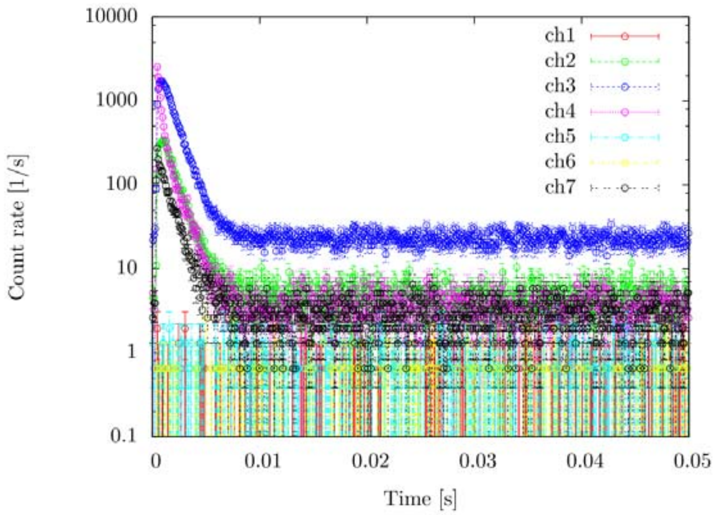

(a) PNS histogram in Case F1-6

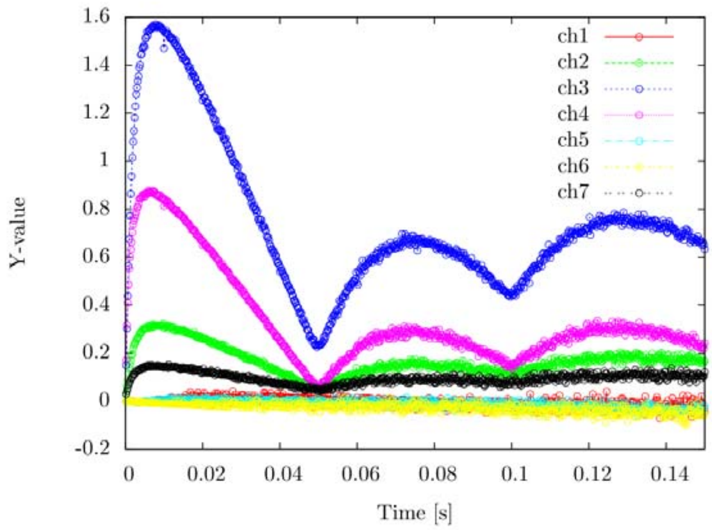

(b) Y-value distribution by Feynman-α method in Case F1-6

Fig. 3-2-2-6 Experimental resutls by PNS and Noise methods in Case F1-6

3-2-3. Case F2 (# of fuel plates: 4440 in Fig. 2-4(b))

Table 3-2-3-1 Core condition in Case F2-1 (# of fuel plates: 4440)

Case	C1	C2	C3	S4	S5	S6	k_{eff}
F2-1	1200.00	1200.00	1200.00	1200.00	1200.00	1200.00	0.99328

Table 3-2-3-2 Measured results of α [1/s] and ρ [$] in Case F2-1

	α [1/s]		ρ [$]	
Detector	Feynman-α	α-fitting	Area (Sjostrand)	Area (Gozani)
BF-3 #1 (Ch#1)	378.35 ± 4.00	378.90 ± 2.26	0.638 ± 0.003	0.639 ± 0.004
BF-3 #2 (Ch#2)	368.72 ± 4.36	375.31 ± 2.10	0.637 ± 0.002	0.630 ± 0.002
BF-3 #3 (Ch#3)	371.42 ± 3.98	377.47 ± 1.05	0.647 ± 0.002	0.626 ± 0.001
BF-3 #4 (Ch#4)	517.43 ± 10.05	377.55 ± 3.46	1.399 ± 0.006	0.631 ± 0.001
LiCaF (Ch#5)	371.82 ± 3.89	382.46 ± 1.72	0.644 ± 0.002	0.635 ± 0.001
Fiber #1 (Ch#6)	194.66 ± 220.45	-	-	0.594 ± 0.046
Fiber #2 (Ch#7)	472.97 ± 74.56	-	-	0.655 ± 0.017

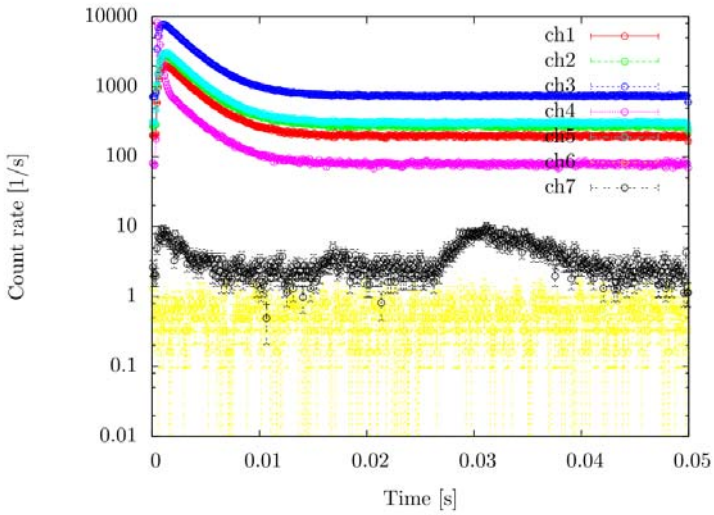

(a) PNS histogram in Case F2-1

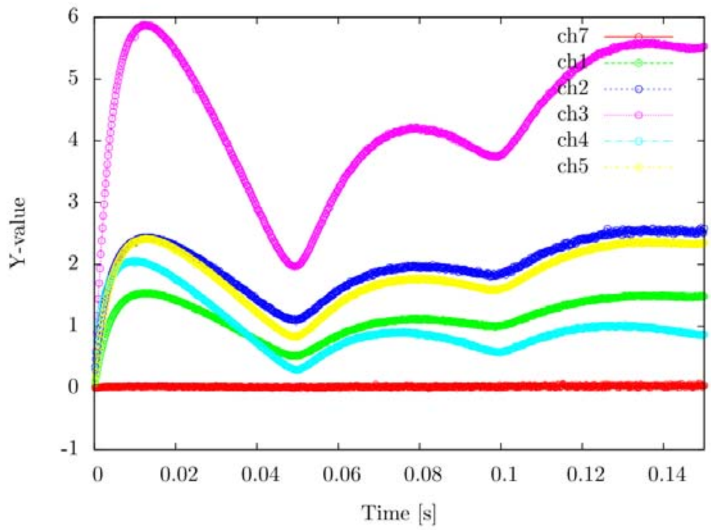

(b) Y-value distribution by Feynman-α method in Case F2-1

Fig. 3-2-3-1 Experimental resutls by PNS and Noise methods in Case F2-1

3-2-4. Case F3 (# of fuel plates: 4320 in Fig. 2-4(c))

Table 3-2-4-1 Core condition in Case F3-1 (# of fuel plates: 4320)

Case	C1	C2	C3	S4	S5	S6	k_{eff}
F3-1	1200.00	1200.00	1200.00	1200.00	1200.00	1200.00	0.98004

Table 3-2-4-2 Measured results of α [1/s] and ρ [$] in Case F3-1

	α [1/s]		ρ [$]	
Detector	Feynman-α	α-fitting	Area (Sjostrand)	Area (Gozani)
BF-3 #1 (Ch#1)	670.37 ± 4.72	697.62 ± 5.30	2.043 ± 0.012	2.092 ± 0.018
BF-3 #2 (Ch#2)	690.57 ± 9.73	691.99 ± 5.10	2.029 ± 0.010	2.063 ± 0.010
BF-3 #3 (Ch#3)	684.02 ± 4.10	699.73 ± 2.81	2.128 ± 0.007	2.047 ± 0.006
BF-3 #4 (Ch#4)	1255.70 ± 32.52	706.39 ± 8.95	8.132 ± 0.072	2.092 ± 0.007
LiCaF (Ch#5)	666.09 ± 4.93	698.59 ± 4.42	2.111 ± 0.010	2.096 ± 0.004
Fiber #3 (Ch#6)	725.66 ± 7.50	677.05 ± 12.28	3.502 ± 0.036	2.064 ± 0.009
Fiber #2 (Ch#7)	700.66 ± 115.19	-	-	2.075 ± 0.084

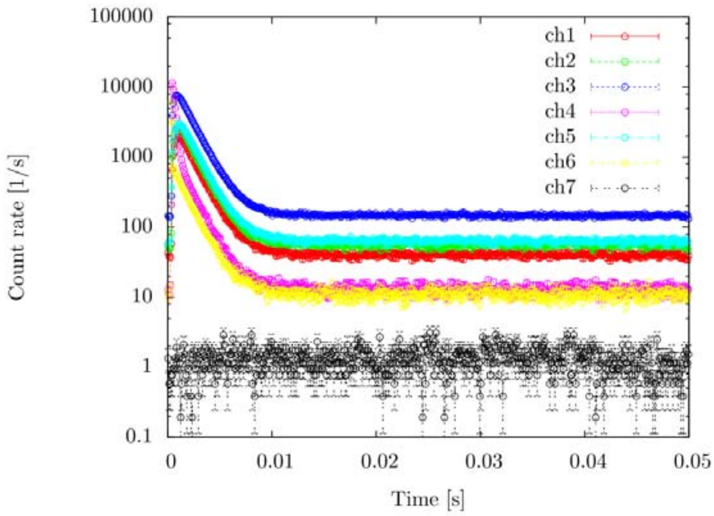

(a) PNS histogram in Case F3-1

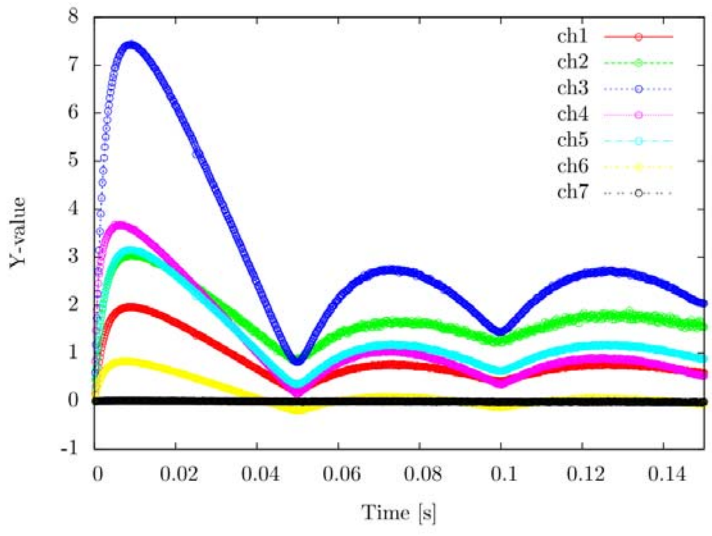

(b) Y-value distribution by Feynman-α method in Case F3-1

Fig. 3-2-4-1 Experimental resutls by PNS and Noise methods in Case F3-1

3-2-5. Case F4 (# of fuel plates: 4200 in Fig. 2-4(d))

Table 3-2-5-1 Core condition in Case F4-1 and F4-2 (# of fuel plates: 4200)

Case	C1	C2	C3	S4	S5	S6	k_{eff}
F4-1	1200.00	1200.00	1200.00	1200.00	1200.00	1200.00	0.96603
F4-2	1200.00	1200.00	1200.00	1200.00	1200.00	1200.00	0.96603

Table 3-2-5-2 Measured results of α [1/s] and ρ [$] in Case F4-1

	α [1/s]		ρ [$]	
Detector	Feynman-α	α-fitting	Area (Sjostrand)	Area (Gozani)
BF-3 #1 (Ch#1)	981.43 ± 7.00	1047.39 ± 10.08	3.693 ± 0.024	3.756 ± 0.038
BF-3 #2 (Ch#2)	983.15 ± 8.05	1036.24 ± 10.26	3.661 ± 0.021	3.670 ± 0.022
BF-3 #3 (Ch#3)	1001.46 ± 4.15	1035.20 ± 5.49	3.921 ± 0.014	3.615 ± 0.013
BF-3 #4 (Ch#4)	2410.26 ± 60.24	1046.45 ± 19.88	27.699 ± 0.317	3.781 ± 0.026
LiCaF (Ch#5)	963.39 ± 5.85	1038.53 ± 8.12	3.789 ± 0.020	3.780 ± 0.012
Fiber #3 (Ch#6)	1059.11 ± 10.46	1019.33 ± 27.46	7.523 ± 0.086	3.699 ± 0.036
Fiber #2 (Ch#7)	1436.49±187.86	-	-	4.255 ± 0.280

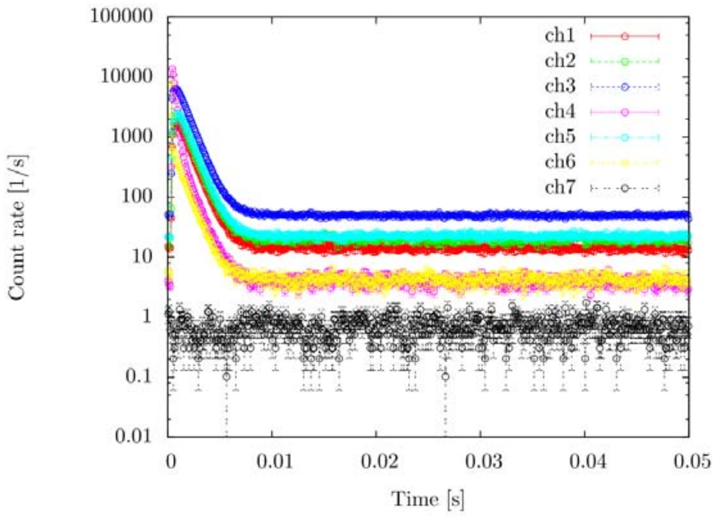

(a) PNS histogram in Case F4-1

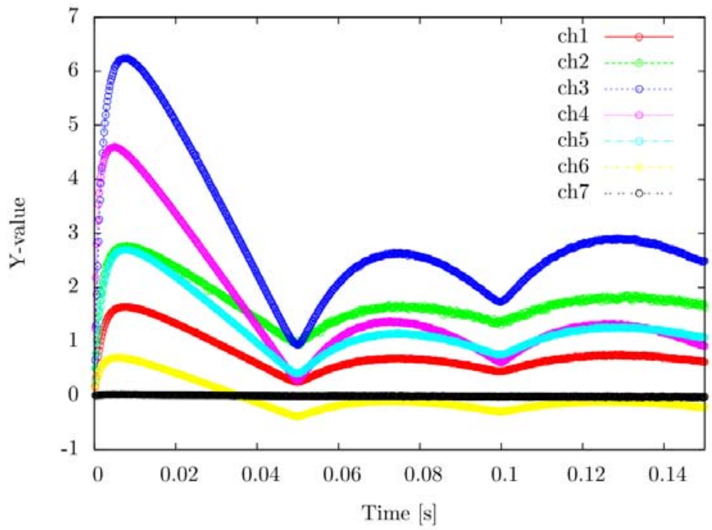

(b) Y-value distribution by Feynman-α method in Case F4-1

Fig. 3-2-5-1 Experimental resutls by PNS and Noise methods in Case F4-1

Table 3-2-5-3 Measured results of α [1/s] and ρ [$] in Case F4-2

	α [1/s]		ρ [$]	
Detector	Feynman-α	α-fitting	Area (Sjostrand)	Area (Gozani)
LiCaF (Ch#1)	950.13 ± 3.00	987.08 ± 3.65	3.816 ± 0.029	4.283 ± 0.037
BF-3 #2 (Ch#2)	984.69 ± 3.01	1014.65 ± 3.29	3.823 ± 0.014	4.323 ± 0.020
FC #2 (Ch#3)	944.57 ± 4.79	974.36 ± 6.49	3.973 ± 0.009	4.319 ± 0.023
FC #3 (Ch#4)	989.59 ± 3.61	997.24 ± 6.52	4.084 ± 0.005	4.440 ± 0.023
Fiber #1 (Ch#5)	-	-	-	-
Fiber #2 (Ch#6)	1125.74 ±52.42	1123.54 ± 45.39	3.772 ± 0.005	4.491 ± 0.153
Fiber #3 (Ch#7)	1412.79 ±68.42	-	-	-

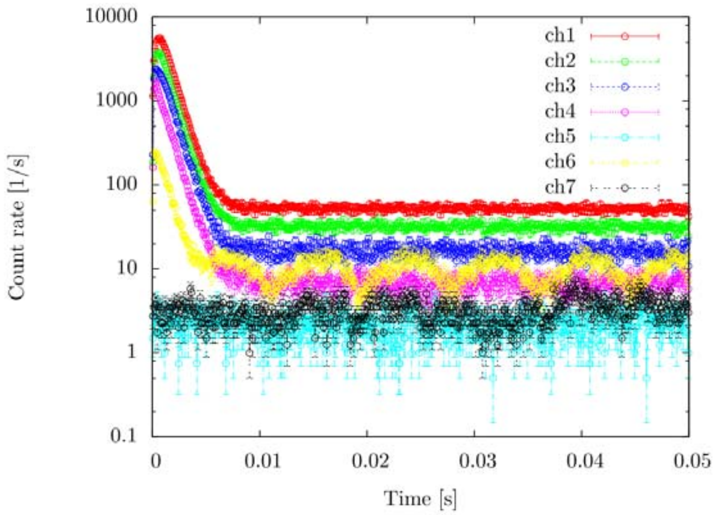

(a) PNS histogram in Case F4-2

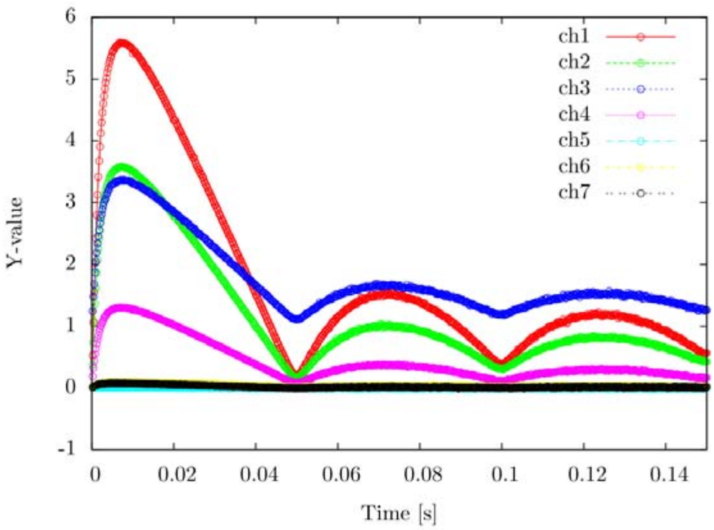

(b) Y-value distribution by Feynman-α method in Case F4-2

Fig. 3-2-5-2 Experimental resutls by PNS and Noise methods in Case F4-2

3-2-6. Case F5 (# of fuel plates: 4080 in Fig. 2-4(e))

Table 3-2-6-1 Core condition in Case F5-1 (# of fuel plates: 4080)

Case	C1	C2	C3	S4	S5	S6	k_{eff}
F5-1	1200.00	1200.00	1200.00	1200.00	1200.00	1200.00	0.95560

Table 3-2-6-2 Measured results of α [1/s] and ρ [$] in Case F5-1

	α [1/s]		ρ [$]	
Detector	Feynman-α	α-fitting	Area (Sjostrand)	Area (Gozani)
BF-3 #1 (Ch#1)	1100.61 ± 3.91	1142.68 ± 11.03	4.858 ± 0.137	5.441 ± 0.174
BF-3 #2 (Ch#2)	1110.85 ± 4.07	1143.44 ± 10.66	4.834 ± 0.067	5.332 ± 0.092
BF-3 #3 (Ch#3)	1114.54 ± 2.81	1167.77 ± 7.55	5.008 ± 0.049	5.388 ± 0.066
BF-3 #4 (Ch#4)	2632.74 ±26.57	2179.82 ±535.32	-	-
LiCaF (Ch#5)	1667.01 ±3.83	1131.01 ± 10.00	6.468 ± 0.034	6.676 ± 0.062
Fiber #2 (Ch#6)	1913.19 ±152.93	1494.85 ±130.19	6.346 ± 0.010	8.592 ± 0.839
Fiber #3 (Ch#7)	1299.97 ±87.56	1425.24 ±158.51	6.264 ± 0.008	8.043 ± 0.956

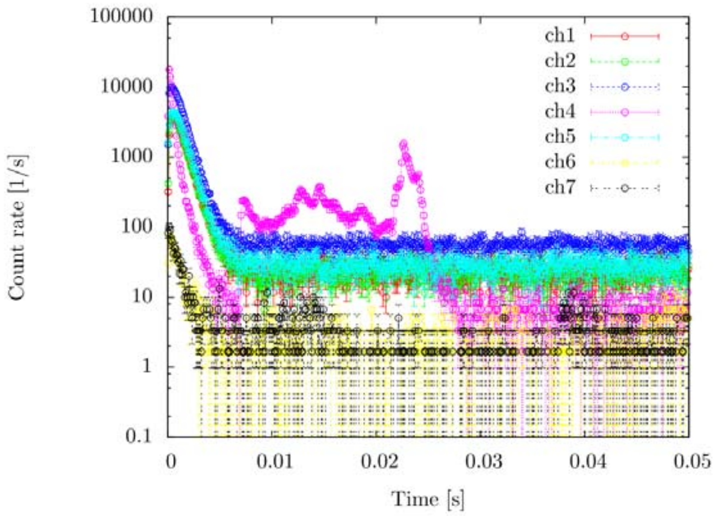

(a) PNS histogram in Case F5-1

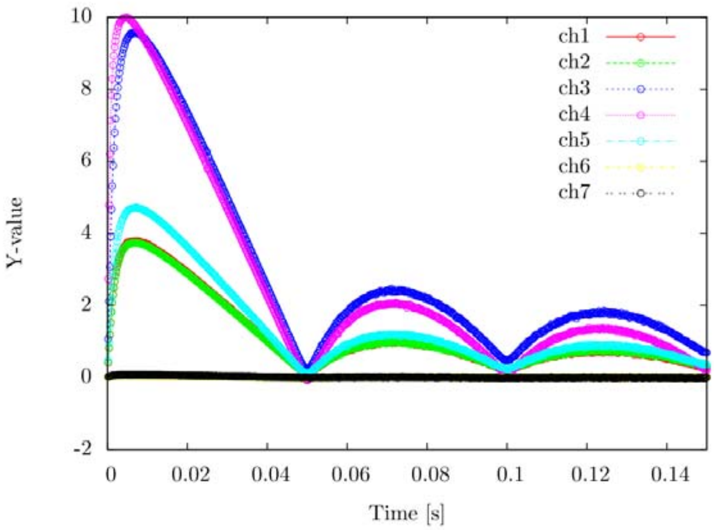

(b) Y-value distribution by Feynman-α method in Case F5-1

Fig. 3-2-6-1 Experimental resutls by PNS and Noise methods in Case F5-1

3-2-7. Case F6 (# of fuel plates: 3960 in Fig. 2-4(f))

Table 3-2-7-1 Core condition in Case F6-1 (# of fuel plates: 3960)

Case	C1	C2	C3	S4	S5	S6	k_{eff}
F6-1	1200.00	1200.00	1200.00	1200.00	1200.00	1200.00	0.95047

Table 3-2-7-2 Measured results of α [1/s] and ρ [$] in Case F6-1

	α [1/s]		ρ [$]	
Detector	Feynman-α	α-fitting	Area (Sjostrand)	Area (Gozani)
BF-3 #1 (Ch#1)	1147.81 ± 3.98	1214.68 ± 5.09	5.306 ± 0.061	6.025 ± 0.079
BF-3 #2 (Ch#2)	1170.63 ± 4.25	1227.65 ± 4.73	5.354 ± 0.030	6.023 ± 0.043
BF-3 #3 (Ch#3)	1178.31 ± 3.63	1236.21 ± 3.33	5.556 ± 0.022	5.973 ± 0.030
BF-3 #4 (Ch#4)	2810.88 ±24.95	1616.85 ±23.53	7.888 ± 0.010	8.108 ± 0.144
LiCaF (Ch#5)	1127.06 ± 4.03	-	-	-
Fiber #2 (Ch#6)	1198.27 ± 70.04	1301.00 ± 39.65	7.846 ± 0.004	6.366 ± 0.189
Fiber #3 (Ch#7)	1304.92 ± 40.08	-	-	-

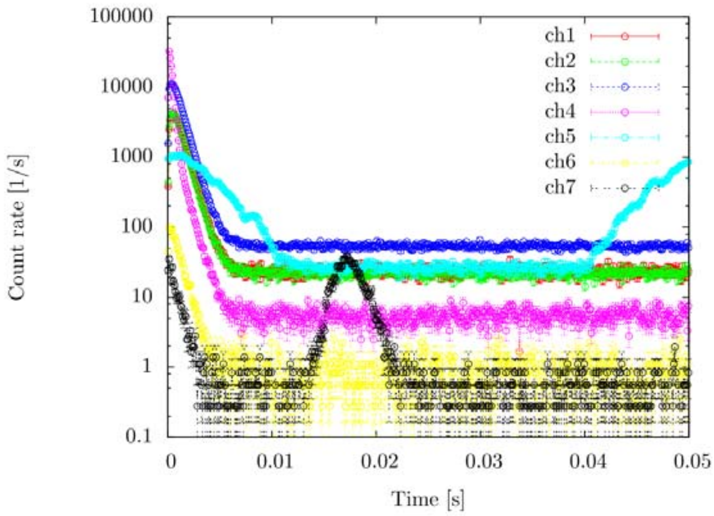

(a) PNS histogram in Case F6-1

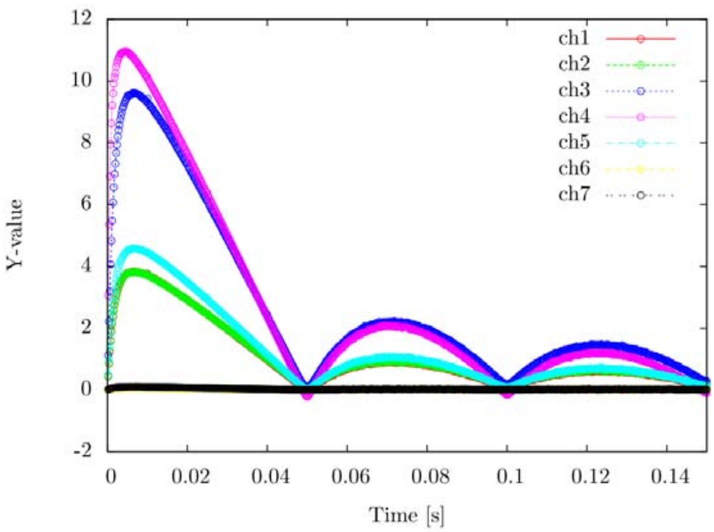

(b) Y-value distribution by Feynman-α method in Case F6-1

Fig. 3-2-7-1 Experimental resutls by PNS and Noise methods in Case F6-1

3-2-8. Case F7 (# of fuel plates: 3840 in Fig. 2-4(g))

Table 3-2-8-1 Core condition in Case F7-1 and Case F7-2 (# of fuel plates: 3840)

Case	C1	C2	C3	S4	S5	S6	k_{eff}
F7-1	1200.00	1200.00	1200.00	1200.00	1200.00	1200.00	0.92509
F7-2	1200.00	1200.00	1200.00	1200.00	1200.00	1200.00	0.92509

Table 3-2-8-2 Measured results of α [1/s] and ρ [$] in Case F7-1

	α [1/s]		ρ [$]	
Detector	Feynman-α	α-fitting	Area (Sjostrand)	Area (Gozani)
BF-3 #1 (Ch#1)	1486.99 ± 6.33	1642.83 ± 9.39	8.718 ± 0.167	9.542 ± 0.209
BF-3 #2 (Ch#2)	1526.32 ± 5.96	1663.99 ± 9.55	8.364 ± 0.076	9.003 ± 0.111
BF-3 #3 (Ch#3)	1565.34 ± 4.34	1675.08 ± 7.43	8.932 ± 0.058	8.849 ± 0.080
BF-3 #4 (Ch#4)	3620.56 ± 17.16	2546.56 ±43.44	15.485 ± 0.029	17.614 ± 0.575
LiCaF (Ch#5)	1445.92 ± 5.88	1606.93 ± 8.73	14.215 ± 0.049	8.930 ± 0.068
Fiber #2 (Ch#6)	1972.45 ±169.96	-	-	-
Fiber #3 (Ch#7)	1723.10 ±113.58	-	-	-

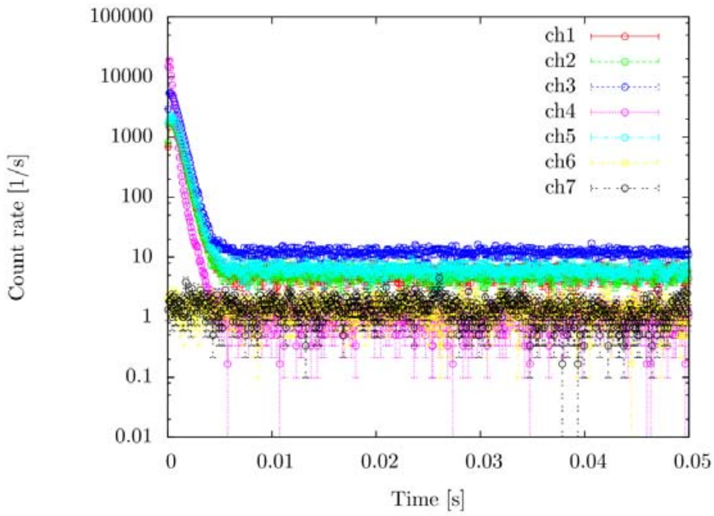

(a) PNS histogram in Case F7-1

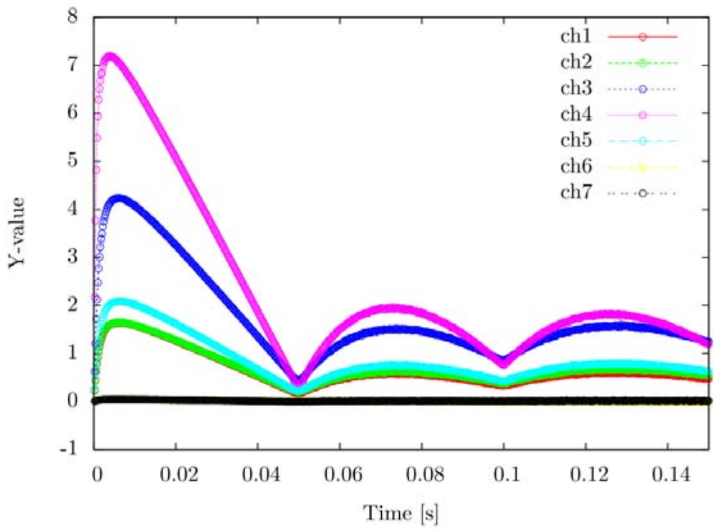

(b) Y-value distribution by Feynman-α method in Case F7-1

Fig. 3-2-8-1 Experimental resutls by PNS and Noise methods in Case F7-1

Table 3-2-8-3 Measured results of α [1/s] and ρ [$] in Case F7-2

	α [1/s]		ρ [$]	
Detector	Feynman-α	α-fitting	Area (Sjostrand)	Area (Gozani)
BF-3 #1 (Ch#1)	1502.75 ± 6.73	1615.9 ± 10.3	8.406 ± 0.182	8.958 ± 0.223
BF-3 #2 (Ch#2)	1522.17 ± 6.67	1659.6 ± 11.7	8.346 ± 0.088	8.974 ± 0.130
BF-3 #3 (Ch#3)	1480.47 ± 8.41	1589.6 ± 16.7	9.338 ± 0.057	9.285 ± 0.132
BF-3 #4 (Ch#4)	1561.98 ± 8.74	1529.3 ± 17.4	10.097 ± 0.035	9.256 ± 0.126
LiCaF (Ch#5)	1459.16 ± 6.75	1631.9 ± 9.7	9.699 ± 0.058	9.781 ± 0.095
Fiber #2 (Ch#6)	1582.17 ±148.61	-	-	-
Fiber #3 (Ch#7)	1286.24 ±105.37	-	-	-

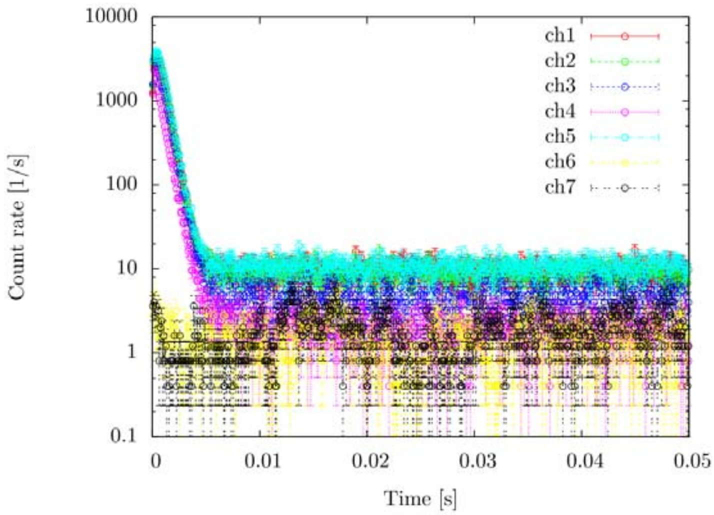

(a) PNS histogram in Case F7-2

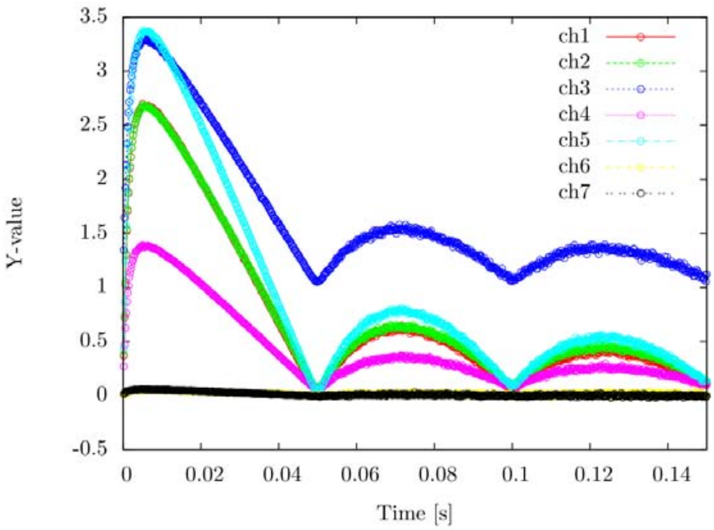

(b) Y-value distribution by Feynman-α method in Case F7-2

Fig. 3-2-8-2 Experimental resutls by PNS and Noise methods in Case F7-2

Phase II

Study on Reaction Rate Distributions

11th June, 2018

Appendix-II

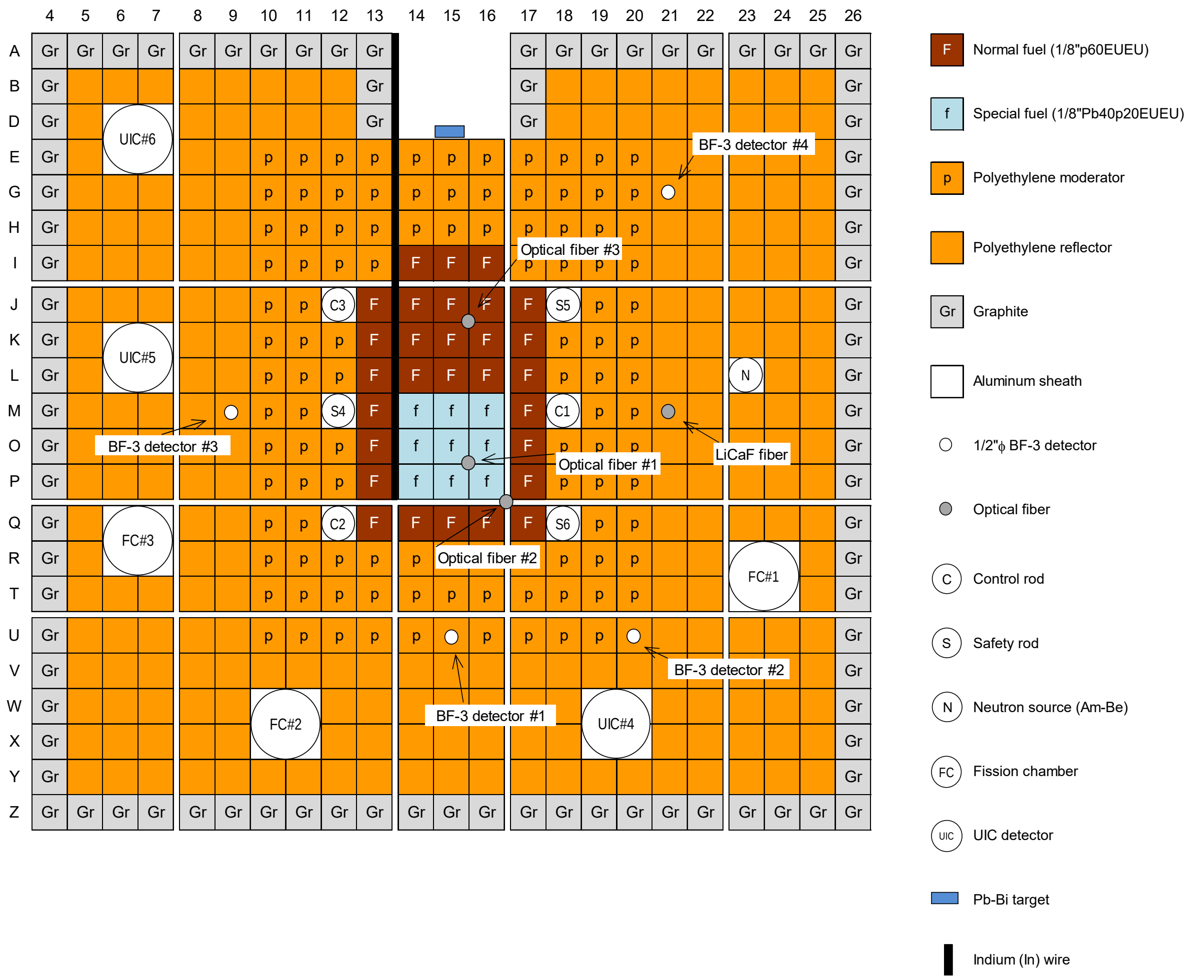

Fig. 4-1 Core configuration of ADS with 100 MeV protons

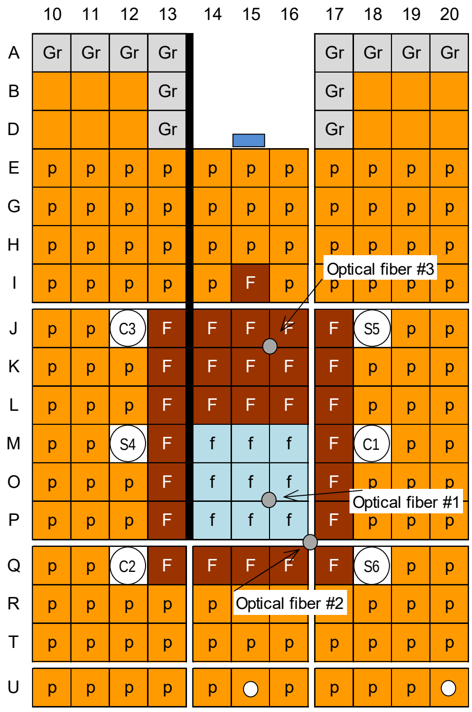

(a) Case F3

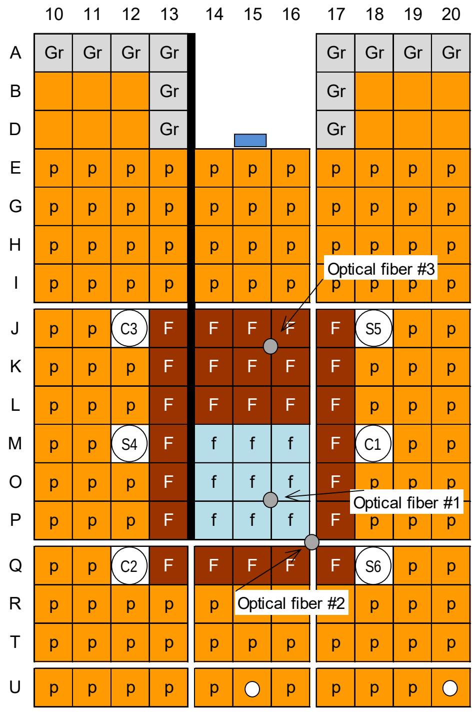

(b) Case F4

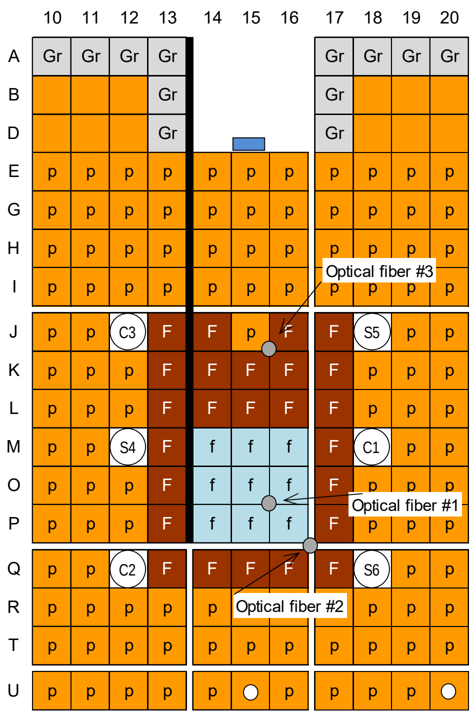

(c) Case F5

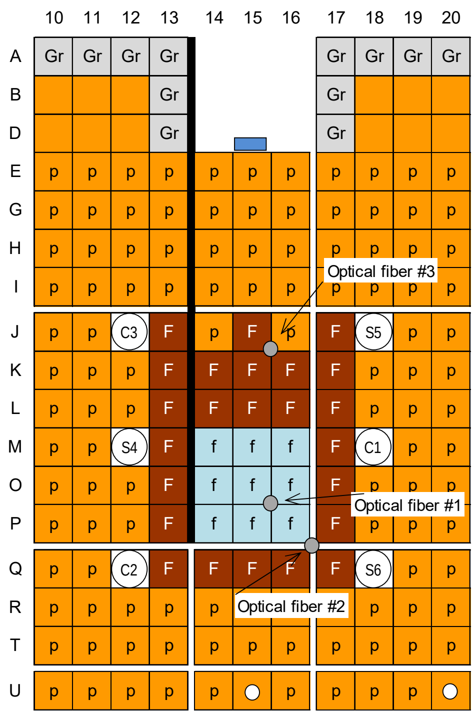

(d) Case F6

Fig. 4-2 Core configuration of reaction rate distributions in ADS with 100 MeV protons

4. Results of Experiments

4-1. Reaction Rate Distributions

4-1-1. Core condition

Table 4-1-1-1 Specification of measurement of reaction rate distribution in Fig. 4-1

Reaction	Location	Foil/Wire
^{115}In(*n*, *n*')^{115m}In	Target (15, D; Fig. 4-1)	10*10*1 mm (Foil)
^{115}In(*n*, γ)^{116}In	Core (13-14, A-P; Fig. 4-1)	1 mm diameter, 800 mm long (Wire)

Table 4-1-1-2 Core condition in all the cores shown in Fig. 4-2

	Number of fuel plates	Rod insertion	k_{eff}
Case F3	4320	C1, C2, C3: 1200.00 [mm] S4, S5, S6: 1200.00 [mm]	0.98004
Case F4	4200	C1, C2, C3: 1200.00 [mm] S4, S5, S6: 1200.00 [mm]	0.96603
Case F5	4080	C1, C2, C3: 1200.00 [mm] S4, S5, S6: 1200.00 [mm]	0.95560
Case F6	3960	C1, C2, C3: 1200.00 [mm] S4, S5, S6: 1200.00 [mm]	0.95047

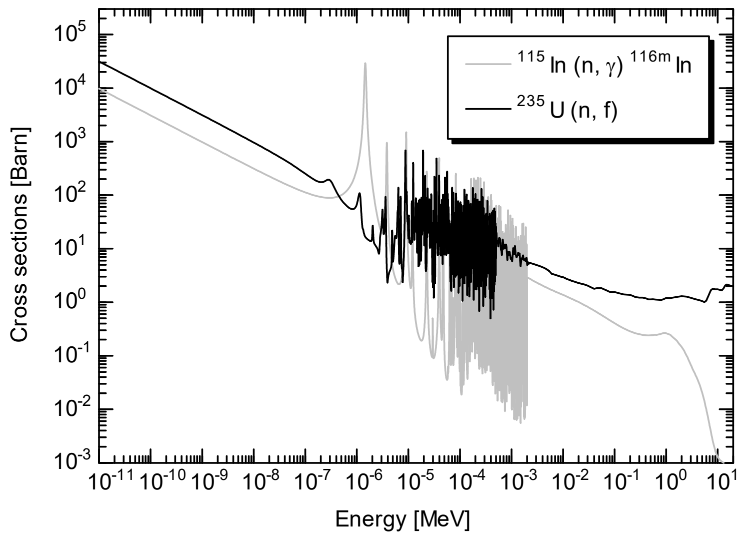

Fig. 4-1-1-1 Proportionality of cross sections of ^{115}In capture and ^{235}U fission reactions

4-1-2. Indium reaction rates

Table 4-1-2-1 Measured reaction rates of In foil at (15, D) in Cases F3 through F-6.

	Measured reaction rate [1/s/cm^3]			
Reaction	Case F3	Case F4	Case F5	Case F-6
^{115}In(*n*, *n*')^{115m}In	(1.970 ± 0.045)E+04	(1.320 ± 0.035)E+04	(2.385 ± 0.020)E+04	(3.482 ± 0.009)E+04

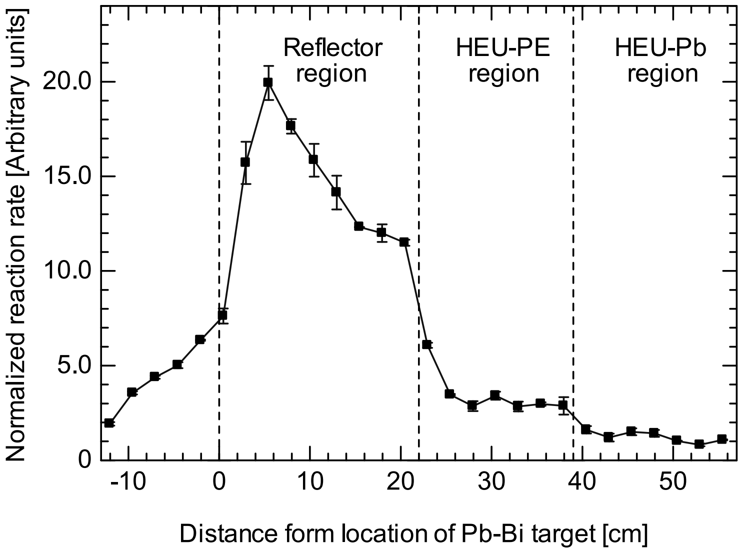

(a) Case F3

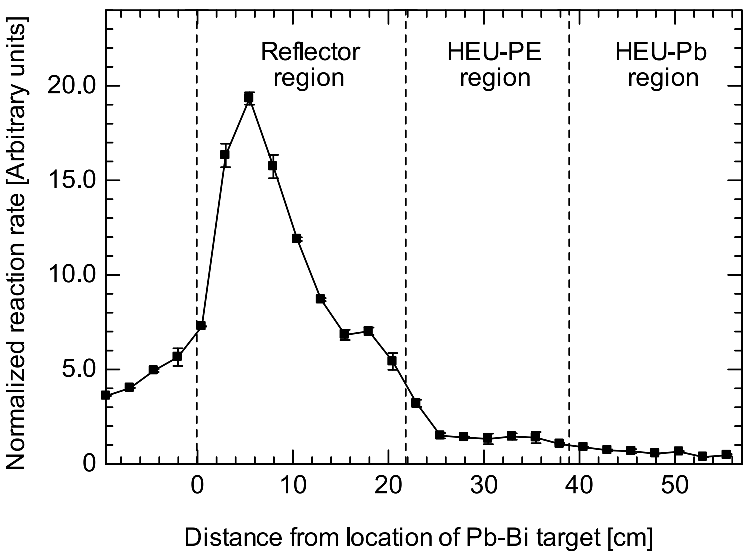

(b) Case F4

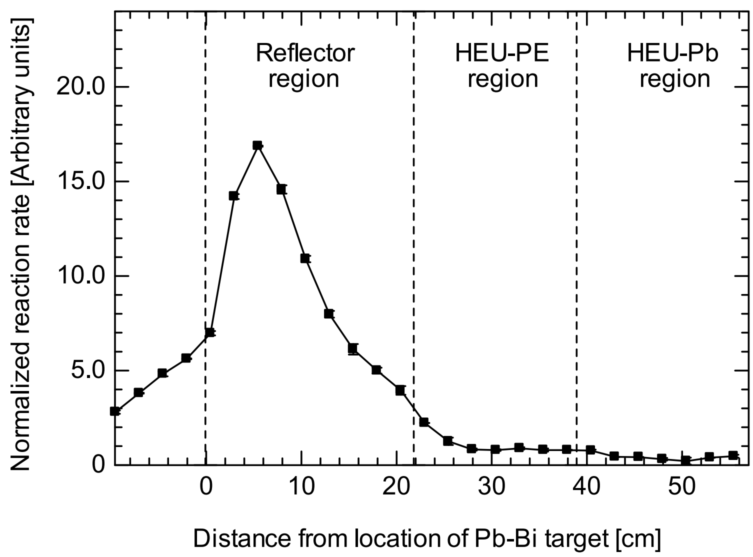

(c) Case F5

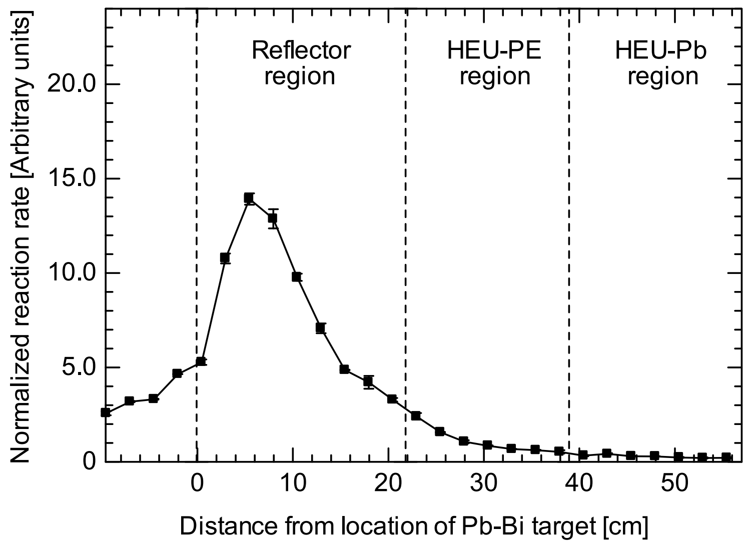

(d) Case F6

Fig. 4-1-2-1 Measured (normalized) reaction rates (^{115}In(n, γ)^{116m}In / ^{115}In(n, n')^{115m}In)

KURNS REPORT OF
INSTITUTE FOR INTEGRATED
RADIATION AND NUCLEAR SCIENCE,
KYOTO UNIVERSITY

発行所　京都大学複合原子力科学研究所
発行日　平成 30 年 6 月
住所　　大阪府泉南郡熊取町朝代西二丁目
　　　　TEL（072）451- 2300